Optimized mesoscale growth of microalgae: A modelling approach

Nicolai Skailand Haddal

November 20, 2017

UNIVERSITY OF BERGEN

Acknowledgements

I would like to thank my supervisors **Børge Hamre** and **Svein Rune Erga** not only for their help and feedback on my thesis, but also for giving me this opportunity to work on a very interesting project.

I would also like to thank **Yi-Chun Chen** and **Håkon Sandven** for their valuable feedback on my thesis.

I would like to thank **Pia Steinrücken** for providing me with the necessary data to complete my thesis.

I would also like to thank my girlfriend **Thea** as well as my parents, family and friends back home for all the support you have given me. I don't know if I could have done this without your help.

Abstract

Photosynthesis is a process that uses water, carbon dioxide and light to create sugar and oxygen. Sugar and oxygen is then used by the cell for maintenance and growth purposes through cellular respiration. We would then expect the growth rate of an algae culture to depend on the amount of radiation available.

This thesis explores how the growth of three strains of P. tricornutum, named FITO, M28 and B58, depends on the amount of radiation received in the form of irradiance, as well as the temperature and the pH. The cultures are grown in bags on a rooftop, the irradiance is measured with a cosine irradiance meter, samples are taken from the algae culture to determine the dry weight or biomass, and the temperature and pH are measured automatically several times during the day. We also create a model that describes the biomass as a function of time, and this model is fitted to the data points we have for biomass.

The correlations between average growth and average temperature and between average growth and average pH are not similar between the strains, however, the correlation between average growth and average irradiance is almost the same for each strain. We also find that the irradiance used can be either in the form of photosynthetically available radiation (PAR) or photosynthetically usable radiation (PUR); the correlation between average growth and PAR is almost identical to the correlation between average growth and PUR.

In our model we have certain parameters, and by fitting the model curve to our different measurement series we get a set of parameter values for each series. We investigate how the maximum growth rate of our model depends on the model parameters, and also how these model parameters depend not only on irradiance, temperature and pH, but on each other. All the correlations between these parameters and between the parameters and irradiance, temperature and pH are weak, the largest ones being between 0.2 and 0.3.

We also find that two of the function parameters, the maximum production and the absorption cross section, have a certain value each for every measurement series that maximizes the maximum growth rate of the model function. We then compare the average fitted parameter values with the average optimal parameter values, and find that the average fitted parameter values for the maximum production and the absorption cross section are 0.74 d^{-1} and 5.7 $\mathrm{dm}^2\ \mathrm{g}^{-1}$, respectively, while the average optimal parameter values for the maximum production and the absorption cross section are 4.5 d^{-1} and 3.2 $\mathrm{dm}^2\ \mathrm{g}^{-1}$, respectively. That is, the average fitted the maximum production is smaller than the average optimal the maximum production, while the average fitted the absorption cross section is higher than the average optimal the absorption cross section. To optimize growth, then, we should consider finding other strains and maybe species of algae that have different average values of the maximum production and the absorption cross section.

Another interesting result is that the growth per area, according to the model, is constant with depth. That means that model-wise there are not any limitations on the depth, at least not for bags that are between 1 cm and 1 m deep. That is, to maximize growth, we should look at other parameters, and look at the depth from a more practical viewpoint.

Contents

List of Figures

List of Tables

1 Introduction

1.1 Light and Life

All around us, we see not only different forms of life, but different wavelengths of light. Two very common forms of life are plants and animals, and the different kinds of wavelengths available to the naked eye lie in the range between approximately 400 and 700 nanometers.

Most if not all animals eat either plants, meat or both types of food for nourishment, and most if not all plants use photosynthesis for nourishment. Regardless of whether or not you are a vegetarian, your life literally depends on certain organisms' ability to make use of photosynthesis. The reason why photosynthesis is so important for you is because this is how sugar is created, and this sugar is used to give you the energy your body needs to function.

But why do I mention the wavelength range of visible light? As it turns out, the part in plant cells that drives photosynthesis has not just one, but two photosystems. Each of these two photosystems absorb light of different wavelengths to drive photosynthesis (Falkowski & Raven, 2007; Kirk, 1994).

1.1.1 Early atmosphere

Approximately 4.6 billion years ago, the Earth was formed together with the Sun. At this point in time the Earth was quite hot, and the atmosphere consisted of hydrogen and helium. Back then, our planet did not have a magnetic field to protect the atmosphere from solar winds, and because of this the solar wind blew the Earth's early atmosphere away (Cain, 2009; Zahnle, Schaefer, & Fegley, 2010; Brennan, 2017).

4.4 billion years ago, after the Earth had cooled down, active volcanoes had formed, and these volcanoes spewed out different types of gases. One of the gases spewed out by these volcanoes were carbon dioxide, CO_2. In addition to volcanic activity, bombardment of Earth by asteroids also helped create the new atmosphere (Cain, 2009; Zahnle et al., 2010; Brennan, 2017).

Between 2.7 and 2.2 billion years ago, an early type of bacteria started to use energy from the Sun in photosynthesis and release oxygen as a byproduct, in addition to creating organic carbon molecules from carbon dioxide (Cain, 2009). These bacteria are known as cyanobacteria.

Because of the cyanobacteria's ability to consume CO_2 and produce oxygen, the bacteria changed the atmospheric composition of the Earth, reducing the amount of CO_2 and increasing the amount of oxygen (Cain, 2009).

1.1.2 Solar spectrum

The solar spectrum is the irradiance spectrum of sunlight and the spectrum right outside of the Earth's atmosphere is close to that of a 6000K blackbody, but as the solar radiation penetrates the atmosphere, some of the radiation is attenuated both through absorption and scattering. The radiation that is absorbed increases the energy of the absorbing agent, and the radiation can also be re-emitted by the absorbing agent. Radiation that is scattered will change direction (Bohren & Clothiaux, 2006; Kirk, 1994).

Water vapor, carbon dioxide and oxygen all absorb in the near infrared. Wavelength-dependent Rayleigh scattering, as well as scattering from aerosols and other particles including water droplets also change the spectrum of the radiation that reaches the ground, making the sky look blue. The reason for this is that scattering changes the direction of a photon in the beam, and since scattering is wavelength-dependent, the solar spectrum changes through the atmosphere (Falkowski & Raven, 2007; Bohren & Clothiaux, 2006; Kirk, 1994).

1.1.3 Algae

The term "algae" is a term used for a diverse group of aquatic organisms that are photoautotrophs, that is, they are not only able to generate nutrition through absorbing light, but they can also use this nutrition to nourish themselves. Unlike most land plants, algae lack roots, stems, leaves with a vascular system to circulate water and nutrients through their bodies. In addition, some algae are unicellular, that is, they consist of only one cell. Some algae consist of eukaryotic cells while others consist of prokaryotic cells. If a cell is eukaryotic it has a nucleus in addition to membrane-bound chloroplasts and mitochondria. If a cell is prokaryotic it lacks a nucleus and membrane-bound organelles (Falkowski & Raven, 2007; Vidyasagar, 2016; *Prokaryotic cells*, -).

1.2 Primary Production

As I mentioned earlier, photosynthesis is the process that is driving algae growth. Not only can algae cells produce sugar and oxygen, but they can also consume it via cellular respiration. Cellular respiration can, in a specific sense, be viewed as the opposite of photosynthesis. Although they are two different processes, while photosynthesis uses CO_2, water and sunlight to produce sugar and oxygen, cellular respiration is the process whereby sugar and oxygen is consumed to produce CO_2, water and energy in the form of Adenosine triphosphate (ATP). ATP is a molecule containing three phosphate molecules, and is energetically unstable, hence it releases energy when a phosphate molecules breaks apart from the ATP molecule, creating Adenosine diphosphate (ADP). Energy in the form of ATP is used to power different processes in the cells (Falkowski & Raven, 2007; Amthor, 1994; Hill, 2014; Alters, 2000).

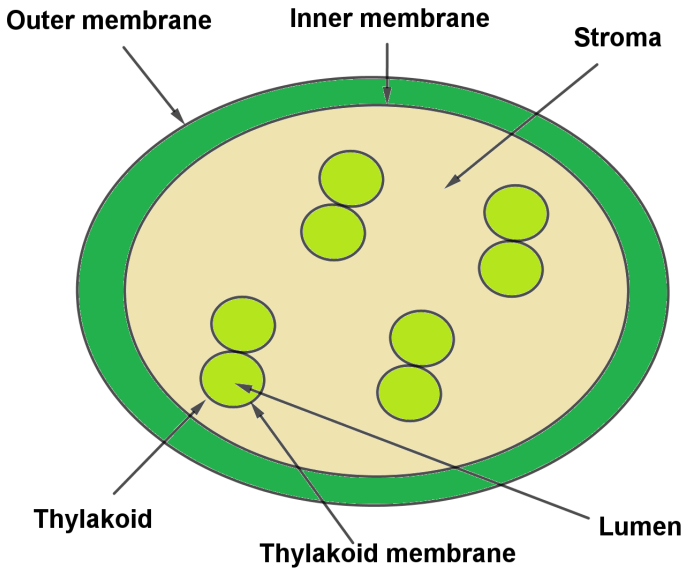

Figure 1: The chloroplast is where photosynthesis and carbon fixation happens; photosynthesis happens along the thylakoid membranes while carbon fixation happens in the chloroplast stroma.

1.2.1 Photosynthesis

Figure 1 shows the chloroplast inside the eukaryotic cell, and photosynthesis happens along the thylakoid membrane. First, radiation is harvested by the antenna of the first photosystem, somewhat ironically called Photosystem 2, or PS2. The radiation energy travels from the antenna towards the reaction centre of PS2. There, it is used to send an electron along the membrane towards the second photosystem, named Photosystem 1 or PS1. A side effect of the release of the electron from PS2 is the oxidation of water. Once the electron reaches PS1, it has used up a lot of its energy and needs a recharge: PS1 also has an antenna, and the energy harvested by the PS1 antenna travels towards a PS1 reaction centre, giving the free electron some energy. The electron is then used to create Nicotinamide adenine dinucleotide phosphate (reduced form), often called NADPH, which is used in the Calvin-Benson cycle to create sugar, or glucose. Glucose is then used in cellular respiration (Falkowski & Raven, 2007; Kirk, 1994; Govindjee, 2012; Blankenship, 2013).

1.2.2 Cellular respiration

Cellular respiration is linked to cellular growth. The reason for this is that, in order to grow, the cell needs energy not only to make new cells but also to maintain itself. This energy is obtained through cellular respiration, which happens mainly along the mitochondrial membrane. Cellular respiration is divided into four processes, namely glycolysis, the pentose phosphate pathway, the Krebs cycle and the electron transport chain. The net result of all these processes is that sugar (glucose) and oxygen is used, forming carbon dioxide, water and energy. But the energy is in the form of the molecule ATP. As I mentioned earlier, this molecule has three phosphate groups, and is quite unstable. When one of the phosphate groups breaks off, ADP is created, and energy is released. This energy can be used for cell maintenance and cell growth. Since cellular growth is linked to cellular respiration, and cellular respiration is linked to photosynthesis, cellular growth is linked to photosynthesis (Falkowski & Raven, 2007; Amthor, 1994; Hill, 2014; Alters, 2000).

1.3 Practical applications of algae

Algae have several practical uses. Some of these uses are:

1. Agar - A gelatin-like product made from red algae that can be used in food preservation, cosmetics, medicines, dentistry, brewing, wine making and as a thickening agent in several desserts (*Agar*, 2017).

2. Alginate - A product obtained from algae that can be used to create hydrogels used in wound healing, drug delivery and tissue engineering (Lee & Mooney, 2012).

3. Climate change - Approximately 50 percent of photosynthetic activity on Earth takes place in aquatic environments. Combining this with the fact that photosynthesis takes use of CO_2, you find that aquatic photosynthesis, or rather, aquatic carbon fixation is of high importance in the regulation of the Earth's climate (Liu, 2013).

4. Energy source - Microalgae are able to provide different types of biofuels including methane, biodiesel and bio-hydrogen. Algae have a smaller environmental impact compared with terrestrial sources of biomass used for biofuels, and production of algae biofuels minimize land use compared with biofuels produced from terrestrial plants (Chisti, 2007; Hannon, Gimpel, Tran, Rasala, & Mayfield, 2010).

5. Fertilizer - By using algae to create bio-fertilizer and then by applying bio-fertilizer to enhance the nutrient content of farm soil it is possible to increase the productivity of farm crops (Chatterjee et al., 2017).

6. Pollution control - Cyanobacteria can be used to degrade different types of environmental pollutants including metal ions, salinity and pesticides. (Chatterjee et al., 2017).

7. Pigments - In order for algae to harvest light, the cells contain pigments. In order to extract certain pigments, for example polar pigments, like carotenoids, hydrophilic solvents like methanol can be used (Falkowski & Raven, 2007; Henriques, Silva, & Rocha, 2007).

8. Polyunsaturated fatty acids (PUFAs) - Microalgae can be used as an alternative to fish oil as a source of PUFAs, and these PUFAs can be used both in health and dietary products as well as in aquaculture feeds (Steinrücken, Erga, Mjøs, Kleivdal, & Prestegard, 2017).

9. Cosmetics - Algae extracts can be used against skin aging and de-pigmentation (Wang, Chen, Huynh, & Chang, 2015).

1.4 Motivation and aim of the thesis

As explained, algae grow in water. In addition, the growth depends at least on the amount of radiation present for the cells to absorb, as well as temperature and nutrients, as will be explained in the theory section. Since algae in the ocean receive almost only sunlight, not only atmospheric attenuation of light needs to be accounted for, but also aquatic attenuation of light if the algae are submerged in water. Not only do the algae cells use radiative energy directly in photosynthesis, but some radiative energy also affect the temperature of the system.

In the science of aquatic photosynthesis there are many models describing different aspects of photosynthesis, but what if we could create a model that describes the growth rate as a function of irradiance and temperature, and possibly pH as well? We might need more than three parameters for our model in the initial phase, but once we have a model with certain parameters, we can find a combination of parameter values that gives us a model that fits well with the measured data, and then try to find out how these parameters depend on for example irradiance and temperature, and thereby create a model for algae growth dependent on only irradiance and temperature, if possible, of course.

Not only would we want to have such a model in order to describe how algae growth depends on certain physical values, but we could also use this model to predict the optimal growth conditions. Once we have a simple yet effective model for describing growth, we have a useful tool for improving the growth of algae.

So, to summarize, the aims of the thesis are as follows:

1. Create a model for algae growth

2. Find optimal growth conditions for algae

1.5 Outline

Section two goes into detail about the theory behind some of the concepts presented in the introduction, as well as introduce some other concepts necessary to create our model.

Section three presents the instruments that have been used to gather the necessary data for this thesis.

Section four explains what methods we used to obtain our data as well as how we will use the data to reach the aims of the thesis.

Section five will present the results we have obtained from analyzing our data. That is, how different variables depend on each other, how the growth varies with time, correlation coefficients, the model for growth et cetera. We will not only present the results, but we will also discuss the results and how they can be used to reach our thesis aims.

Section six will include the conclusions of the thesis.

Section seven will include suggestions to further work on the thesis aims.

The last part of the thesis includes references used for the thesis.

2 Theory

2.1 Photosynthesis

Photosynthesis can be divided into two processes; the light reactions that occur, in eukaryotic cells, along the thylakoid membranes and the dark reactions that occur, in eukaryotic cells, in the chloroplast stroma. The net result of photosynthesis is that CO_2, water and energy in the form of photons is used to create carbohydrates and oxygen (Falkowski & Raven, 2007; Kirk, 1994; Govindjee, 2012; Blankenship, 2013).

2.1.1 Light reactions

Photosynthesis starts with the light reactions, and the first step is for Photosystem 2 (PS2) to harvest light energy via its pigment-protein antenna. The energy harvested by this antenna can migrate through a pigment-protein complex all the way to the reaction center via one of two energy transfer mechanisms (Falkowski & Raven, 2007; Kirk, 1994; Blankenship, 2013).

1. The Förster mechanism, which is a non-radiative dipole-dipole coupling mediated by intermolecular forces. The energy is located on individual pigments, and the energy transfer is usually downhill; that is, from a higher energetic state to a lower energetic state (Falkowski & Raven, 2007; Kirk, 1994).

2. The Dexter mechanism, which is based on the overlapping of wave functions between molecules. The energy is delocalized, and the energy transfer is both uphill and downhill (Falkowski & Raven, 2007).

Once the energy reaches the reaction center of the photosystem the energy can be absorbed by a special chlorophyll a molecule called P680, where chlorophyll a is a type of pigment. Once the P680 molecule absorbs the energy it becomes electronically excited and can reduce a nearby acceptor molecule. When this happens the P680 molecule in the reaction center becomes oxidized which means that there is an electron hole in the reaction center. This electron hole can either be filled by the electron it just donated, via a backreaction, or it can be filled by a neighboring donor molecule, namely the amino acid tyrosine (Y_Z). If tyrosine donates an electron to the hole in the reaction center, it becomes oxidized and in turn oxidizes a Mn atom in a nearby Mn cluster. The oxidation of the Mn atom in turn leads to the oxidation of water which provides the system with electrons, protons and oxygen(Falkowski & Raven, 2007; Kirk, 1994; Govindjee, 2012; Blankenship, 2013). We now move on to the electron transport chain.

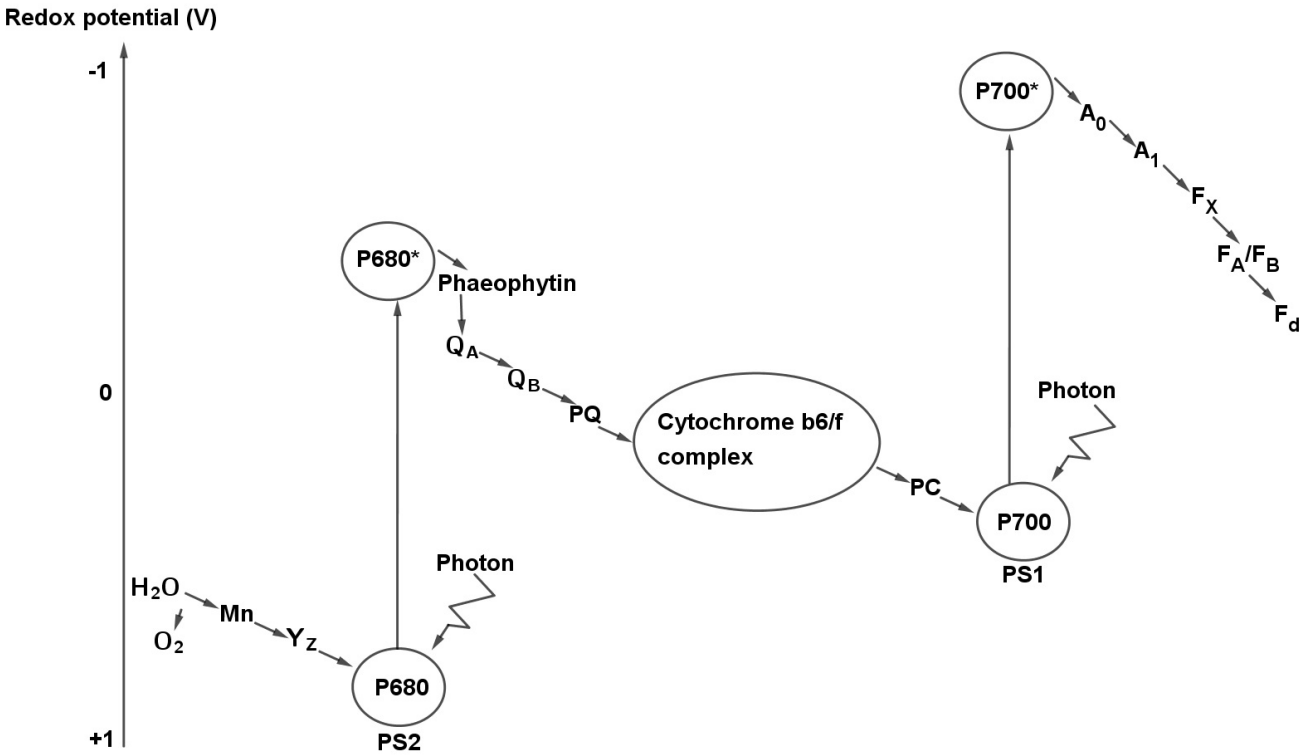

Figure 2: The Z Scheme. As the electron goes from one molecule to the next, the redox potential changes. When the redox potential becomes more negative, the redox energy becomes more positive because of the negative electron charge.

The electron transport chain can be represented with the Z-scheme (Figure 2), which tells us the redox potential of the molecule that the electron is occupying in the electron transport chain. The donor molecule P680 donates its electron to a phaeophytin molecule, which then reduces a bound form of plastoquinone named Q_A. The electron is then transferred via another plastoquinone molecule named Q_B. These plastoquinone molecules are sometimes called quenchers because they quench fluorescence (backreactions) by providing large differences in electric potential, hence reducing the probability of a backreaction. Once Q_B has received two electrons it pulls two electrons from the stroma and then dissociates from its binding site, becoming part of the plastoquinone (PQ) pool, leaving an empty pocket to be filled by an oxidized plastoquinone molecule. This gives us free plastoquinol (PQH_2) which can move towards a complex called the cytochrome b_6/f complex (Falkowski & Raven, 2007; Kirk, 1994; Govindjee, 2012).

The cytochrome complex oxidizes platoquinol, which is accompanied by the release of two protons into the thylakoid lumen (inside of thylakoid), creating an electrochemical gradient. Some of the electrons donated by plastoquinol to the cytochrome complex can cycle back to the donor side of PS2, and this so-called Q cycle doubles the amount of protons moved per electron moved. After receiving and manipulating electrons from plastoquinol the cytochrome complex is reoxidized by a small water-soluble molecule that diffuses in the thylakoid lumen. The electrons are transferred from cytochrome f to PS1 either via a copper-containing protein called plastocyanin (PC), or a soluble iron-containing protein called cytochrome c6, or by both of these (Falkowski & Raven, 2007; Kirk, 1994).

Electrons delivered to PS1 can reduce the chlorophyll a molecule named P700, and if the antenna of PS1 absorbs a photon, this photon energy can lead to the oxidation of P700. P700 becomes oxidized when it donates its electron to a neighbouring chlorophyll a molecule designated A_0, which is followed by an electron transfer to a phylloquinone (vitamin K1) molecule designated A_1. From A_1 the electron is pased on to an iron-sulfur complex, F_X. F_X is then oxidized by a second iron-sulfur complex F_B/F_A which ultimately transfers the electron to an iron protein called ferredoxin. An enzyme named ferredoxin-$NADP^+$ reductase (FNR) helps ferredoxin reduce the molecule Nicotinamide adenine dinucleotide phosphate (NADP), and by adding protons from water to $NADP^-$ we get NADPH (Falkowski & Raven, 2007; Kirk, 1994; Govindjee, 2012; Blankenship, 2013).

Another important molecule created in photosynthesis is ATP. When protons are transported across the thylakoid membrane and into the lumen during the electron transport chain, a pH difference is created and therefore a pH gradient is set up. When the protons move through the ATP synthase complex from the lumen to the stroma they carry energy with them, and this energy is used in phosphorylation via the ATP synthase complex to create ATP. The process of phosphorylation is also reversible, that is, ATP can be used to make ADP, and the direction of the reaction is determined by the equilibrium of the substrates (Falkowski & Raven, 2007; Kirk, 1994; Blankenship, 2013).

2.1.2 Dark reactions

The primary pathway responsible for carbon reduction is called the Calvin cycle, which is often called a dark reaction, and this cycle is responsible for the creation of sugar (Falkowski & Raven, 2007; Govindjee, 2012). There are three steps in the cycle:

1. Carboxylation (where the enzyme Rubisco interacts together with CO_2) of a five-carbon sugar phosphate (Ribulose 1.5-biphosphate or RuBP) which produces 2 molecules of 3-phosphoglyceric acid (3-PGA) (Falkowski & Raven, 2007; Kirk, 1994; Govindjee, 2012).

2. The conversion of 3-PGA to form triose phosphate (glyceraldehyde triphosphate or G3P) with the help of ATP and NADPH (Falkowski & Raven, 2007; Kirk, 1994; Govindjee, 2012).

3. The interconversion of sugars where if we start with 6 molecules of CO_2 in step one, one molecule of hexose is created, in addition to 6 molecules of RuBP needed to go through the cycle once more (Falkowski & Raven, 2007; Kirk, 1994; Govindjee, 2012).

That is, Rubisco interacts with CO_2 through carboxylation to create sugar (hexose). Rubisco can also interact with oxygen instead of CO_2 in a process called oxygenation which is part of a process called photorespiration. While carboxylase activity of Rubisco turns RuBP and CO_2 into 2 molecules of 3-PGA (3P-glycerate), oxygenase activity of Rubisco turns RuBP and oxygen into 1 molecule of 3P-glycerate and 1 molecule of 2P-glycolate. The 2-PGA inhibits the Calvin cycle and must be turned into 3-PGA for recovery by the Calvin cycle. One could describe oxygenase activity as a light-dependent consumption of oxygen (Falkowski & Raven, 2007; Blankenship, 2013).

2.2 Cellular respiration

Cellular respiration is the process where the sugar created by photosynthesis, in addition to oxygen, is used to create water, carbon dioxide and energy in the form of ATP which can be used to maintain the cell and grow new cells. In addition, nitrogen, phosphorus, sulfur and trace metals are needed for the synthesis of many essential cellular components. Cellular respiration is often called dark respiration, and there are four steps in this process: glycolysis, the pentose phosphate pathway, the krebs cycle and oxidative phosphorylation (Falkowski & Raven, 2007; Amthor, 1994; Hill, 2014; Alters, 2000).

Glycolysis takes place partly in the cytoplasm (outside chloroplast) and partly in the chloroplast stroma. In glycolysis sugar is broken apart and glyceraldehyde 3-P is created which is then used to create pyruvate. The major role of glycolysis is to form substrates that can be used for further respiratory processes (Falkowski & Raven, 2007; Amthor, 1994; Hill, 2014; Alters, 2000).

Glycolysis is not the only respiratory pathway that consumes sugar; the pentose phosphate pathway also does. In this pathway the sugar is phosphorylated and then oxidized to produce NADPH, CO_2 and pentose phosphate, the pentose phosphate then being phosphorylated to hexose phosphate and triose phosphate, which can be used in glycolysis. The major role of the pentose phosphate pathway is to provide a nonphotosynthetic source of NADPH (Falkowski & Raven, 2007; Amthor, 1994).

The third respiratory pathway, the Krebs cycle, is located in the mitochondrial matrix which is located between the outer and inner mitochondrial membranes. In the Krebs cycle the pyruvate that was created in glycolysis is oxidized to CO_2 by the help of Nicotinamide adenine dinucleotide (NAD^+) and Flavin adenine dinucleotide (FAD), creating NADH, Dihydroflavine adenine dinucleotide ($FADH_2$) and ATP (Falkowski & Raven, 2007; Amthor, 1994; Alters, 2000).

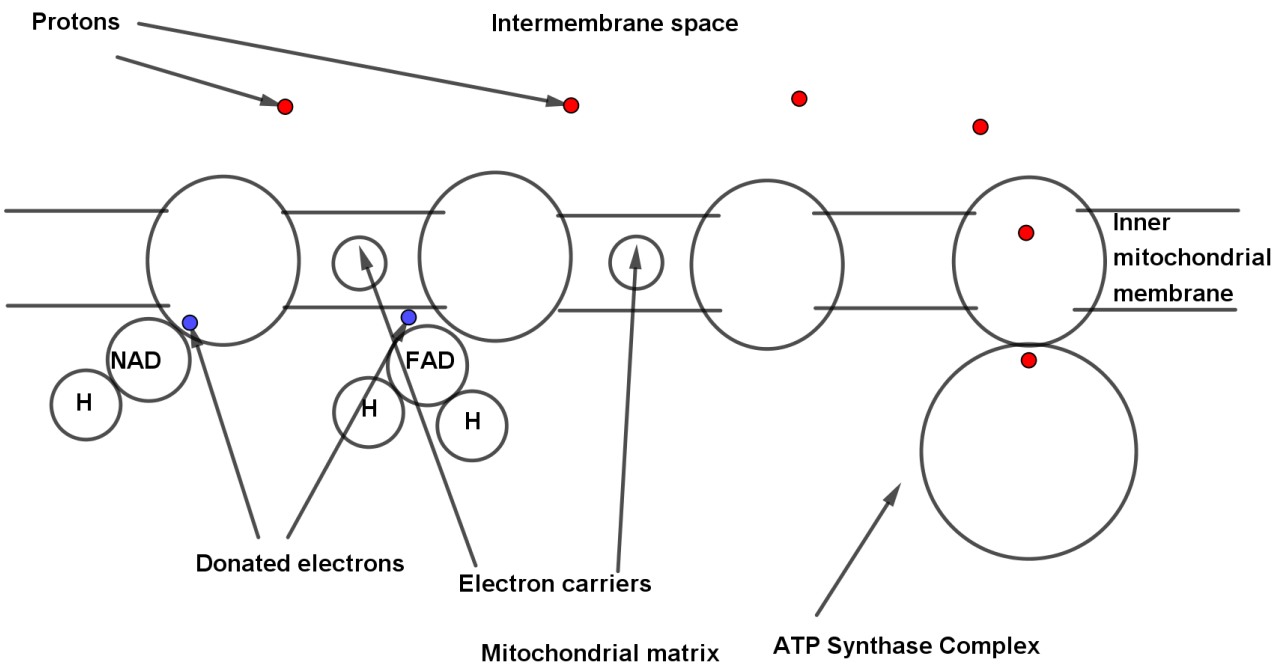

Figure 3: The mitochondrial electron transport chain. As electrons are donated to the electron carriers from NADH and $FADH_2$, the electrons travel along the membrane. This works as a proton pump, pumping protons from the mitochondrial matrix and into the intermembrane space. The protons return to the matrix through the ATP Synthase Complex, and the energy of the protons are used to synthesize ATP.

The last respiratory pathway shown in Figure 3 is oxidative phosphorylation, also known as the electron transport chain (not to be confused with the thylakoid membrane electron transport chain), and this pathway takes place in the mitochondrial intermembrane space. In this pathway ADP is phosphorylated into ATP via an ATP synthase complex similar to that found in the chloroplast. When NADH and $FADH_2$ donate electrons to the inner membrane, the electrons can then move inside the membrane, and the moving electrons work as a proton pump. Once there is an imbalance in the amount of protons between the intermembrane space and the mitochondrial matrix, a proton gradient is established which will push protons through the ATP synthase complex, creating ATP (Falkowski & Raven, 2007; Amthor, 1994; Hill, 2014; Alters, 2000).

2.3 Irradiance and the light attenuation law

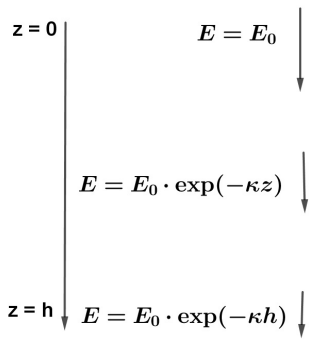

Figure 4: Approximation of atmospheric attenuation of radiation with the help of Beer-Lamberts law.

Figure 4 shows us what can happen when radiation travels through the atmosphere, or any other medium for that matter; the radiation is attenuated. This attenuation happens either by absorption, where atoms, molecules and/or particles in the medium absorb the radiation, or by scattering, whereby the direction of some of the radiation changes.

In this thesis we are using the term irradiance for radiation. There are two common ways of expressing irradiance; either in the form of an energy flux or in the form of a photon flux. In this thesis we will be using the photon flux which describes the number of photons. More explicitly, the irradiance is the amount of photons hitting a surface per unit time per unit surface. An example of irradiance units will therefore be

$$\frac{\text{photons}}{\text{s} \cdot \text{m}^2} \tag{1}$$

A law describing the attenuation of irradiance, therefore, is an exponential law known as Beer-Lambert's law, which says

$$E = E_0 \exp(-\kappa z) \tag{2}$$

where E is the irradiance at depth z, E_0 is the initial irradiance (irradiance at depth $z = 0$), κ is the diffuse attenuation coefficient and z is the depth of the medium. κ can also be expressed in terms of the effective mass specific absorption cross section k which includes extra absorption from longer photon pathways due to scattering

$$\kappa = k\rho \tag{3}$$

where ρ is the volume mass density of the medium. k may depend on wavelength, in which case we should use spectral irradiance instead of irradiance, where the units of spectral irradiance are

$$\frac{\text{photons}}{\text{s} \cdot \text{m}^2 \cdot \text{nm}} \tag{4}$$

where nm are units of wavelength.

2.4 P vs. E curves

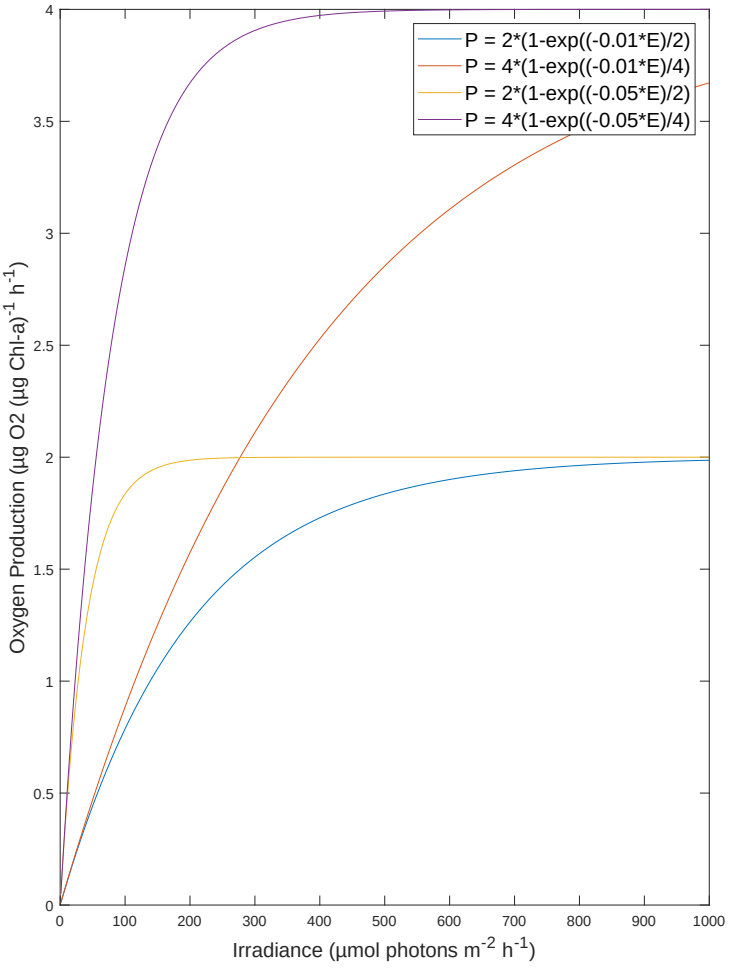

Figure 5: A set of photosynthesis versus irradiance curves. Different values of P_m and α give different curves.

A P vs. E curve, or a photosynthesis vs. irradiance curve, is a model curve that describes for example net oxygen production/consumption as a function of light intensity. When the irradiance levels are low, the production is approximately a linear function of the irradiance, and the ratio between photosynthesis and the irradiance in this portion of the P vs. E profile is often denoted by the symbol α. Hence, α is the slope of the initial linear part of the P vs. E curve. Something not shown in Figure 5 is that for very low irradiance levels, the oxygen production is negative, i.e. oxygen is consumed, yet this part of the curve is also linear (Falkowski & Raven, 2007; Kirk, 1994; Sakshaug et al., 1997).

The equation for a P vs. E curve is as follows:

$$P = P_m \left[1 - \exp\left(\frac{-\alpha E}{P_m} \right) \right] \tag{5}$$

At some irradiance level the production reaches a plateau where the curve is light-saturated, at which the rate of photon absorption greatly exceeds the rate of steady-state electron transport from water to CO_2, and this upper limit of production is denoted P_m or P_{max}. The irradiance that saturates photosynthesis, E_K, is given at the intercept between α and P_m. Not shown in Figure 5 is that at irradiance levels far above the optimal level, photosynthetic rates decline from the light-saturated value and the rate of decline β is analogous to the initial slope α but with an opposite sign. This phenomenon of decline is known as photoinhibition, and the degree of photoinhibition is dependent on both the irradiance and the duration of exposure (Falkowski & Raven, 2007; Kirk, 1994; Sakshaug et al., 1997).

E_K represents an optimum value for irradiance, and at irradiance levels lower than E_K, the rate at which photons are absorbed is lower than the maximum rate of electron transfer from water to CO_2. At irradiance levels higher than the optimal value E_K, the rate of photon absorption is higher than the maximum rate of electron transfer from water to CO_2. Increasing the irradiance above E_K only slightly increases the rate of photosynthesis (Falkowski & Raven, 2007; Kirk, 1994; Sakshaug et al., 1997).

Photoinhibition can be thought of as changing P_m by either reducing the number of photosynthetic units (the units consist of a single PS1 and a single PS2 working together in addition to a set of light-harvesting pigment-proteins) or by increasing the maximum rate of electron transfer, also known as the maximum turnover time. Like I mentioned earlier, when reaction centers receive energy from photons, water is split, which generates oxygen, electrons and hydrogen ions. If a reaction center takes in too much energy/too many photons, and oxygen is not removed quickly enough, the oxygen can reach higher energy levels and oxidize parts of the reaction center (Falkowski & Raven, 2007; Kirk, 1994).

The initial slope of the P vs. E curve, the maximum photosynthetic rate, and the light saturation parameter E_k can be related to three different parameters: n, σ_{PS2} and $\frac{1}{\tau}$, where n is the maximum number of oxygen molecules that can be generated in a single electron turnover, σ_{PS2} is the functional absorption cross section of PS2, and $\frac{1}{\tau}$ is the maximum turnover rate, or the maximum rate in which electrons are transferred from water to CO_2 (Falkowski & Raven, 2007; Sakshaug et al., 1997).

In order to manipulate their absorption cross sections, photosynthetic organisms have developed some mechanisms in order to be able to do this. The variations in absorption cross sections occur on many different time scales, and there are at least three types of adjustments an organism can make to its absorption cross section (Falkowski & Raven, 2007):

1. State transitions - this happens by changing the quantum yield of photosynthesis by physically coupling or decoupling the light-harvesting antennae of the chlorophyll-protein complexes with the reaction centers (Falkowski & Raven, 2007)

2. Nonphotochemical quenching - thermal dissipation of absorbed excitation energy; that is, the absorbed energy is released as heat (Falkowski & Raven, 2007; Sakshaug et al., 1997)

3. Photoacclimation (Falkowski & Raven, 2007)

The state transitions and nonphotochemical quenching mechanisms change the absorption cross section of PS2 in a matter of minutes, but when a photosynthetic organism is placed for a long period of time in a given irradiance range, it acclimates or changes to make better use of this irradiance range within the limits of the genetic potential and environmental constraints of the cell. This long term acclimation to irradiance is called photoacclimation, and this is a process that can change pigmentation (Falkowski & Raven, 2007).

Photosynthetic electron transport is temperature dependent, and for several reasons. Some of the electron transfer processes, which take place in the membranes, are dependent on the fluidity of these membranes, and this fluidity is dependent on temperature. A second effect of temperature in regards to the electron transport is related to thermal effects on intermolecular collision processes; when the temperature increases, the rate of intermolecular collision processes increases (Falkowski & Raven, 2007).

2.5 PAR and PUR

Photosynthetically available radiation (PAR) is the spectrally integrated irradiance between 400 nm and 700 nm.

We can define PAR in the following way:

$$E_{PAR} = \int_{400}^{700} E_\lambda(\lambda) d\lambda \tag{6}$$

where $E_\lambda(\lambda)$ is the spectral irradiance and λ is the wavelength in question.

We can define photosynthetically usable radiation (PUR) in the following way:

$$E_{PUR} = \frac{\int_{400}^{700} E_\lambda(\lambda) a(\lambda) d\lambda}{\int_{400}^{700} a(\lambda) d\lambda} \tag{7}$$

where $a(\lambda)$ is the normalized spectral algae absorption cross section. We now have two ways of calculating irradiance, namely PAR and PUR.

In order for the cell to gain the most energy possible, it can either receive a higher irradiance or it can have a greater absorption cross section. The cell can change its absorption cross section through the three mechanisms previously mentioned; antennae coupling, thermal dissipation or photoacclimation. However, it is good if the cell does not receive too much energy, because if it does it can suffer from photoinhibition. Cells or plants exposed to very high irradiance levels for brief periods reveal little or no effect while cells exposed for longer periods show a decrease in photosynthesis (Falkowski & Raven, 2007; Kirk, 1994).

2.6 Water column example

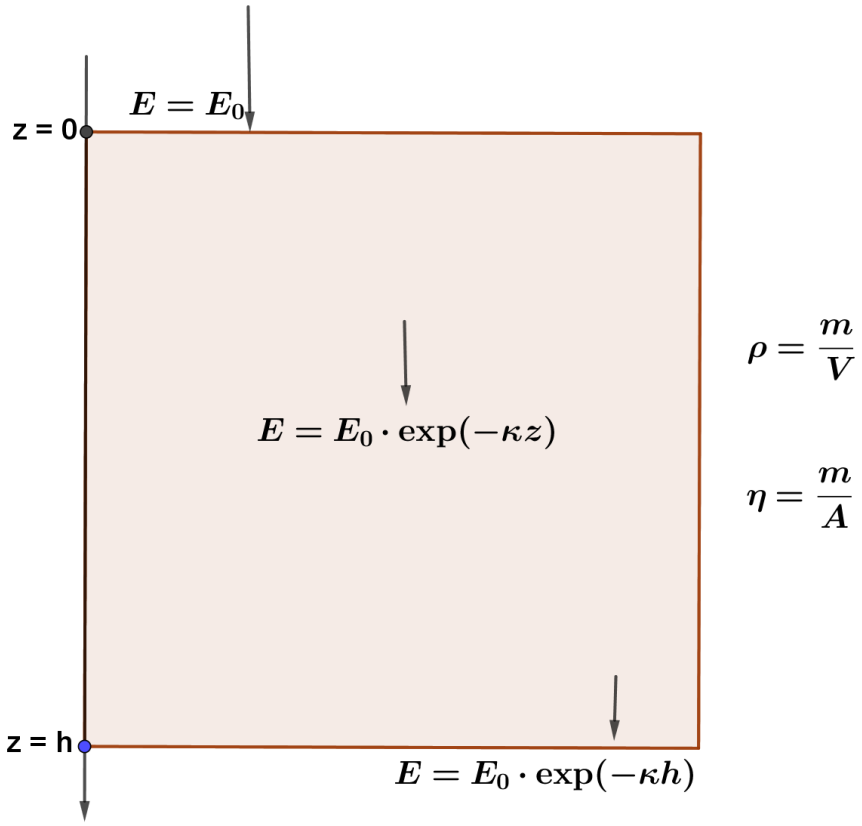

Figure 6: A water column containing algae. Just like in the case of atmospheric attenuation, we can use Beer-Lamberts law for attenuation of light in a water column.

If we have a water column containing algae cells, as shown in Figure 6, and we shine a light on top of the column, the light will get attenuated because of absorption and scattering by the water and the algae cells. The remaining light, however, will reach the algae. Some of the light that reaches the algae will be absorbed and used in photosynthesis, but in order for the algae to grow, the algae cells have to use some of the oxygen that is freed from water when absorbing the light in order to consume sugar.

Let us assume that the growth is a function of irradiance and temperature, as described in the following equation:

$$\frac{d\rho}{dt} = f(E, T)\rho \tag{8}$$

where ρ is the mass per unit volume (g/l) of the algal dry mass, t is time in days, E is the wavelength integrated irradiance (μmol photons per square decimeter per day, where one day is 24 hours) in the form of either PAR or PUR and T is temperature (degrees Celsius).

If we have strong mixing in the algae container ρ will be constant with depth, and we get that

$$\eta = \int_0^h \rho dz = \rho h \tag{9}$$

and hence

$$\rho = \frac{\eta}{h} \tag{10}$$

where η is the mass per unit area (gram per square decimeter), z is the depth in the water column (decimeter) and h is the total depth of the water column (decimeter).

Furthermore, we have that

$$\frac{d\eta}{dt} = \int_0^h \frac{d\rho}{dt} dz = \int_0^h f(E,T)\frac{\eta}{h} dz \tag{11}$$

If we still assume that the mixing is uniform, we have that

$$\kappa = k\frac{\eta}{h} \tag{12}$$

where κ is the diffuse attenuation coefficient of the medium with units (per decimeter), and k is the effective mass specific absorption cross section of the medium with units (square decimeters per gram). And if we use a modified P vs. E model for growth we get that

$$f(E,T) = P_m \left[1 - \exp\left(-\frac{\alpha k E}{P_m}\right) - \xi\right] \tag{13}$$

where $f(E,T)$ is the growth function, P_m is the maximum production with units (per day), α is the positive linear slope of the corresponding P vs. E curve with units (grams per μmol photons), E is the irradiance in the form of either PUR or PAR and ξ is a unitless loss factor.

The loss factor is necessary primarily because without it, production will not become zero as time and hence biomass goes to infinity. As time and hence biomass goes to infinity, resources for growth become limited for some of the cells. In addition, not all of the oxygen is used for growth. Some of the oxygen is used for maintenance respiration, some of it is released by the cell into the surrounding medium, and some of it can oxidize neighboring cells. Hence, even when not all of the oxygen is used by the cell, not all of the oxygen that is actually used by the cell is used for growth per se.

The absorption cross section is necessary in Equation 13 because without it, we can reduce the absorption cross section as much as we want, yet the growth only increases with decreasing absorption cross section. A large absorption cross section will attenuate too much radiation in the top layer, yet a small absorption cross section will make the cells absorb too little radiation throughout the column, preventing growth.

Furthermore, we have that

$$E = E_0 \exp(-k\rho z) = E_0 \exp(-k\frac{\eta}{h}z) \tag{14}$$

By combining equations 11, 13 and 14, we get a new equation:

$$\frac{d\eta}{dt} = P_m \eta \left(1 - \xi - \frac{1}{h}\int_0^h \exp\left[-\frac{\alpha k}{P_m} E_0 \exp\left(-k\frac{\eta}{h}z\right)\right] dz\right) \tag{15}$$

This last equation is very difficult, if not impossible, to solve analytically. What we will do instead is to solve it numerically.

3 Instruments

In this section we will look at the instruments used to gather our data. To measure irradiance, we used an irradiance sensor of the Ramses type, manufactured by TriOS, with the ID 80E2. To measure biomass, we used a Mettler Toledo (MT5) micro weight. The temperature and pH were measured automatically by using a thermistor and an electrode pH meter, respectively.

3.1 Irradiance Sensor

3.1.1 Specifications

The irradiance sensor named 80E2 measures irradiance in a wide spectrum, namely, the UV-visible range (320-1000 nm). It has 194 usable channels, a spectral range of 319.5-951.8 nm, and an accuracy of 6-10%. In addition, its spectral accuracy is 0.3 nm (Nedrebø, 2017; Tveiterås, 2013).

Figure 7: A Ramses 80E2 Cosine Irradiance sensor.

The TriOS Ramses cosine irradiance sensors (Figure 7) use a cosine collector made out of silica which is placed at the front of the instrument in order to diffuse light into the optical fiber behind it (Tveiterås, 2013). The output we get when we use the irradiance sensor is power per wavelength, that is,

$$\frac{\mathrm{mW}}{\mathrm{m}^2 \cdot \mathrm{nm}} \tag{16}$$

3.1.2 Inner Workings

The Ramses radiometers use an MMS-1 spectrometer made by Zeiss. In Figure 8 we can see that from the diffuser (tip of the instrument), the light travels through the optical fiber and into the spectrometer. After the light has entered the spectrometer, the light hits the holographic grid in the back, which works like a diffraction grating, separating the light into different wavelengths. The light is also reflected by this grating, and each wavelength is reflected with different angles, such that the different wavelengths hit separate diodes in the photodiode array, that is, each channel has its associated wavelength (Nedrebø, 2017; Tveiterås, 2013).

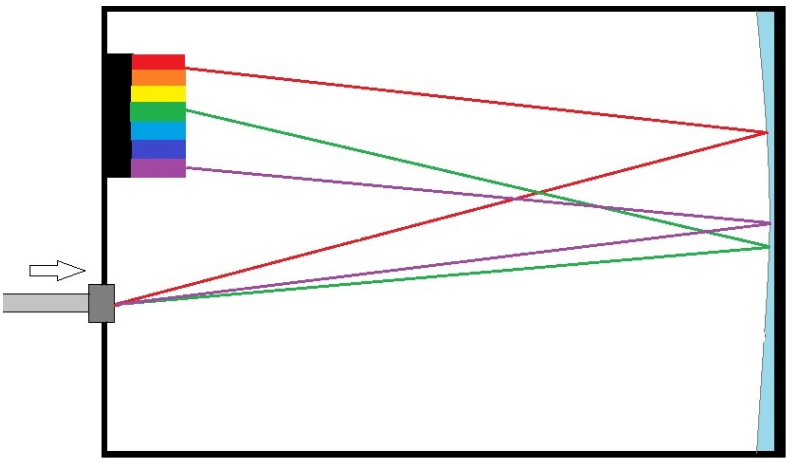

Figure 8: Inside of a spectrometer. The light enters the spectrometer through the optical fiber on the left side. It is then diffracted by the grating to the right and reflected back to the photodiodes shown with the colors red, orange, yellow, green, blue, indigo and violet.

3.1.3 Calibration

Every now and again, the irradiance sensor must be calibrated in order for the results to be accurate. One way of calibrating the sensor is to use a method of relative calibration. By using the same light source every time and keeping the sensor and light source in the same positions as in previous calibrations, the instrument can be calibrated (the light source shines close to a blackbody and has a spectrum that is constant with time).

First, the instrument and light source are put into position and aligned properly. The light bulb is mounted in a housing while the radiometer is placed in two cradles, and the distance between the objects is measured from the foot of the light bulb housing to the nose of the detector. Then, the light source is heated up (0V to 12V takes 5 minutes, and once it has reached 12V, it needs 5 minutes to become stable). When the light bulb is presumably stable, we take a few test spectra to check for stability. Once stable, we take three spectra that we will use as measurements in the relative calibration. When the calibration has been finished, the light bulb voltage is lowered from 12V to 0V over 5 minutes in order to preserve the light bulb.

From the measured spectra we can create drift factors by dividing the spectrum values for the initial reference spectrum by the spectrum values for the current spectrum. By using interpolation we can get drift factors for all times between measured spectra, and by multiplying these drift factors with the measured spectrum from the field we can obtain the relative calibrated spectrum.

The initial reference spectrum is the spectrum obtained with the first time with this set up, that is, when the devices had just arrived from the manufacturer. If we compare the calibration spectrum at some point in time to this first point in time, there should be drift in the devices. We use relative and not absolute calibration because absolute calibration requires knowledge about the exact spectral irradiance emitted by the calibration lamp at a given distance.

To make sure the calibration lamp is stable, we can compare the drift factors with different radiometers.

3.2 Microweight

The Mettler Toledo MT5 micro weight was used to measure the dry weight of the algal mass. It has a fine range and a course range of 1 μgram and 0.01 μgrams, respectively. It has a readability of 1 μgram, a weighing capacity of 5100 mg, a repeatability of 0.8 μgrams between 0 and 2 grams and a repeatability of 0.9 μgrams between 2 and 5 grams. It also has a linearity of $\pm$ 4 μgrams and a linearity of $\pm$ 2 μgrams referred to 500 mg, as well as a typical stabilization time of either 9, 12 or 16 seconds (*Operating instructions Mettler Toledo MT/UMT Balances*, -).

3.3 Thermistor

Thermistors were used to measure the temperatures in the bags. There are at least two types of thermistors; NTC and PTC thermistors. NTC stands for negative temperature coefficient, and PTC stands for positive temperature coefficient; if the temperature coefficient is negative, the resistance decreases with increasing temperature, while if the temperature coefficient is positive, the resistance increases with increasing temperature (*PTC thermistor*, -; *NTC Thermistors*, -). That is, by measuring the resistance over the thermistor, we can find the temperature.

3.4 pH meter

A pH meter is an electrical device that can be used to measure hydrogen-ion (H^+) activity in a solution. A pH meter is made up of a voltmeter attached to two electrodes; a pH-responsive electrode and an unvarying reference electrode. When we immerse the electrodes in a solution together, they act like a battery, and the pH-responsive electrode develops an electric potential or charge that is directly related to the solution's H^+ activity (*PH meter*, -).

4 Method

4.1 Data analysis without model

The overall aim of the thesis is to find the necessary conditions for optimal algae growth on land. The three types of algae we will analyze are strains of P. tricornutum (P. tricornutum is a diatom, a type of eukaryote) called FITO (Figure 9), M28 (Figure 10) and B58 (Figure 11), and these three strains were grown in separate bags on a rooftop from April 2016 to October 2016. The bags had depths of approximately 3.75 cm and were supplied carbon dioxide and nutrients needed for growth. The dry mass for each strain was recorded not more than once a day. The temperature and pH in the bags was measured automatically, and the irradiance (PAR) on the roof was recorded with a cosine irradiance spectrometer.

We analyze the data by using Matlab and we investigate several points of interest. First of all we investigate how the volume mass density (biomass) or the dry mass changes with time. There are 15 measurement series for each strain, so there is a total of 45 measurement series for the volume mass density, or biomass, since the volume of the bag is approximately constant throughout the growth periods. After each measurement series the algae culture is diluted and so the volume mass density is decreased. We also use the biomass (dry weight) to calculate the average growth rates between each point of biomass and see how it changes with time, as well as the relative growth rates. After we calculate the average growth rates and relative growth rates, we set up histograms that show the distributions of the growth rates for each of the strains.

In addition, we investigate how these growth rates depend on irradiance (PAR), temperature and pH. To do this we first calculate the average irradiance, average temperature and average pH between each biomass point. Then, we not only create scatterplots between the average growth and average irradiance, temperature and pH, but we also calculate the linear correlation coefficients. These scatterplots and linear correlations are calculated for each strain separately.

Additionally, we look at how the average temperature in each bag depends on the average irradiance, and we look at how the average growth rates and relative growth rates depend on biomass. Then, we create surface plots that show how the average growth rate depends on average irradiance and average temperature, omitting the dependence of the average growth rate on pH.

After this, we use another pair of data sets of irradiance obtained with a cosine irradiance spectrometer, combined with data on absorption cross sections for FITO and M28, to calculate the average irradiance between the biomass points both in the form of PUR and PAR for each strain separately. Then, these average PUR and average PAR values are plotted together with the average growth rates for FITO and M28, and the linear correlations between these variables are calculated as well.

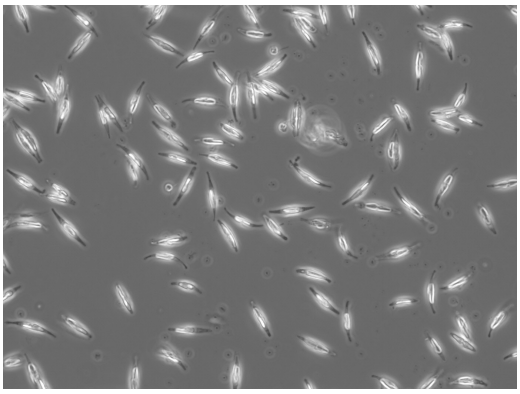

Figure 9: Picture of FITO, courtesy of Pia Steinrücken at UiB (University of Bergen).

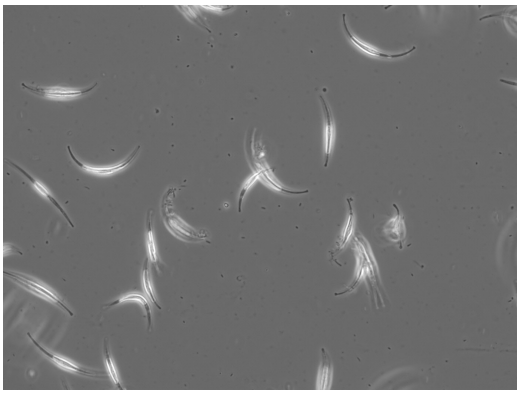

Figure 10: Picture of M28, courtesy of Pia Steinrücken at UiB (University of Bergen).

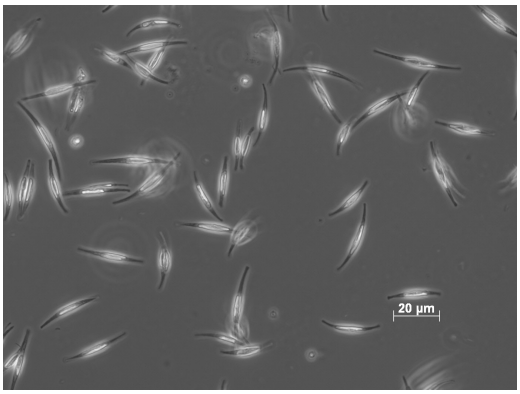

Figure 11: Picture of B58, courtesy of Pia Steinrücken at UiB (University of Bergen).

4.2 Data analysis with model

In the theory section, we found an equation describing the time derivative of the areal mass density as a function of several parameters. This equation contains the integral of an exponential function of another exponential function, which makes it quite difficult if not impossible to solve analytically. What we can do, however, is to solve it numerically. Using a trapezoid integral we can integrate down the water column for each point in time to find the total change in areal mass density for each point in time. Once we have this total change for the first point in time, we can calculate the areal mass density for the second point in time with a numerical method. Using this second areal mass density we can calculate the second change in areal mass density and use this to calculate the areal mass density for the third point in time, et cetera.

First, we make intervals δt and δz and then use these to describe what values t and z are going to take when we solve the equation numerically. Then we find the starting biomass point for the measurement series we want to investigate. After this is done we find a suitable value for E_0 from our previous data analysis, and set the depth of the water column equal to the total thickness of the bag and its contents (between 3.5 and 4 cm, so let's say 3.75 cm for compromise). The values of P_m, α, k and ξ that give us the best model fit are not so easy to find. What we can do, however, is to create a cost function that Matlab has to minimize via another Matlab function called fminsearch. For each measurement series the cost function is equal to the sum of the squares of the distances between the model curve and the data points for biomass. By using fminsearch on this cost function, Matlab finds the least square sum for us as well as the parameter values P_m, α, k and ξ providing this least square sum. Figure 12 shows a model curve, while Figure 13 shows a model curve obtained by using the least square sum with fminsearch on the first measurement series for FITO.

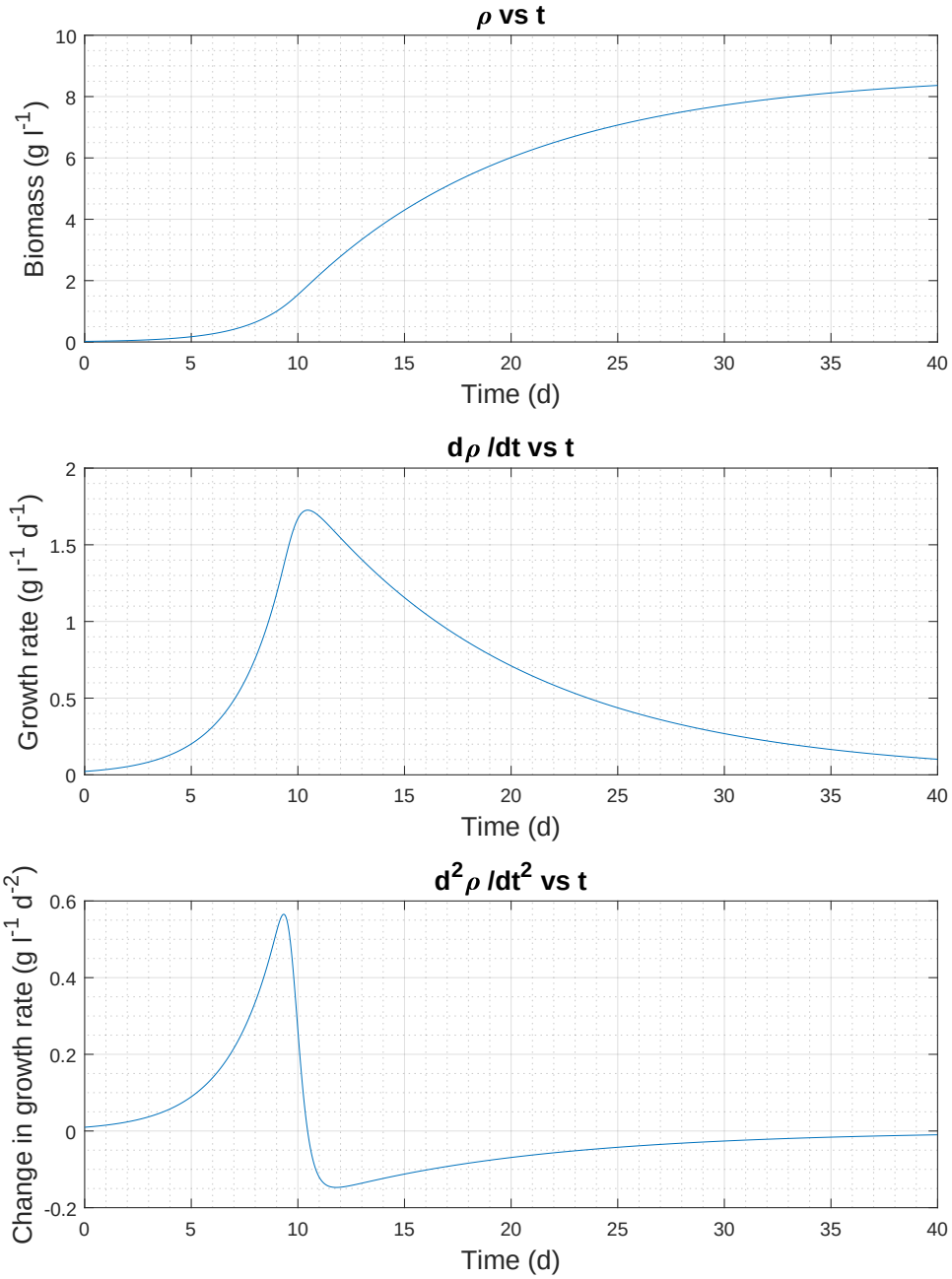

Figure 12: A model for algae growth. Upper graph of figure shows ρ (volume mass density) versus time, middle graph shows the time derivative of ρ, while bottom graph shows the double time derivative of ρ.

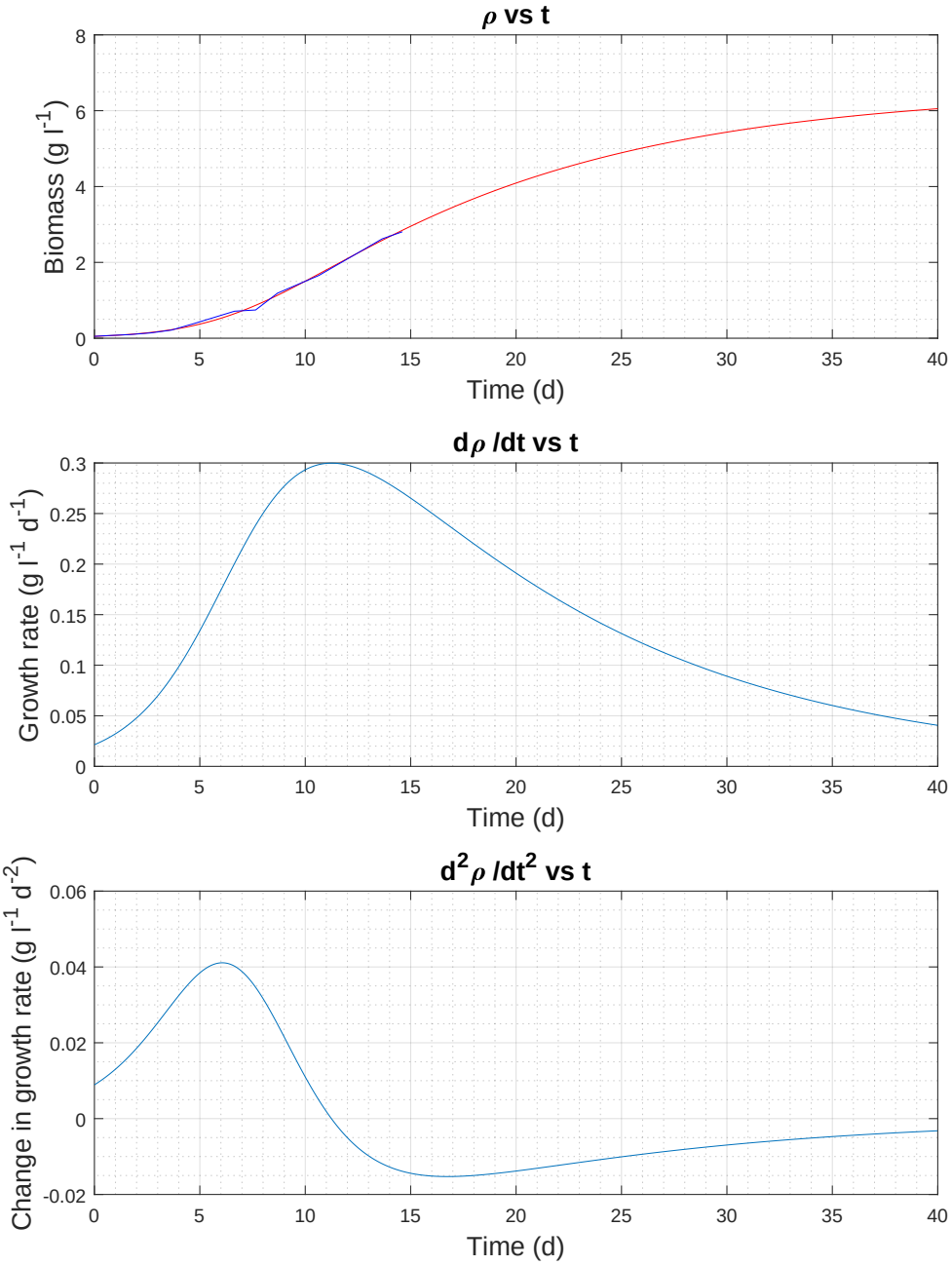

Figure 13: Model for algae growth versus data points. In top part of figure, red curve is model curve while blue is data point curve. Blue curves in middle and lower parts of figure are based on model. Sum of least squares used as mathematical criterion for goodness of fit. Figure is based on measurement series one for FITO.

After we find decent parameter values for a measurement series we show graphically how the model curves respond to changes in the parameter values so as to better explain what each parameter contributes to the model curve. In addition, we create a surface plot showing how the maximum growth depends on a combination of parameter values forP_m and α for a specific measurement series, which then can be used to not only find good growth conditions, but can also be used to find parameter combinations for that measurement series which give a specific growth rate. To find out whether or not the sampling times play a big role in the results, we find the relative differences between the growth rates some hours before and after the maximum growth rate and the maximum growth rate itself.

We go through all 45 measurement series and find the least square sum and the corresponding parameter values P_m, α, k and ξ. We then not only plot these parameter values against the average irradiance, average temperature and average pH of the corresponding measurement series, but we also calculate the linear correlation coefficients. We also plot the parameter values P_m, α, k and ξ against each other and calculate these linear correlation coefficients.

In addition, we pick a measurement series, find the parameter values that give the best fit, and then vary each parameter around the corresponding best fit value one at a time. For each parameter value we pick out the maximum growth, and we then plot the maximum growth against the corresponding parameter value to show how the maximum growth of a measurement series depends on the parameters. If we are lucky, we also find some maxima for these plots. We also look at a model curve for a small depth as well as the maximum change in mass per area for depths between 1 cm and 1 m.

Then, we use the 45 measurement series in the following way: Going through each measurement series, we insert the parameter values that gave us the least square sum for the measurement series into the model. By then varying one of the following parameter at a time by inserting for example 50 different values for it, and for each of those 50 different values we get one maximum growth rate, we find the maximum of these 50 different maximum growth rate values as well as the corresponding parameter value. By doing this for P_m and k for each measurement series, we find 45 maxima and 45 sets of parameter values. We are then able to find the average value for each of the three parameters, the standard deviations, and construct histograms that show the distribution for each of these three parameter values. Lastly, we find the ultimate optimal growth conditions.

5 Results and discussion

5.1 Results without model

5.1.1 Biomass over time

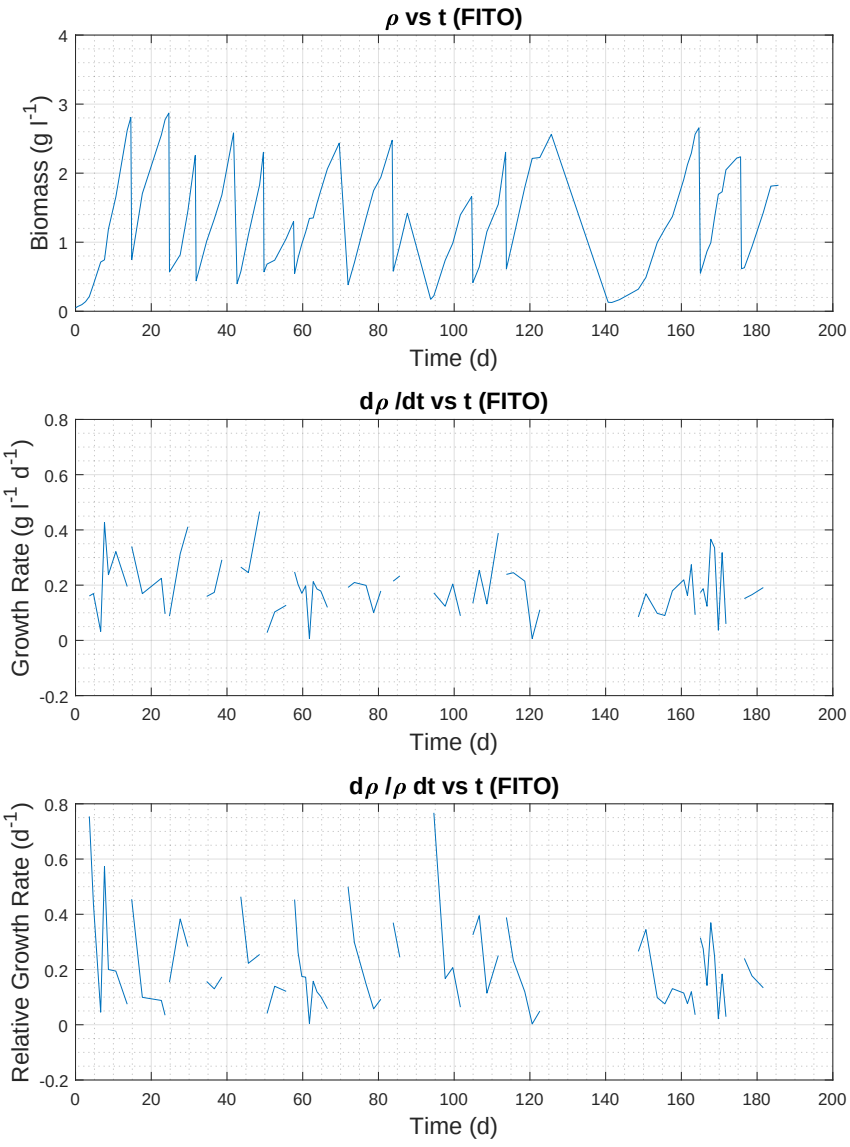

Figure 14: Graphs for biomass (upper), growth rate (middle) and relative growth rate (lower) versus time for the strain FITO.

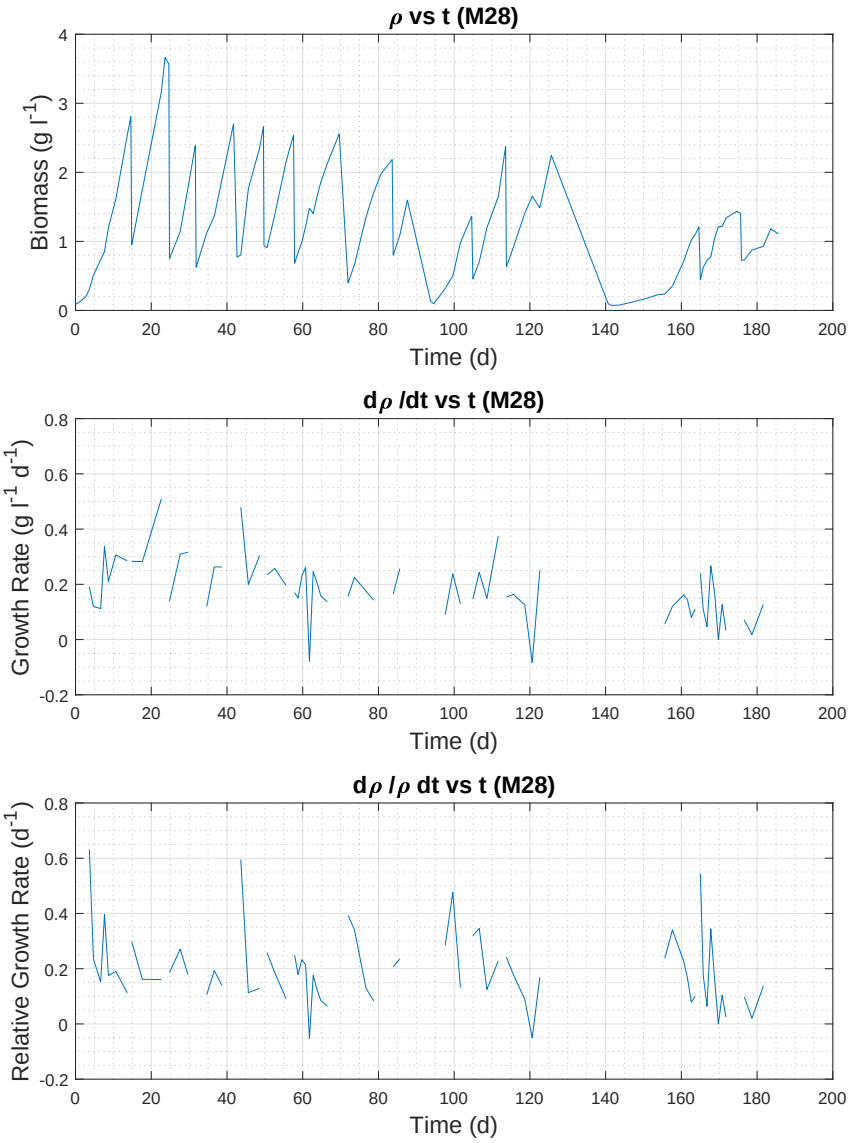

Figure 15: Graphs for biomass (upper), growth rate (middle) and relative growth rate (lower) versus time for the strain M28.

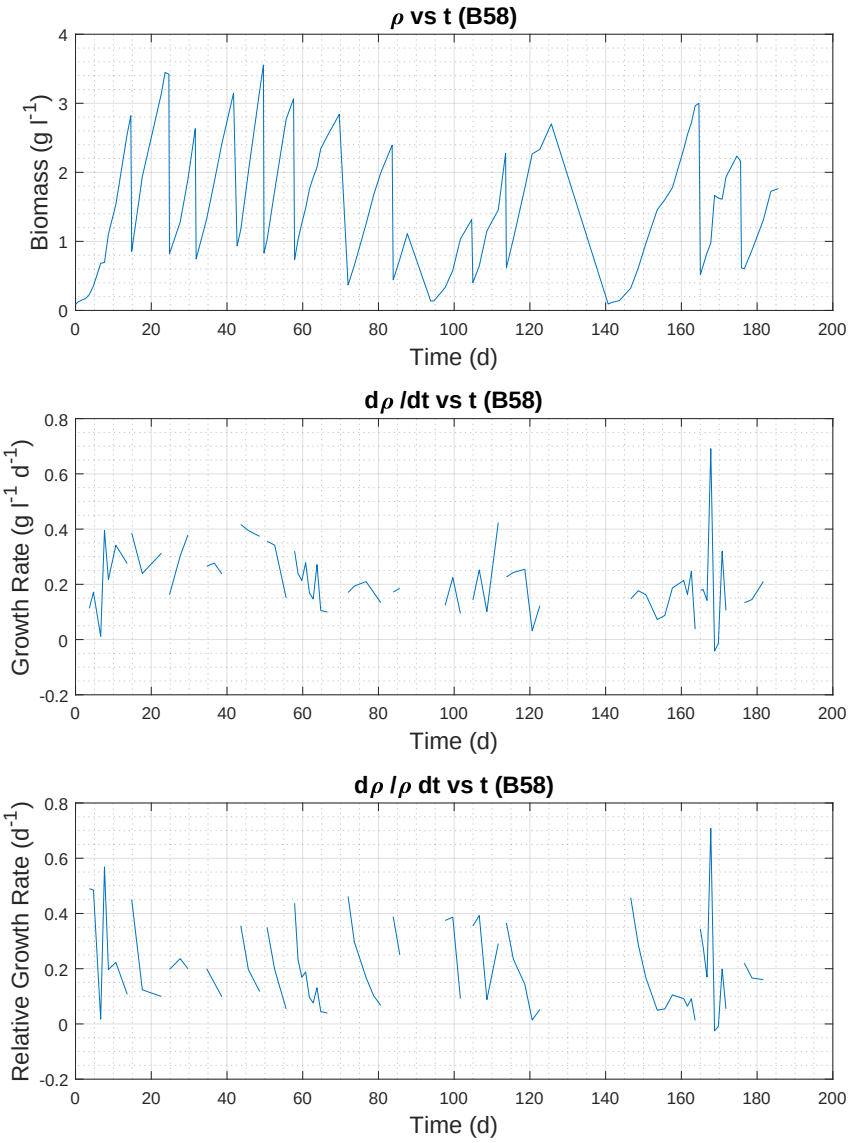

Figure 16: Graphs for biomass (upper), growth rate (middle) and relative growth rate (lower) versus time for the strain B58.

Figures 14, 15 and 16 show how the biomass or volume mass density, growth rate and relative growth rate for each of the three strains FITO, M28 and B58 depend on time. Some of the growth rates and relative growth rates have been omitted, for example the growth rate between the measurement series (since the negative growth rate there is caused by dilution), in addition to the growth rates for low and high biomasses, making the remaining growth rates be the growth rates for the somewhat linear phases of growth. As we can see from the biomass versus time plots, the growth seems to have three phases: an initial exponential phase where the biomass is small, an intermediate linear phase where the biomass is usually somewhere between 1 and 3 grams per liter, and a flattening phase where the growth starts to approach zero. Even though what might look like a flattening phase might not be a flattening phase, it is a well-known phenomenon in biological systems that once the biomass reaches a certain level, the growth goes to zero either because of a lack of nutrients or some other reason.

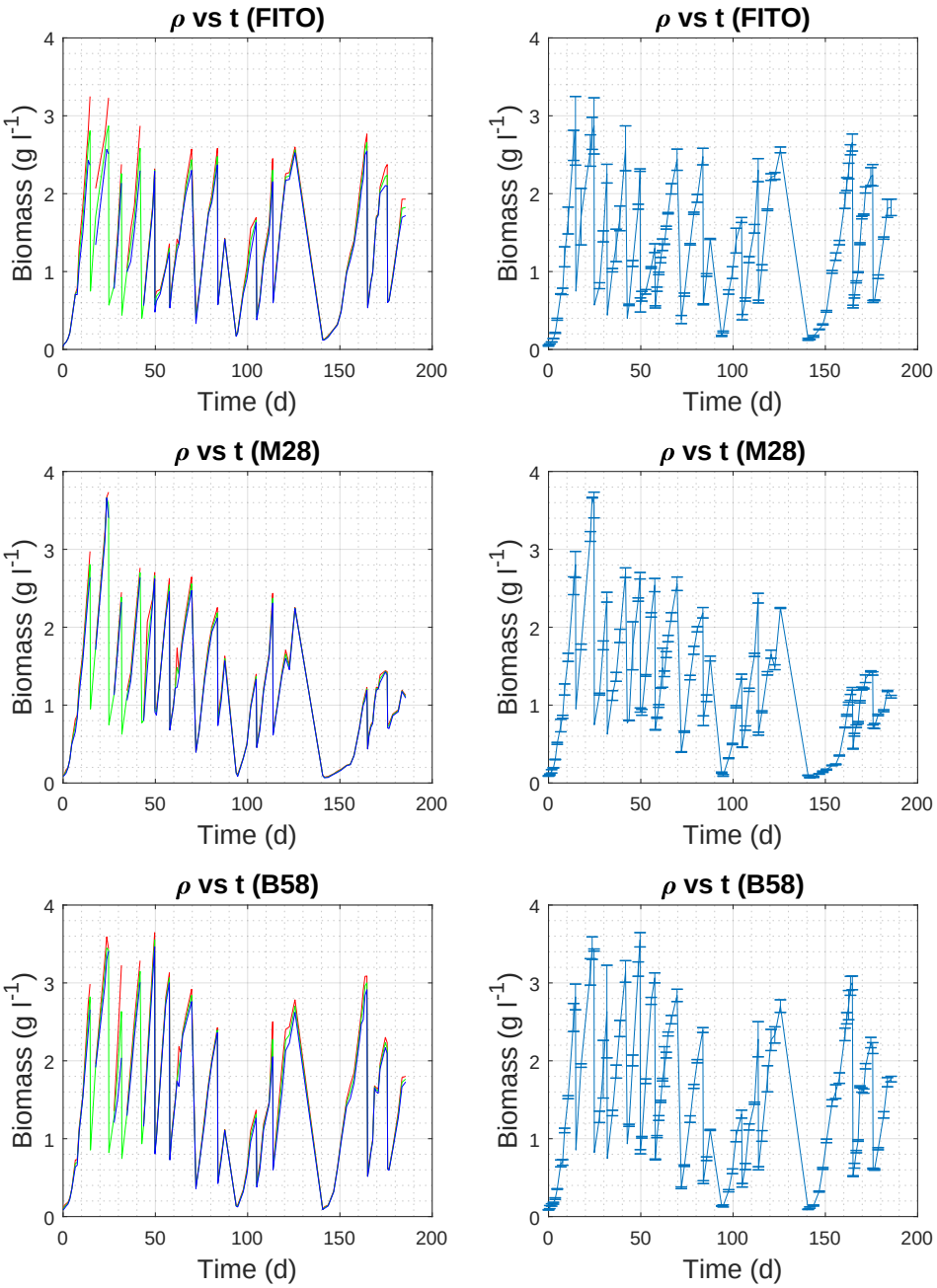

Figure 17: Graphs showing biomass (standard deviations included in two ways) versus time for the strains FITO, M28 and B58. For the left part of the figure, red graph is average plus standard deviation, green graph is average, while blue graph is average minus standard deviation.

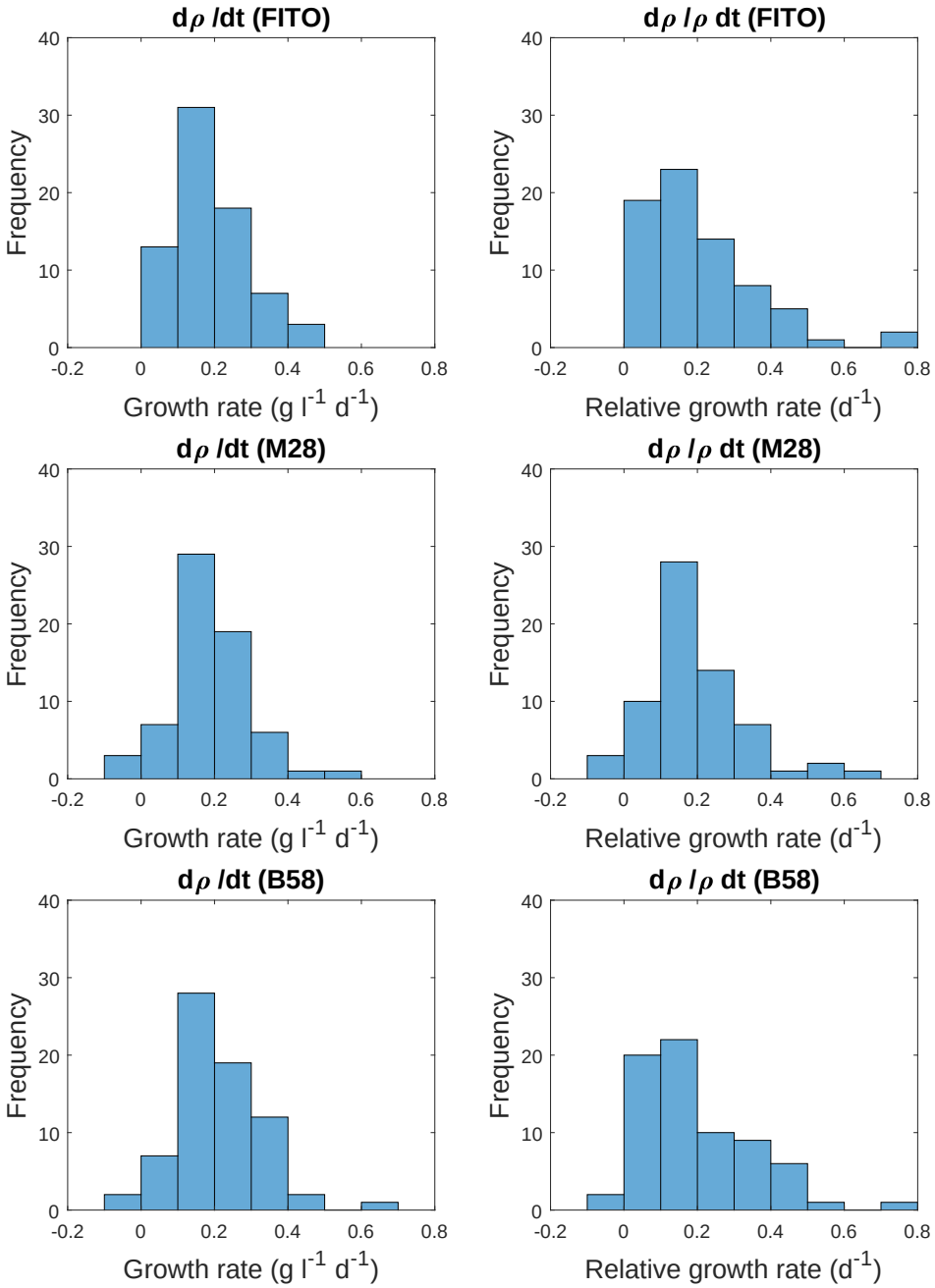

Figure 18: Histograms showing the distributions of growth rates (left side) and relative growth rates (right side) for the strains FITO (upper), M28 (middle) and B58 (lower).

In Figure 17 we see curves of biomass (with standard deviations) versus time for the three strains of algae. In Figure 18, we see that the distributions of growth rates for all three strains og algae has a somewhat bell-shaped distribution. If the distribution is bell-shaped, this means that the mean growth rates are in the centers of the growth rate distributions, while there are equally many growth rates a certain number above and below the mean. The distribution of relative growth rates for M28 seems somewhat bell-shaped, while the distributions of relative growth rates for FITO and B58 not so much.

Table 1: Standard deviation of the growth rate distribution divided by the mean of the growth rate distribution for the three strains FITO, M28 and B58.

Algae	$\mathrm{d}\rho/\mathrm{dt}$	$\mathrm{d}\rho/\rho\ \mathrm{dt}$
FITO	0.51	0.77
M28	0.58	0.68
B58	0.56	0.74

Table 1 shows the ratio of the standard deviation of the growth rate distribution divided by the mean of the growth rate distribution. This number tells us what the relationship between the standard deviation and the mean of the distribution is, and is a way of quantifying the spread of the distribution.

5.1.2 Biomass, irradiance, temperature and pH

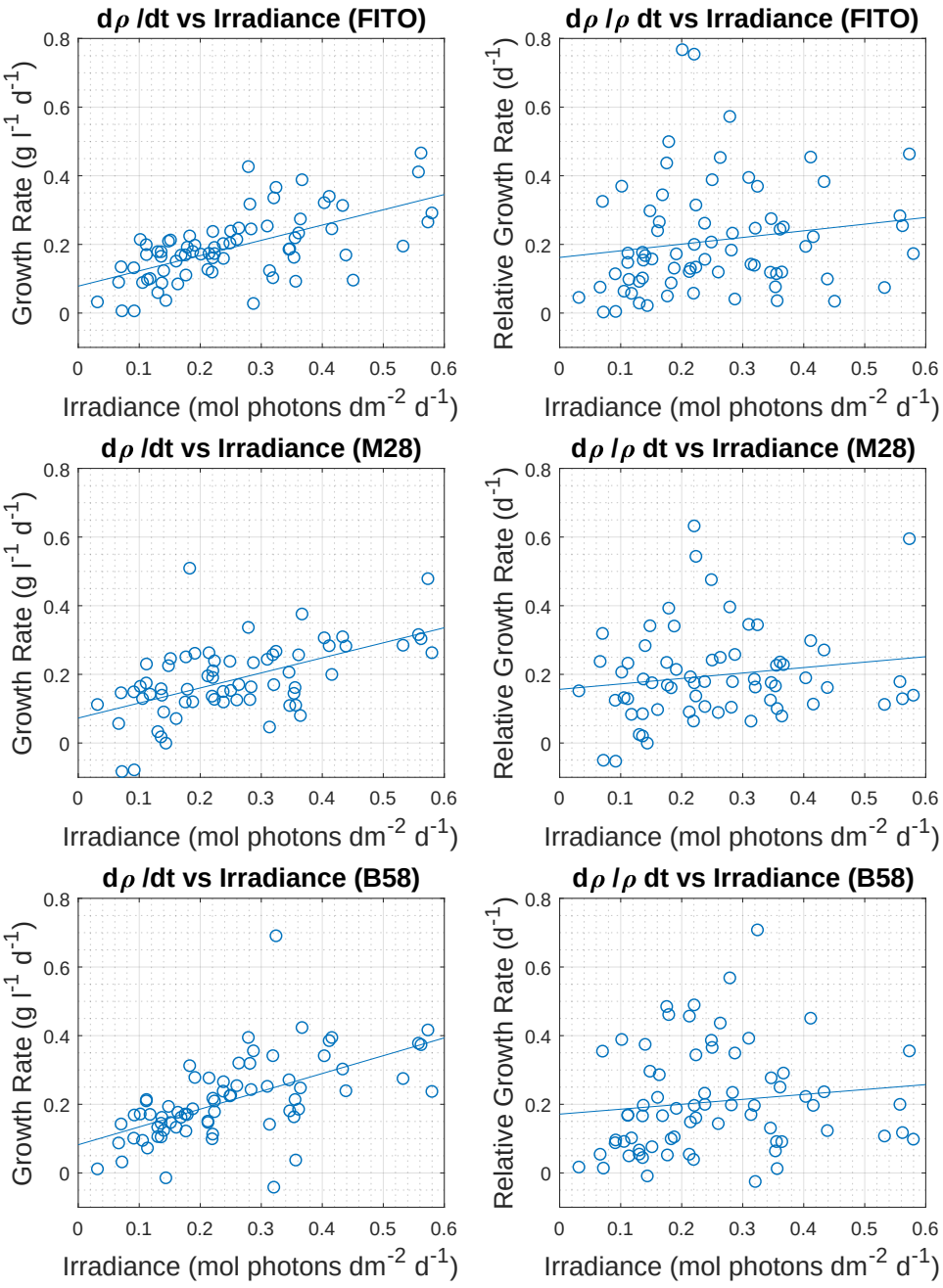

Figure 19: Scatterplots of growth rates (left side) and relative growth rates (right side) versus average irradiance (PAR) for the strains FITO (upper), M28 (middle) and B58 (lower). Least square lines are included.

Figure 19 shows scatterplots of growth rates and relative growth rates for the strains FITO, M28 and B58 versus the average irradiance (PAR) calculated between every pair of biomass points. The biomass is recorded not more than once a day, but once it is recorded, it is recorded for all three strains, while the irradiance is recorded approximately two times every minute. By studying these scatterplots, we can see that there is a positive linear correlation between the growth rates and average irradiance, and a weaker yet positive correlation between the relative growth rates and the average irradiance. By studying the scatterplots of growth rates versus average irradiance further, and looking at the theory, there is reason to believe that the relationship between the growth rates and the average irradiance might not be entirely linear, but rather represent a P vs. E curve, that is, photosynthetic production versus irradiance. According to the theory on P vs. E curves, once the irradiance gets high enough, the growth will flatten out. If the irradiance gets even higher, photoinhibition occurs, wherein the photosynthetic machinery of the algae cells, or rather, the reaction centers, become damaged because of oxidation. It is difficult, however, to see the effects of photoinhibition from these graphs. Perhaps more data points are needed, and maybe even higher irradiances are needed to spot photoinhibition.

Table 2: Linear correlation coefficients between growth rates and relative growth rates and average irradiance (PAR).

Algae	$\mathrm{d}\rho/\mathrm{dt}$ vs Irradiance	$\mathrm{d}\rho/\rho\mathrm{dt}$ vs Irradiance
FITO	0.61	0.16
M28	0.55	0.16
B58	0.58	0.12

Table 2 shows the linear correlation coefficients between the growth rates and average irradiances as well as the linear correlation coefficients between the relative growth rates and average irradiances for the strains FITO, M28 and B58. What we can see is that the correlations for growth rates are much stronger than the correlations for relative growth rates, as can also be seen from Figure 19. However, there is not a lot of variation between these linear correlations for each strain of algae.

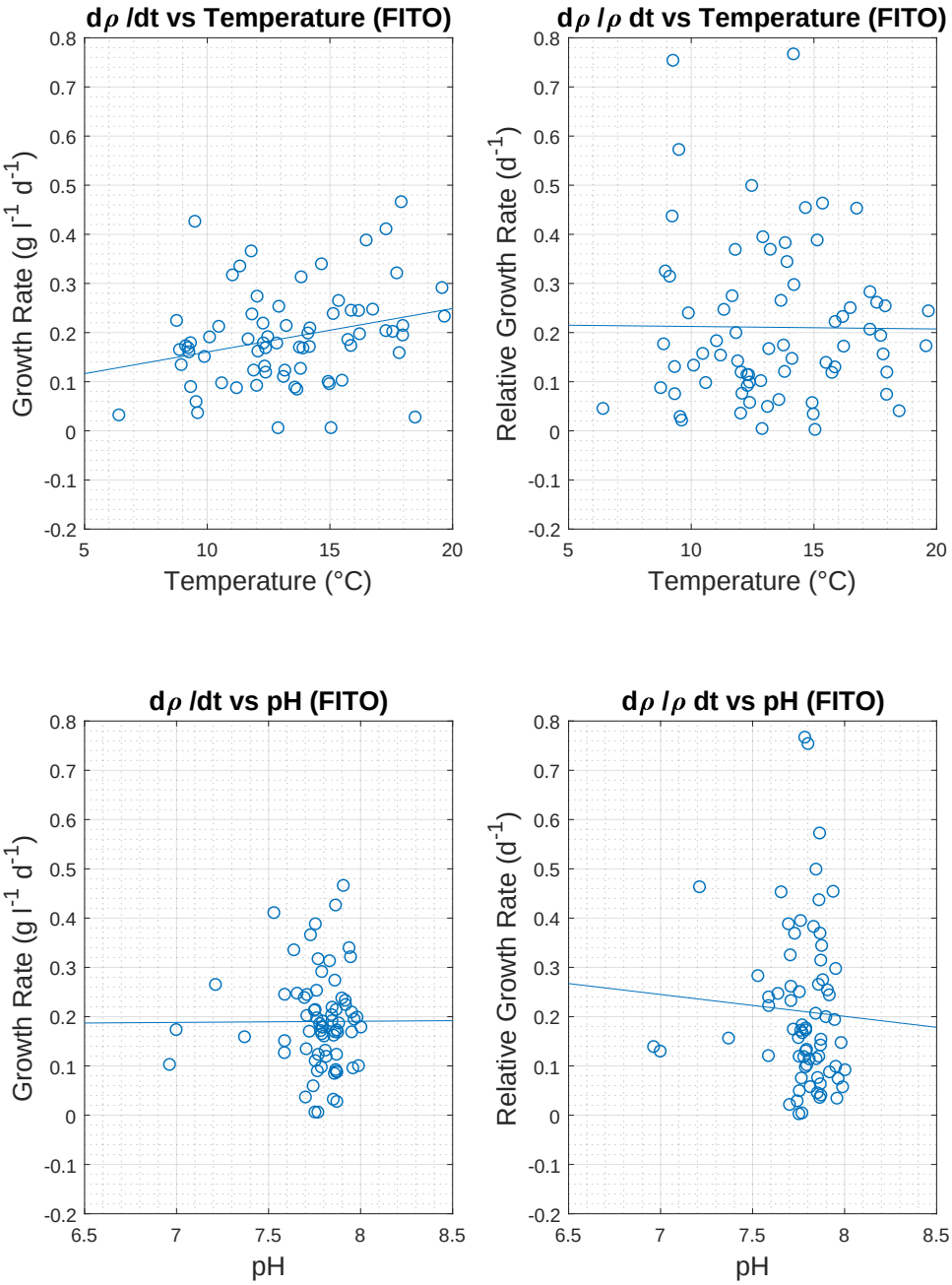

Figure 20: Growth rates (left side) and relative growth rates (right side) versus average temperature (top) and average pH (bottom) for the strain FITO.

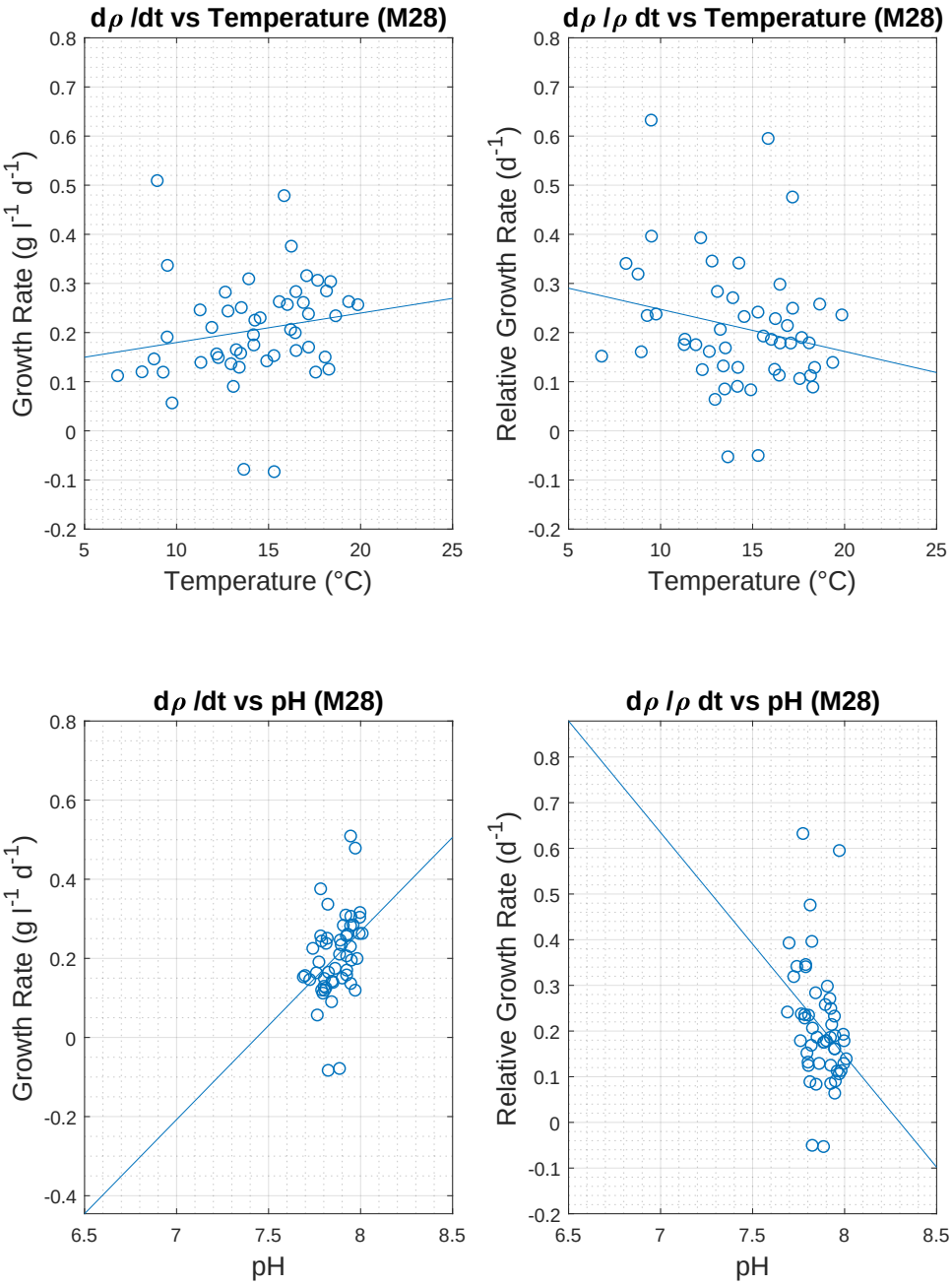

Figure 21: Growth rates (left side) and relative growth rates (right side) versus average temperature (top) and average pH (bottom) for the strain M28.

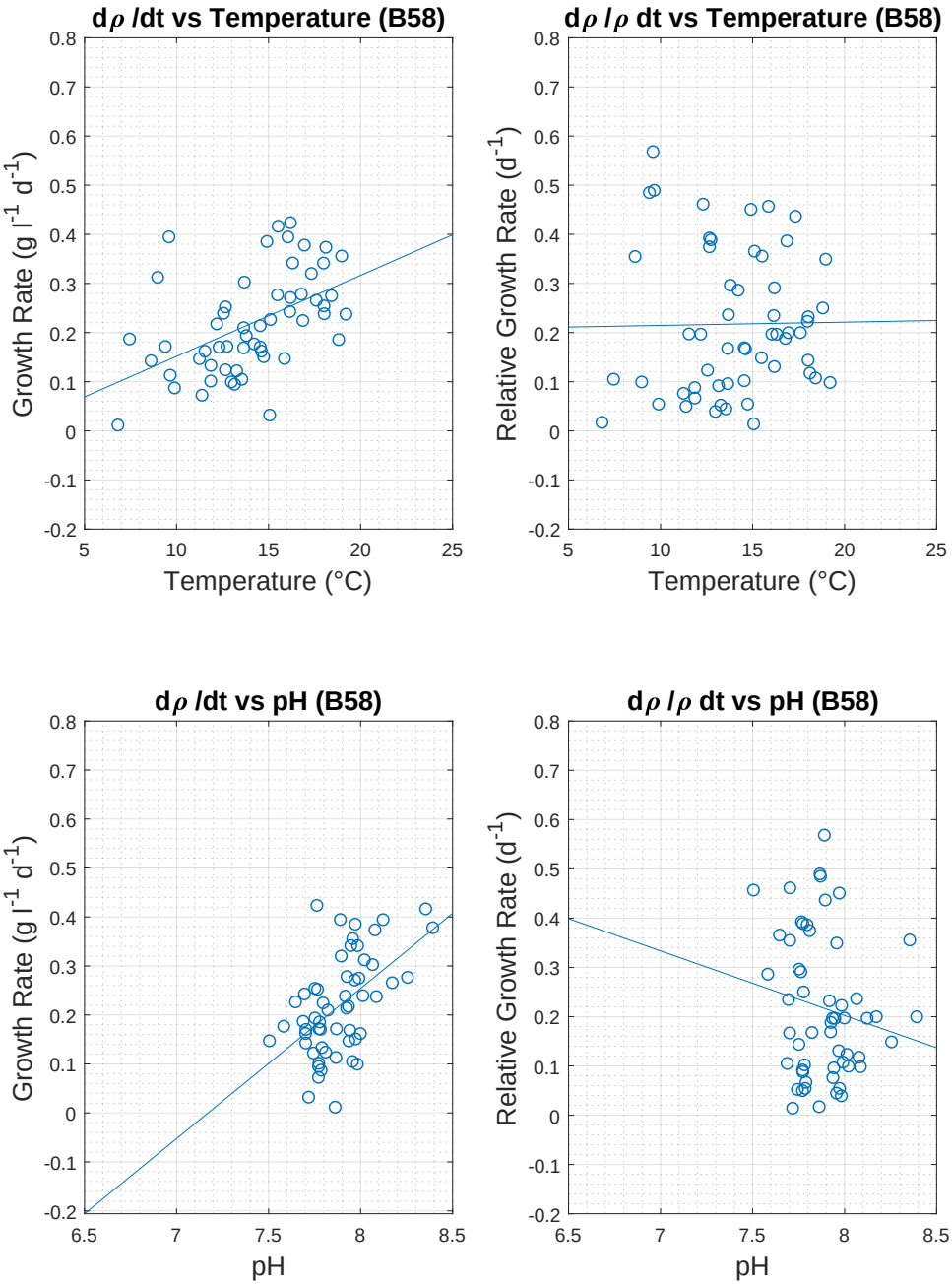

Figure 22: Growth rates (left side) and relative growth rates (right side) versus average temperature (top) and average pH (bottom) for the strain B58.

Table 3: Linear correlation coefficients between growth rates, relative growth rates and average temperature for the strains FITO, M28 and B58.

Algae	$d\rho/dt$ vs Temperature	$d\rho/\rho dt$ vs Temperature
FITO	0.27	-0.0095
M28	0.18	-0.21
B58	0.50	0.014

Table 3 shows the linear correlation coefficients between growth rates and average temperatures as well as the linear correlation coefficients between the relative growth rates and average temperatures for the strains FITO, M28 and B58. Both by looking at figures 20, 21 and 22 and by looking at the correlation coefficients we can see that the linear correlations between the growth rates and average temperatures are positive, but the correlation for B58 is definitely the stronger one. The same correlations for FITO and M28 are much weaker, and by looking at the clusters in the figures for FITO (Figure 20) and M28 (Figure 22) it might seem like there really is not any linear correlation at all.

When looking again at figures 20, 21 and 22 and by looking at the correlation coefficients we can see that the linear correlation between the relative growth rates and the average temperatures are all small, and some being negative. The strongest one is the one for M28, which is approximately -0.21.

Table 4: Linear correlation coefficients between growth rates, relative growth rates and average pH for the strains FITO, M28 and B58.

Algae	$d\rho/dt$ vs pH	$d\rho/\rho dt$ vs pH
FITO	0.0046	-0.052
M28	0.38	-0.32
B58	0.53	-0.16

Table 4 shows the linear correlation coefficients between growth rates and average pHs as well as the linear correlation coefficients between the relative growth rates and average pHs for the strains FITO, M28 and B58. For the limited pH range we have, the results are very mixed. The biggest correlation between the growth rates and average pHs is approximately 0.53 (B58), while the smallest one is below 0.01 (FITO)! In all these cases of correlations between growth rates and relative growth rates and average pH, the horizontal cluster tendency seems to be quite strong.

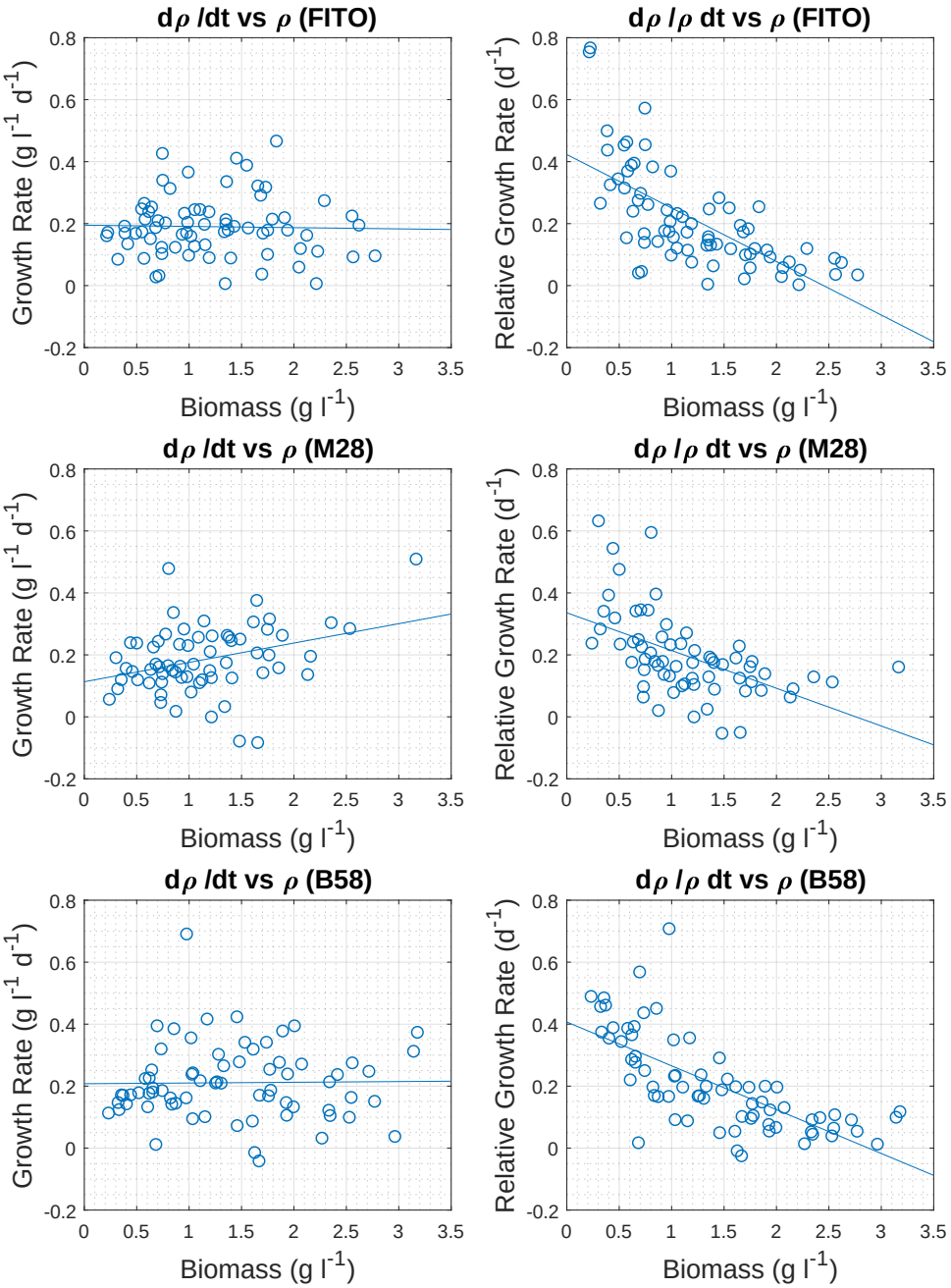

Figure 23: Scatterplots of growth rates (left side) and relative growth rates (right side) versus biomass for the strains FITO (upper), M28 (middle) and B58 (lower).

Table 5: Correlations between growth rate and relative growth rate and biomass.

Algae	dρ/dt vs ρ	dρ/ρdt vs ρ
FITO	-0.0258	-0.68
M28	0.33	-0.52
B58	0.015	-0.71

Figure 23 shows scatterplots of growth rates and average growth rates for FITO, M28 and B58 versus biomass, and Table 5 shows the linear correlation coefficients between growth rates and biomass, as well as the correlations between relative growth rates and biomass for FITO, M28 and B58. For the growth rates, the correlation seems to be either almost zero or positive but weak. By looking at the figure, we can see that the scatterplots of growth rates versus biomass are more or less clustered horizontally in each case. Looking at the relative growth rates, the correlation between the relative growth rates and biomass seem to be consistently negative. Something interesting to note is that the scatterplots for relative growth rates versus biomass seem to be organized in such a way that a curve with the function $y = \frac{c}{x}$, where c is a constant, would fit the plot quite well. This would not really be surprising considering the growth rate scatterplots have horizontal lines, i.e. the growth rate is almost constant with biomass (c is the growth rate and x is the biomass).

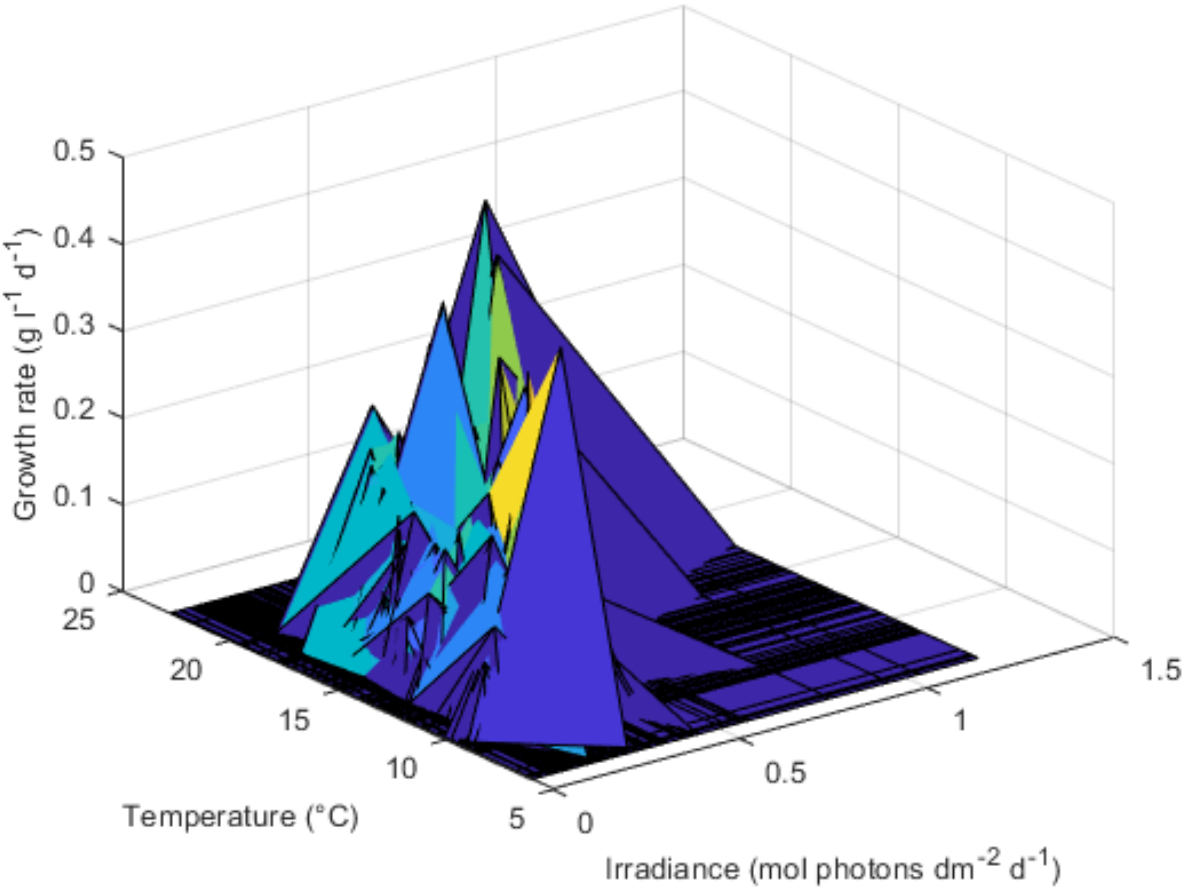

Figure 24: Surface plot of growth rates versus average temperature and irradiance (PAR) for FITO.

Figure 24 shows a surface plot of growth rates versus average temperature and average irradiance (PAR) for the strain FITO. Although it's difficult to extract information from a surface plot like this without being able to rotate it, we can locate one area where the growth is pretty decent. If we have an average temperature of approximately 18 degrees Celsius and an average irradiance of approximately 0.8 mol photons per square decimeter per day, we have values for average temperature and irradiance that give us some of the highest peaks in the surface plot.

For FITO, regardless of whether or not the average temperature is high or low within the range of average temperatures, the growth can be large given that the average irradiance has a high enough value. The average irradiance needed seems to be somewhat proportional to the average temperature, that is, if the average temperature is low, a low average irradiance will give a high growth rate. The primary factor affecting growth seems to be the average irradiance, and so as long as the average temperature is within a certain range, the average irradiance is the deciding factor for growth.

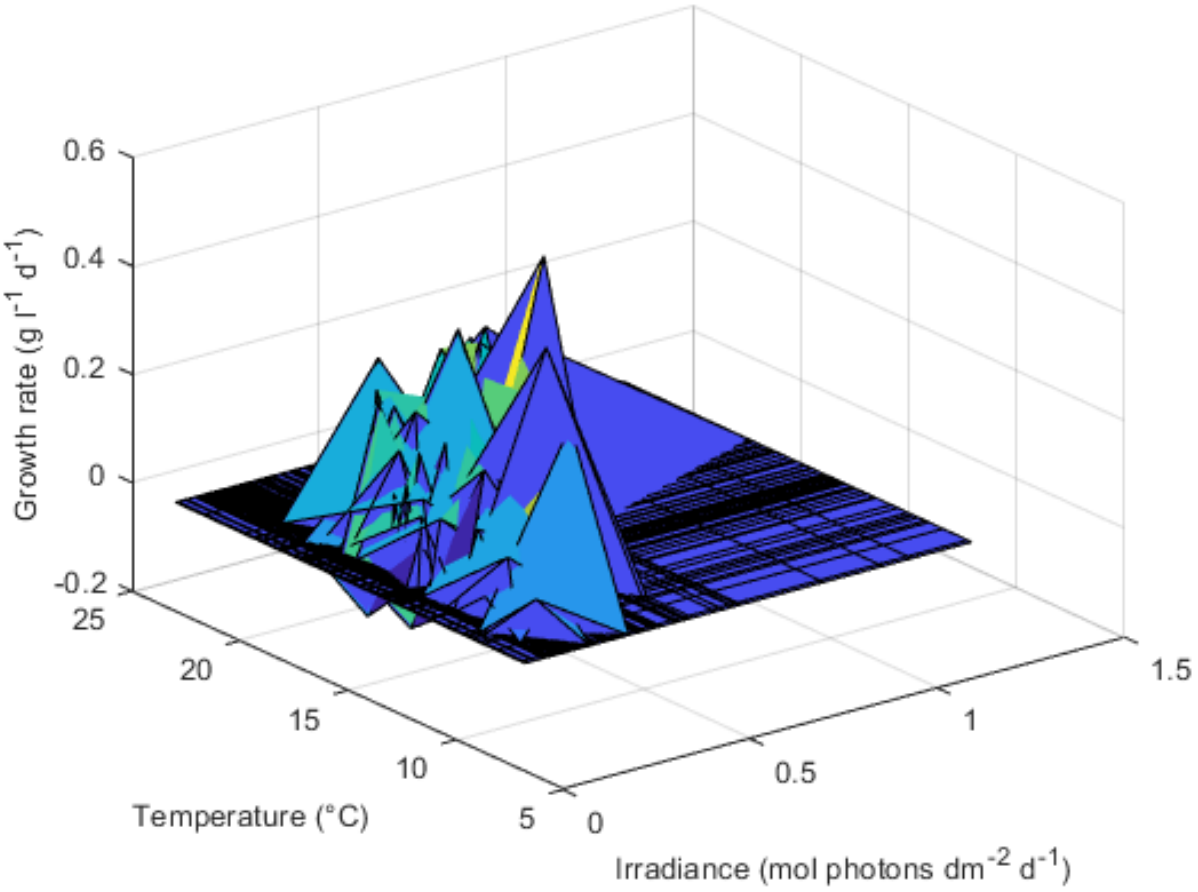

Figure 25: Surface plot of growth rates versus average temperature and irradiance (PAR) for M28.

Figure 25 shows a surface plot of growth rates versus average temperature and average irradiance (PAR) for the strain M28. Although it's difficult to extract information from a surface plot like this without being able to rotate it, we can locate one area where the growth is pretty decent. If we have an average temperature of approximately 20 degrees Celsius and an average irradiance of approximately 0.6 or 0.7 mol photons per square decimeter per day, we have values for average temperature and irradiance that give us some of the highest peaks in the surface plot.

For M28 the result seems to be somewhat the same as the result for FITO; regardless of whether or not the average temperature is high or low within the range of average temperatures, the growth can be large given that the average irradiance has a high enough value. The average irradiance needed seems to be somewhat proportional to the average temperature here as well. The primary factor seems to be the average irradiance, and so as long as the average temperature is within a certain range, the average irradiance is the deciding factor for growth.

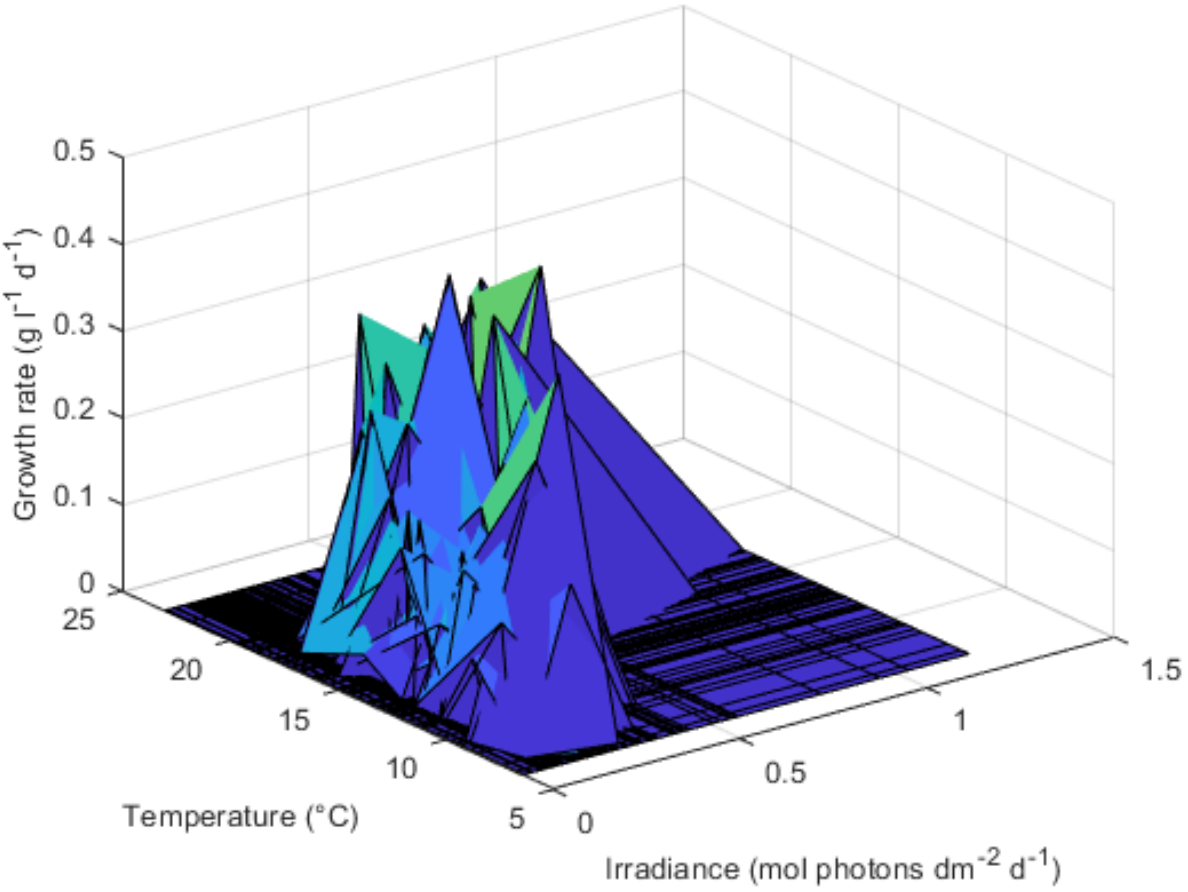

Figure 26: Surface plot of growth rates versus average temperature and irradiance (PAR) for B58.

Figure 26 shows a surface plot of growth rates versus average temperature and average irradiance (PAR) for the strain B58. Although it's difficult to extract information from a surface plot like this without being able to rotate it, we can locate one area where the growth is pretty decent. If we have an average temperature of approximately 15 degrees Celsius and an average irradiance of approximately 0.4 or 0.5 mol photons per square decimeter per day, we have values for average temperature and irradiance that give us some of the highest peaks in the surface plot.

For B58 the result seems to be that in order for growth to be the most efficient, the average irradiance needs to be within a certain interval. Too low irradiances will not give very high growth, but the irradiance does not have to be too high. Within a certain average temperature range and a certain average irradiance range the growth seems to be almost independent of both average temperature and irradiance.

5.1.3 Temperature versus irradiance

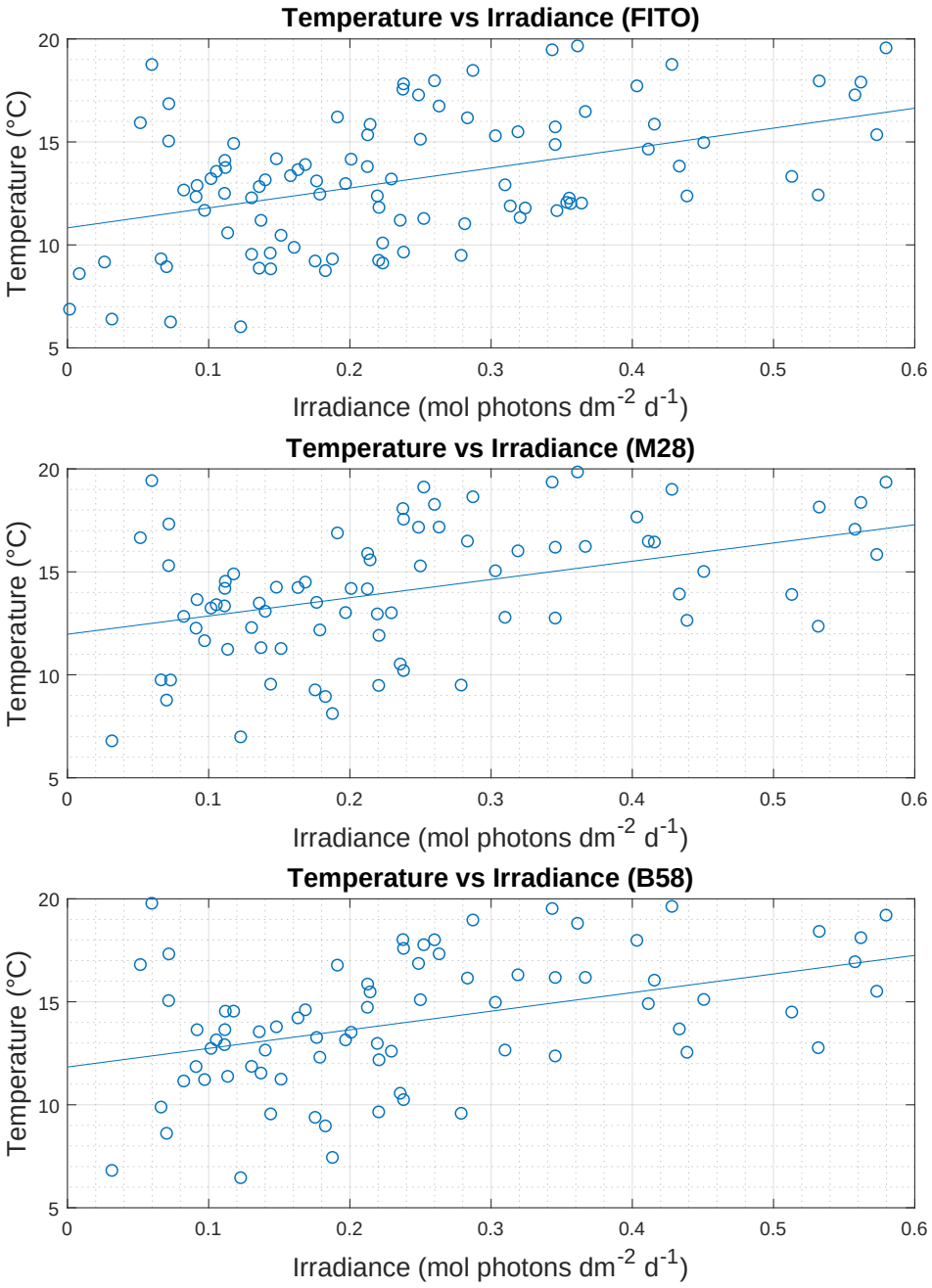

Figure 27: Scatterplots of average temperatures versus average irradiance (PAR) for FITO (top), M28 (middle), bottom (B58).

Table 6: Linear correlation coefficients between average irradiance (PAR) and average temperature for FITO, M28 and B58.

Algae	Temperature vs Irradiance
FITO	0.57
M28	0.55
B58	0.56

In Figure 27, we can see a positive linear correlation between the average temperature and the average irradiance for all three strains of algae. We would expect the temperature to depend on the irradiance given that absorption of radiation is able to heat an object.

In Table 6 we can see that the linear correlation coefficients for each of the strains is quite similar to one another, the smallest being approximately 0.55 for M28 and the biggest being approximately 0.57 for FITO.

Since there is a decently strong link between the average temperature and the average irradiance, and the link is almost the same across the strains, then this means that if there is a certain optimal range of temperature and irradiance values for growth it is possible for a high average irradiance to decrease the growth without photoinhibition occurring. If a high average irradiance that does not cause photoinhibition causes an average temperature that is too high, this is most likely not optimal for the growth, and if the average irradiance is very low, this causes an average temperature that might also be too low. That is, there does indeed exist optimal values for the average irradiance and the average temperature.

5.1.4 PAR and PUR

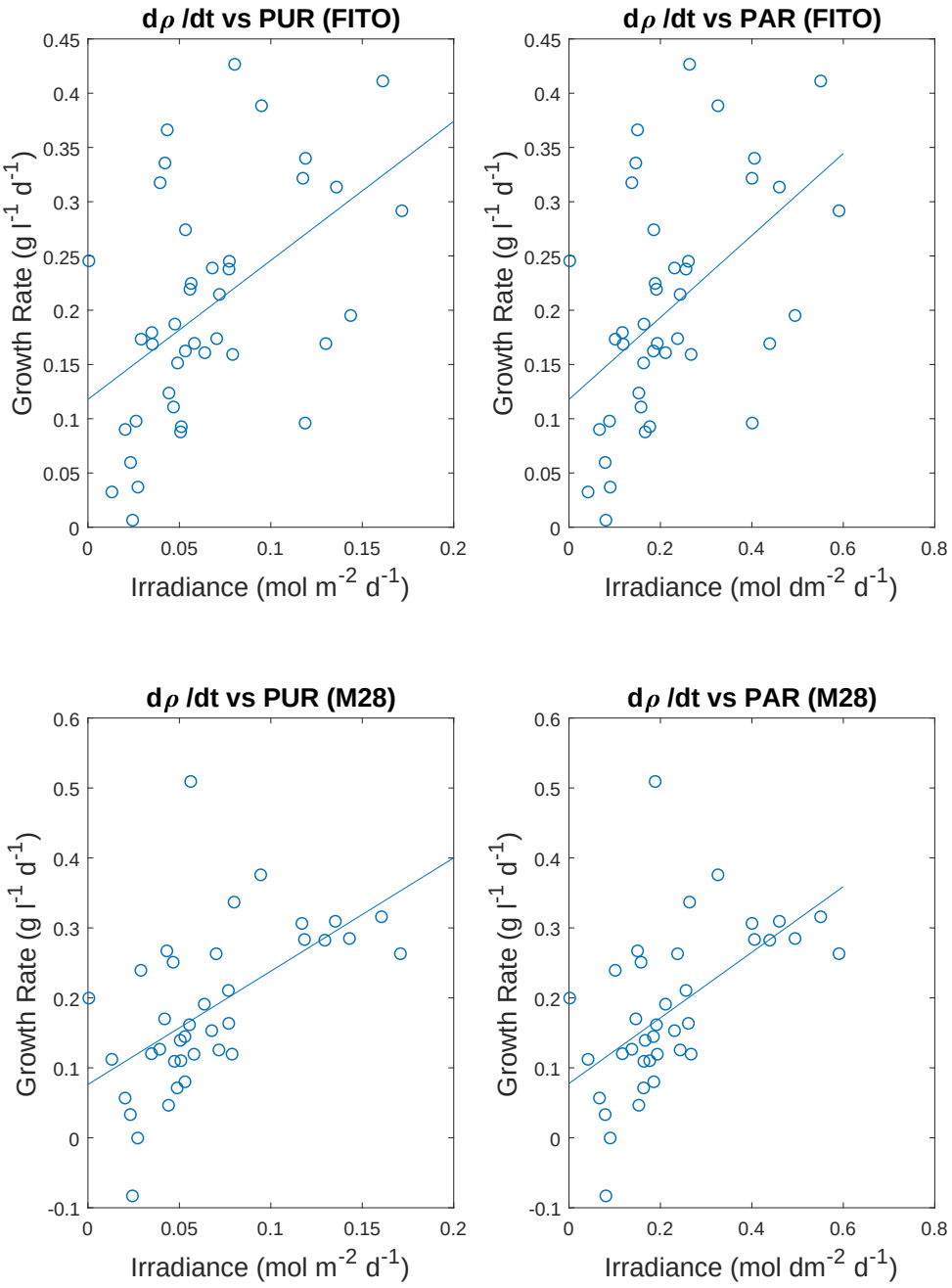

Figure 28: Growth rates versus PUR (left side) and PAR (right side) for the strains FITO (top) and M28 (bottom).

Figure 28 shows scatterplots between growth rates and average irradiances both in the form of PAR and PUR for two strains of algae, namely FITO and M28. Interestingly, the difference in the growth rate's dependency on PUR and PAR seems to be smaller than the difference in the growth rate's dependency on the particular strain. By comparing PUR, FITO with PUR, M28, or for that matter PAR, FITO with PAR, M28, we can see that there is quite the difference in these scatterplots as compared with comparing PUR, FITO with PAR, FITO or PUR, M28 with PAR, M28. The correlation seems to be stronger for M28 than for FITO in either case, however.

It is difficult to detect anything other than linear patterns in the PUR-PAR-scatterplots for FITO, but for M28 the growth rate seems to stagnate at higher irradiance levels. The scatterplots might completely change with more data points, however it might also be the case that a P vs. E curve would fit the PUR-PAR-scatterplots for M28 well, seeing as these scatterplots seem to have an initial linear phase and then a flat phase.

Table 7: Linear correlation coefficients between growth rates and PAR and PUR for FITO and M28.

Algae	$\mathrm{d}\rho/\mathrm{dt}$ vs PUR	$\mathrm{d}\rho/\rho\mathrm{dt}$ vs PAR
FITO	0.50	0.50
M28	0.57	0.57

Table 7 shows the correlation coefficients between the growth rates for FITO and M28 and the average irradiance either in the form of PUR or PAR. As we can see, there is a difference of approximately 0.07 between FITO and M28, but between PUR and PAR for the same strain the correlation coefficients are nearly unchanged. This means that whether you use PUR or PAR as a measure of irradiance, you can still predict the growth rate with almost the same accuracy.

5.2 Results with model

5.2.1 Introduction to model results

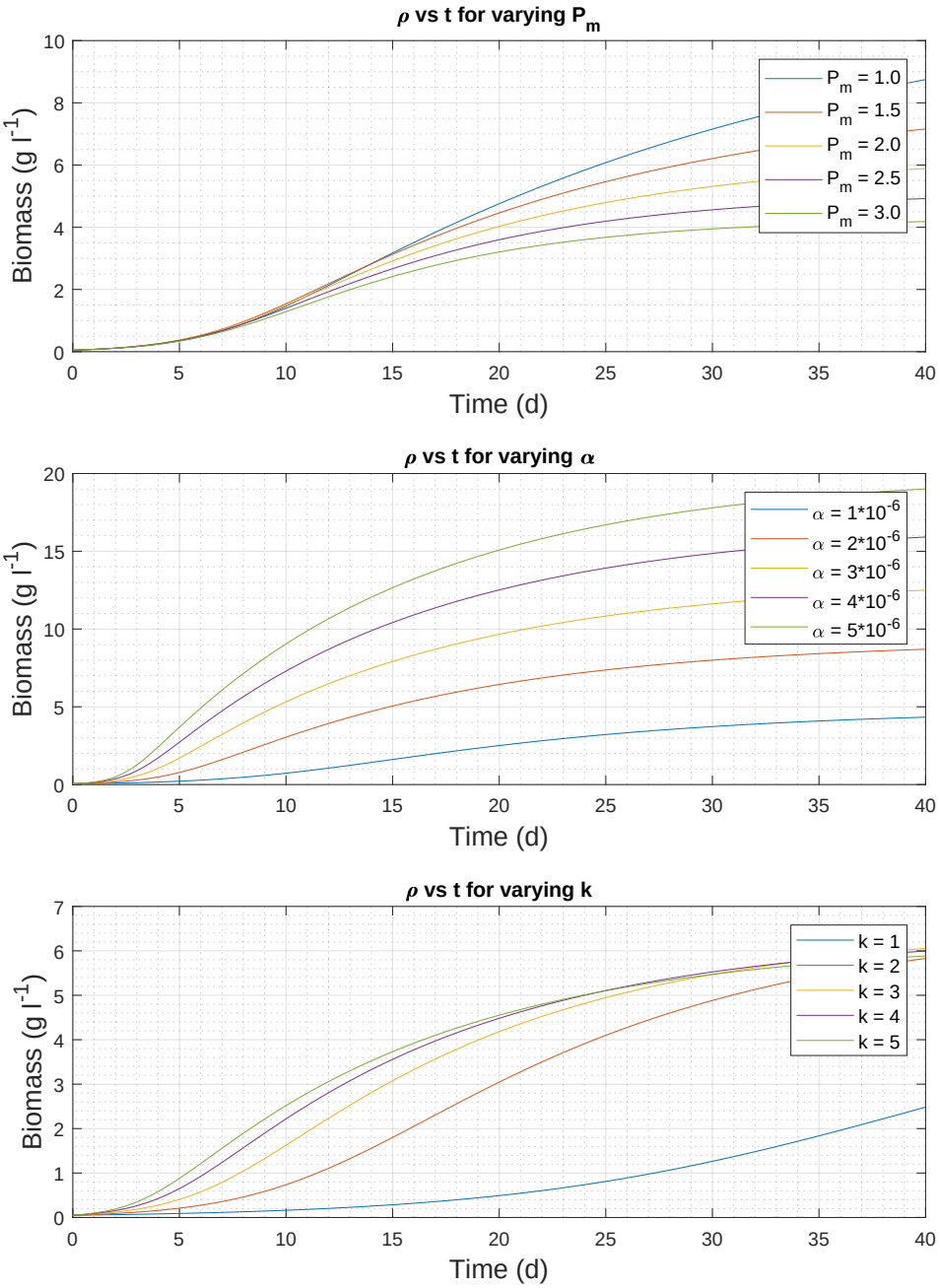

Figure 29: Model graphs for different values for P_m (Upper), α (Middle) and k (Lower). Each parameter is varied one at a time. Figure is based on measurement series one for FITO.

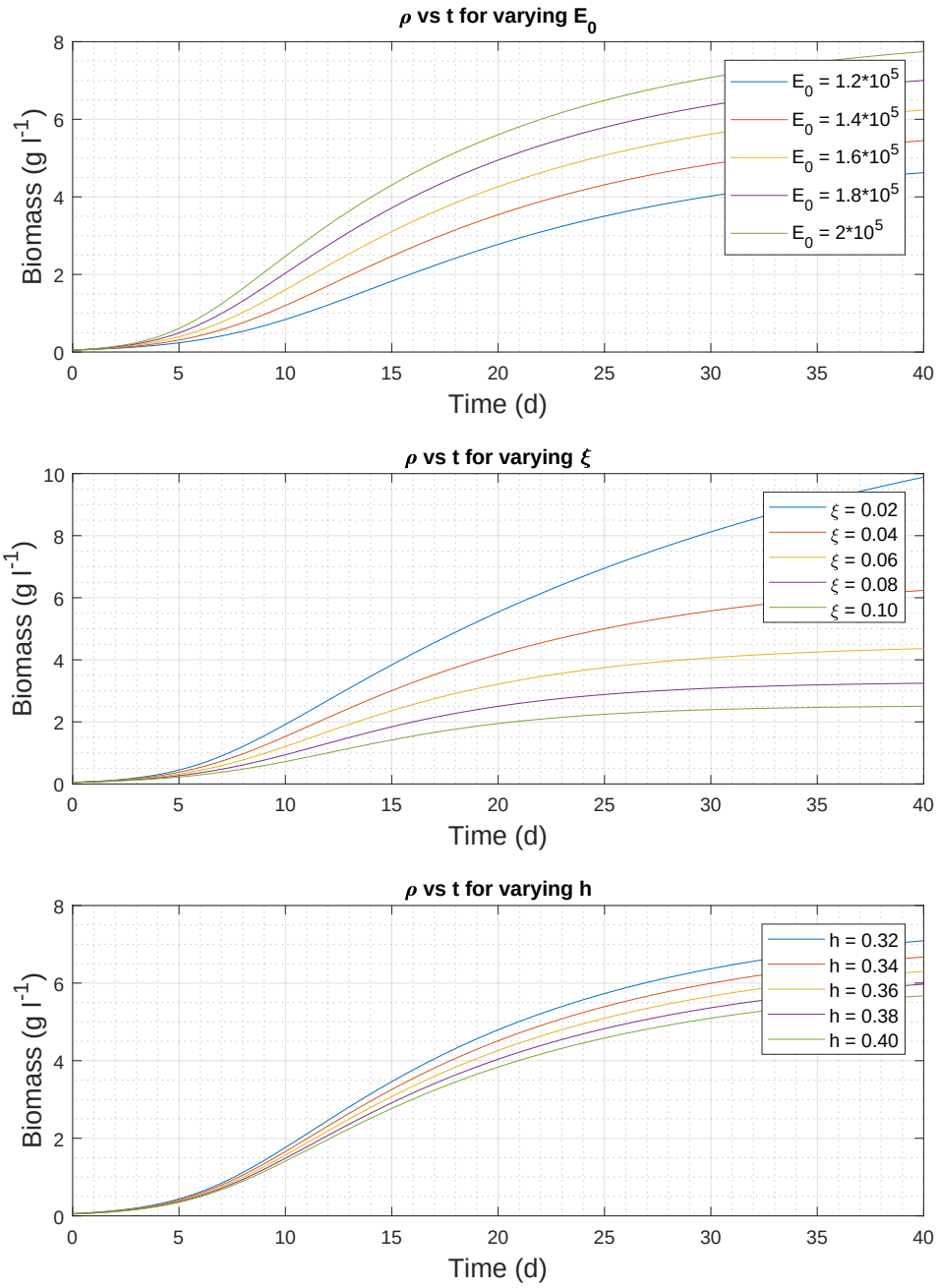

Figure 30: Model graphs for different values for E_0 (Upper), ξ (Middle) and h (Lower). Each parameter is varied one at a time. Figure is based on measurement series one for FITO.

Figures 29 and 30 show how the model curve that describes volume mass density, or biomass, as a function of time, depends on the parameters P_m, α, k, E_0, ξ and h in the given parameter value intervals.

For the given interval, the saturation level for biomass decreases with increasing P_m, and the maximum growth rate is also reduced, but not by a lot. However, as we will see later, whether or not an increase in P_m will decrease the maximum growth depends on what interval for P_m we are looking at. Even though the maximum growth rate changes with P_m it does not change a lot, and so changing P_m in order to maximize growth has a limited effect.

In the given interval for values of α, both the maximum growth rate and the saturation level increases with increasing α. α seems to have a decent impact on the maximum growth rate, however, if we have a low α and start our algae culture with a small biomass, it takes longer time for this culture to reach a biomass that yields maximum growth. Hence, the time it takes for a culture to reach the point of maximum growth is inversely proportional to α, while the maximum growth is proportional to α, and so an increase in α is good for growth no matter how small an algae culture you start out with.

In the given interval for values of the absorption cross section k, the maximum growth rate seems to increase only slightly with increasing absorption cross section, but by at least looking for the curves for $k = 2$, 3, 4 and 5 it seems that the saturation level is unchanged. However, there might be other values for k that could show the opposite. For these values of k, a low k makes an algae culture with a low biomass spend a lot of time to reach a point of maximum growth. In addition the point of maximum growth seems to occur for smaller biomasses with increasing absorption cross section k, and so not only the maximum growth increases, but also the maximum relative growth.

In the given interval for values of the incoming irradiance E_0, both the maximum growth rate and the saturation level increases quite a bit with increasing irradiance. However, since the model does not take photoinhibition into account, this is not a completely accurate picture for higher irradiances.

In the given interval for values of the loss factor ξ, both the maximum growth rate and the saturation level decreases with increasing values of the loss factor. That is, to maximize growth, we want the loss factor to be as small as possible.

In the given interval for values of the depth h, both the maximum growth rate and the saturation level decreases with increasing depth, and the difference in biomass between the curves for varying values of h seem to increase with increasing time or increasing biomass.

Although many of the parameters have the same type of impact on the model curve, the exact way these parameters impact the model curve seem to differ slightly. What we want to do, according to these curves, to maximize growth is to have a low P_m, a high α, an at least not too low absorption cross section k, a high irradiance E_0 but not too high, a small loss factor ξ and a small depth h. We will investigate the effect of these model parameters further.

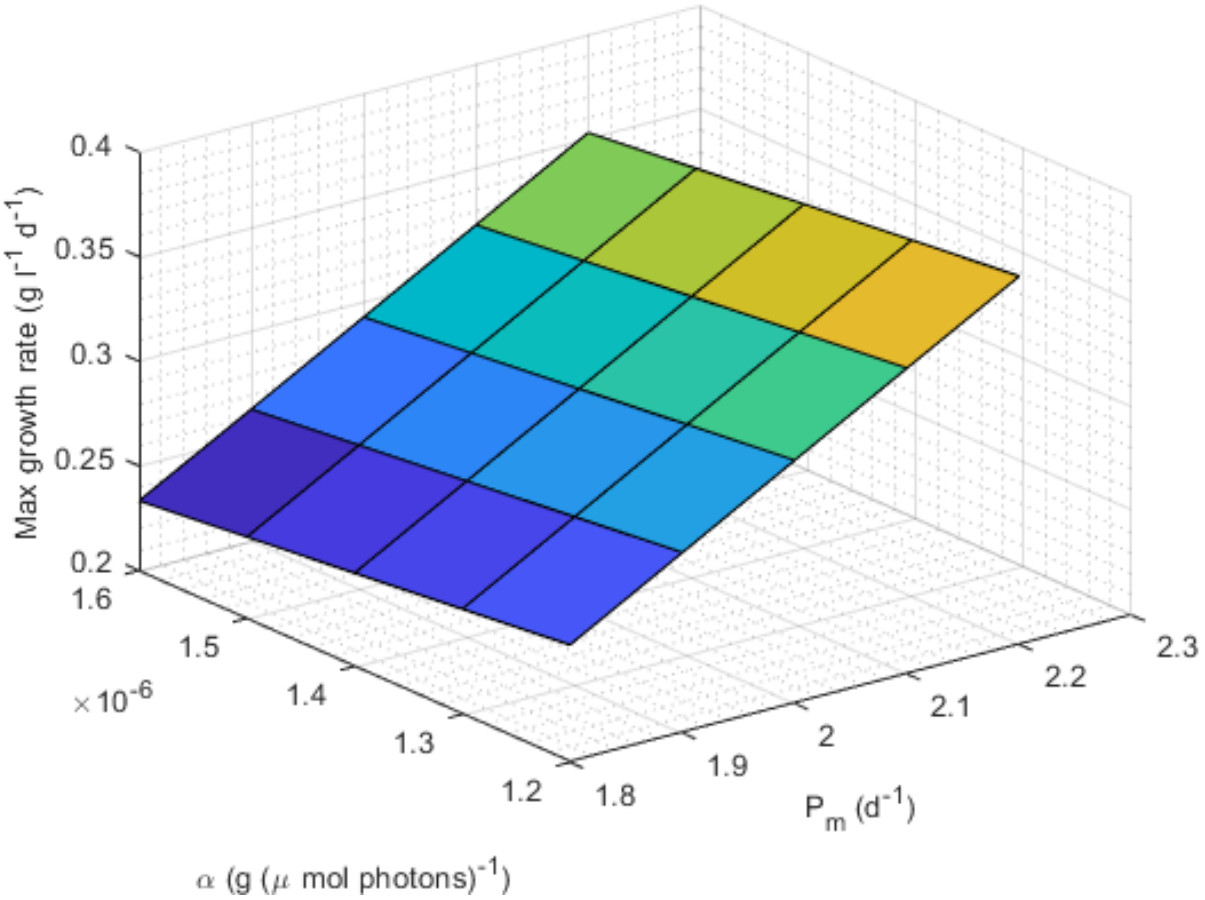

Figure 31: Surface plot of maximal model based growth rate versus specific values of P_m and α. Figure is based on measurement series one for FITO.

From Figure 31 we can see that for these specific values of P_m and α, the maximum model based growth rate depends linearly on both of the variables.

If we look at our series of data, we find that the maximum growth rate for the series of data this figure is based on is approximately 0.3. We can try to find a combination of values for P_m and α that give us a maximum model based growth rate of 0.3 in order to find a set of parameter values P_m and α that will give us a model that has the same maximum growth rate as the series this is based on. If we're lucky, the maximum growth will also happen at approximately the same biomass as in the series, and the model curve and the measurement series will be similar in the point of maximum growth, as shown in Figure 32.

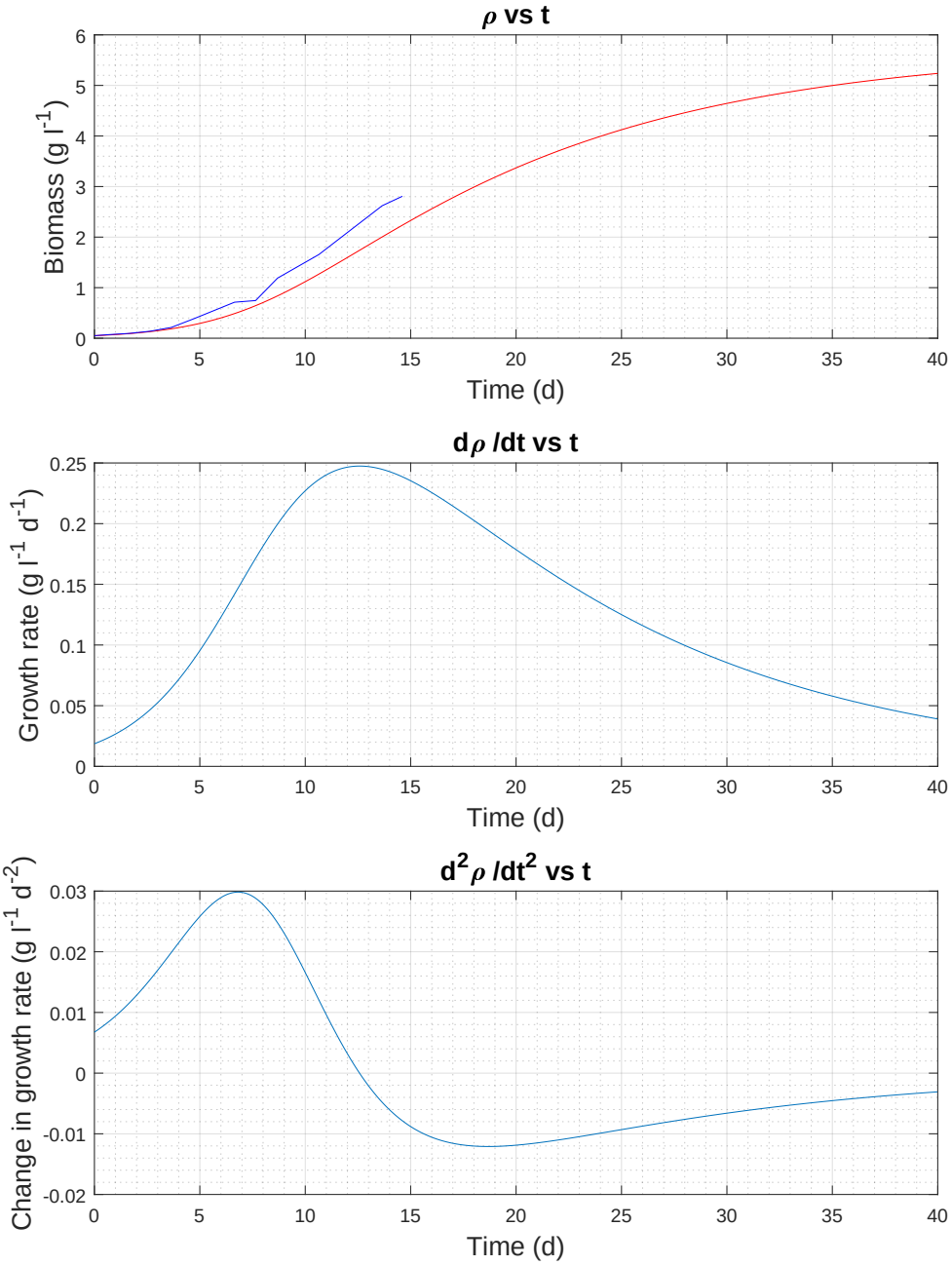

Figure 32: Model curve based on Figure 31. In top part of figure, red curve is model curve while blue is data point curve. Blue curves in middle and lower parts of figure are based on model.

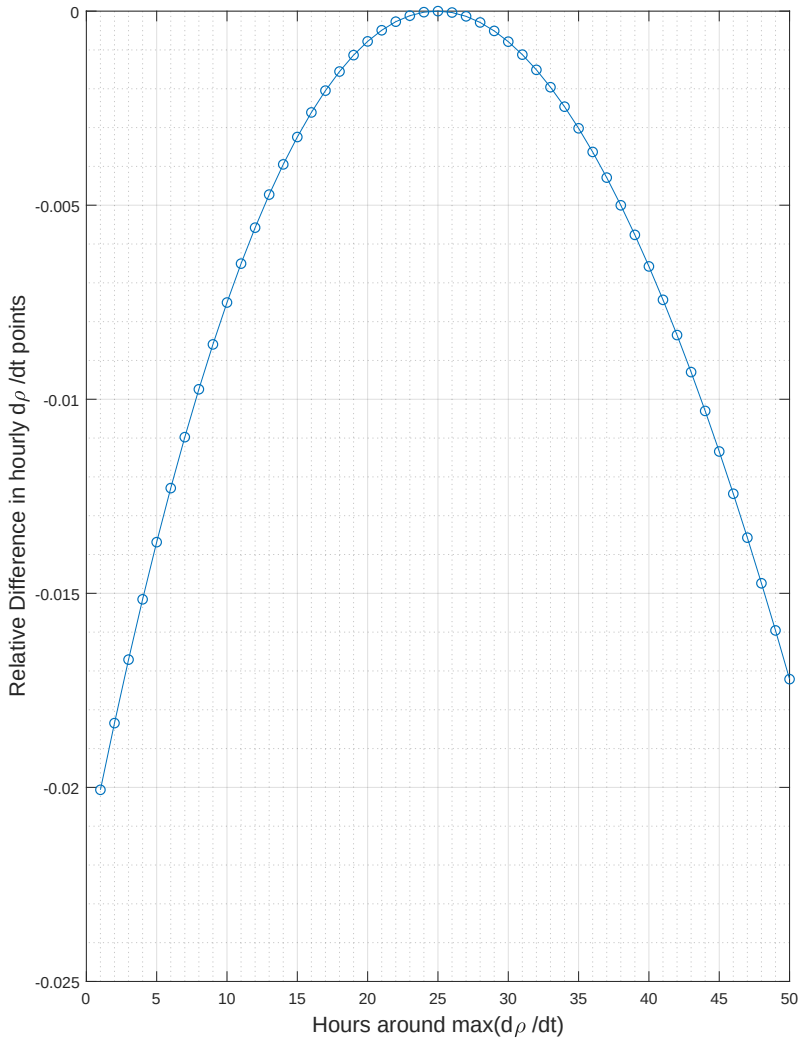

Figure 33: Relative difference in hourly dη/dt points based on model. Maximum growth occurs at t = 25 on x-axis. Figure is based on measurement series one for FITO.

Figure 33 shows the relative difference between growth rates and the maximum growth rate itself (based on model). Hour 25 on the x-axis is the point of maximum growth since the relative difference between the maximum growth rate and itself is 0. At hour 0 on the x-axis, which is approximately 25 hours before the point in time of maximum growth, the growth rate is 2% smaller than the maximum growth rate. This means that in approximately one day (24 hours), the growth rate around the point of maximum growth only changes with around 2%. This is important both for sampling and for harvesting purposes.

5.2.2 Model parameter correlations

Table 8: Parameter values for the different measurement series for FITO found with least square sum and the Matlab function fminsearch.

Measurement series	P_m $[d^{-1}]$	α $[10^{-7}$ $g(\mu mol$ photons$)^{-1}]$	k $[dm^2 g^{-1}]$	ξ
1	1.9	14	2.9	$4.2{\cdot}10^{-2}$
2	0.69	24	6.6	$3.2{\cdot}10^{-1}$
3	0.22	180	1.2	$1.0{\cdot}10^{-1}$
4	0.77	5.4	4.9	$1.4{\cdot}10^{-9}$
5	0.39	11	9.5	$6.0{\cdot}10^{-9}$
6	0.11	88	1.6	$6.5{\cdot}10^{-2}$
7	1.3	8.8	5.0	$8.0{\cdot}10^{-2}$
8	1.0	12	14	$4.6{\cdot}10^{-2}$
9	0.44	34	1.8	$2.3{\cdot}10^{-1}$
10	2.8	17	4.7	$7.8{\cdot}10^{-2}$
11	1.4	22	1.5	$1.0{\cdot}10^{-1}$
12	1.1	17	5.7	$1.8{\cdot}10^{-1}$
13	0.15	14	5.4	$1.4{\cdot}10^{-2}$
14	0.48	38	9.2	$3.4{\cdot}10^{-1}$
15	0.35	27	1.3	$1.5{\cdot}10^{-1}$

Table 9: Parameter values for the different measurement series for M28 found with least square sum and the Matlab function fminsearch.

Measurement series	P_m $[d^{-1}]$	α $[10^{-7}$ $g(\mu mol$ photons$)^{-1}]$	k $[dm^2 g^{-1}]$	ξ
1	0.69	10	3.4	$2.7{\cdot}10^{-2}$
2	0.35	20	5.2	$2.1{\cdot}10^{-1}$
3	0.18	88	1.6	$5.3{\cdot}10^{-2}$
4	0.21	11	3.7	$1.4{\cdot}10^{-2}$
5	0.59	140	7.6	$5.4{\cdot}10^{-1}$
6	0.19	370	9.1	$2.5{\cdot}10^{-1}$
7	4.1	8.1	3.4	$2.2{\cdot}10^{-2}$
8	2.9	46	2.1	$1.5{\cdot}10^{-1}$
9	0.18	140	2.3	$3.2{\cdot}10^{-6}$
10	0.26	220	23	$4.9{\cdot}10^{-2}$
11	0.79	7.4	3.4	$4.8{\cdot}10^{-10}$
12	0.43	80	38	$5.8{\cdot}10^{-2}$
13	0.11	88	1.7	$5.5{\cdot}10^{-2}$
14	0.14	88	1.7	$5.5{\cdot}10^{-2}$
15	0.061	87	1.6	$6.8{\cdot}10^{-2}$

Table 10: Parameter values for the different measurement series for B58 found with least square sum and the Matlab function fminsearch.

Measurement series	P_m $[d^{-1}]$	α $[10^{-7}$ $g(\mu mol$ photons$)^{-1}]$	k $[dm^2g^{-1}]$	ξ
1	0.39	17	3.2	$9.2{\cdot}10^{-2}$
2	0.69	22	6.6	$2.3{\cdot}10^{-1}$
3	0.18	88	1.6	$5.4{\cdot}10^{-2}$
4	0.81	20	1.8	$2.1{\cdot}10^{-1}$
5	0.73	19	1.8	$2.5{\cdot}10^{-1}$
6	0.63	32	3.5	$3.0{\cdot}10^{-1}$
7	0.75	19	9.9	$1.5{\cdot}10^{-1}$
8	0.70	19	5.4	$1.7{\cdot}10^{-1}$
9	0.78	13	6.5	$1.9{\cdot}10^{-1}$
10	1.2	240	7.7	$7.8{\cdot}10^{-1}$
11	0.43	15	1.5	$1.1{\cdot}10^{-2}$
12	0.69	23	4.9	$2.9{\cdot}10^{-1}$
13	0.26	12	8.7	$5.9{\cdot}10^{-2}$
14	0.67	54	6.4	$5.2{\cdot}10^{-1}$
15	0.15	250	1.4	$1.0{\cdot}10^{-1}$

Table 11: Mean and standard deviations for parameter values across all measurement series

Parameter	Mean	Std. Dev.
P_m $[d^{-1}]$	0.74	0.80
α $[10^{-7}$ $g(\mu mol$ photons$)^{-1}]$	61	80
k $[dm^2g^{-1}]$	5.7	6.4
ξ	0.15	0.16

Tables 8, 9, 10 and 11 show the parameter values that we found for each measurement series by using least square sum method combined with the Matlab function fminsearch, as well as the mean and standard deviation of all those parameter values. In each case the standard deviation is larger than the mean, which means that there is a large uncertainty for the values of these parameters.

Table 12: Average parameter values for each strain of algae.

Parameter	FITO	M28	B58
P_m $[d^{-1}]$	0.88	0.75	0.60
α $[10^{-7}$ $g(\mu mol$ photons$)^{-1}]$	34	94	56
k $[dm^2 g^{-1}]$	5.0	7.2	4.7
ξ	0.12	0.10	0.23

Table 12 show the average parameter values that we found for the measurement series by using least square sum method combined with fminsearch, but in this table the averages are for each strain of algae and not for the entirety of the measurement series.

As we can see, there are some differences in the average parameter values between the strains. FITO has the largest average value of P_m, M28 has the largest average values of α and k, while B58 has the largest average value of ξ. Although the average parameter values for each strain are quite close to one another, the parameter with the largest variation is α, where the lowest average is $3.4{\cdot}10^{-7}$ g (mol photons)$^{-1}$ and the highest average is $9.4{\cdot}10^{-7}$ g (mol photons)$^{-1}$.

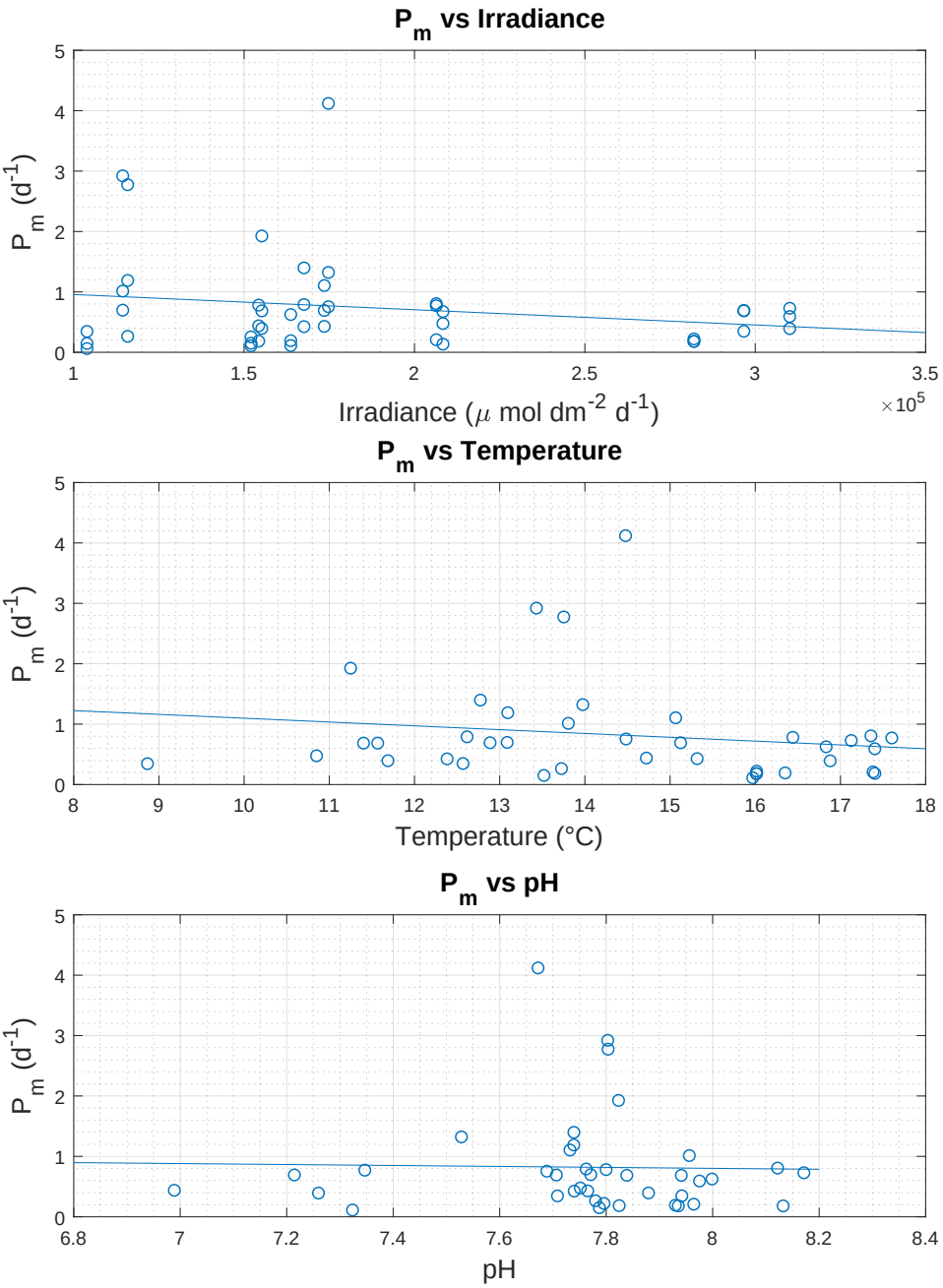

Figure 34: Scatterplot of P_m versus average irradiance, average temperature and average pH.

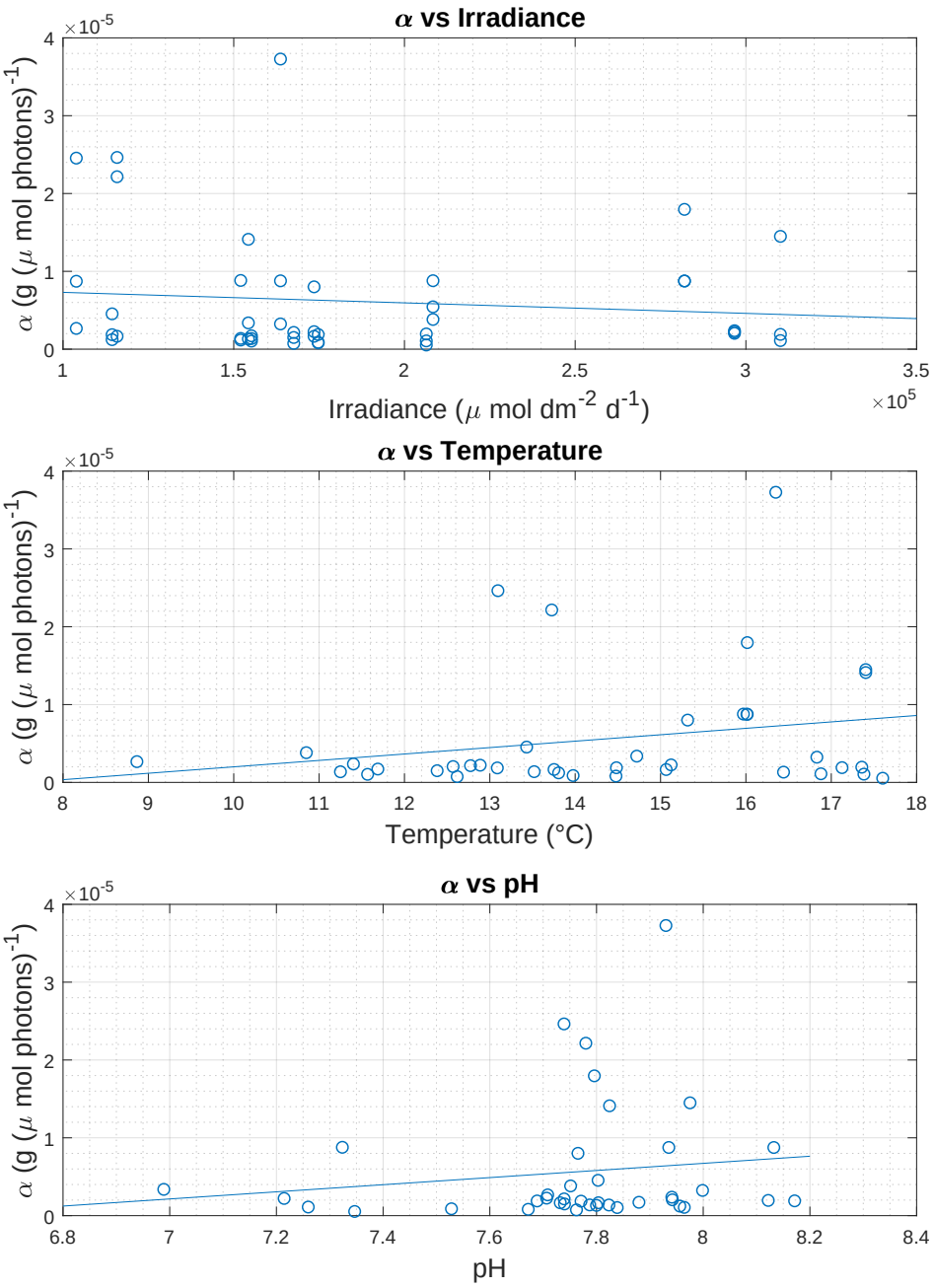

Figure 35: Scatterplot of α versus average irradiance, average temperature and average pH.

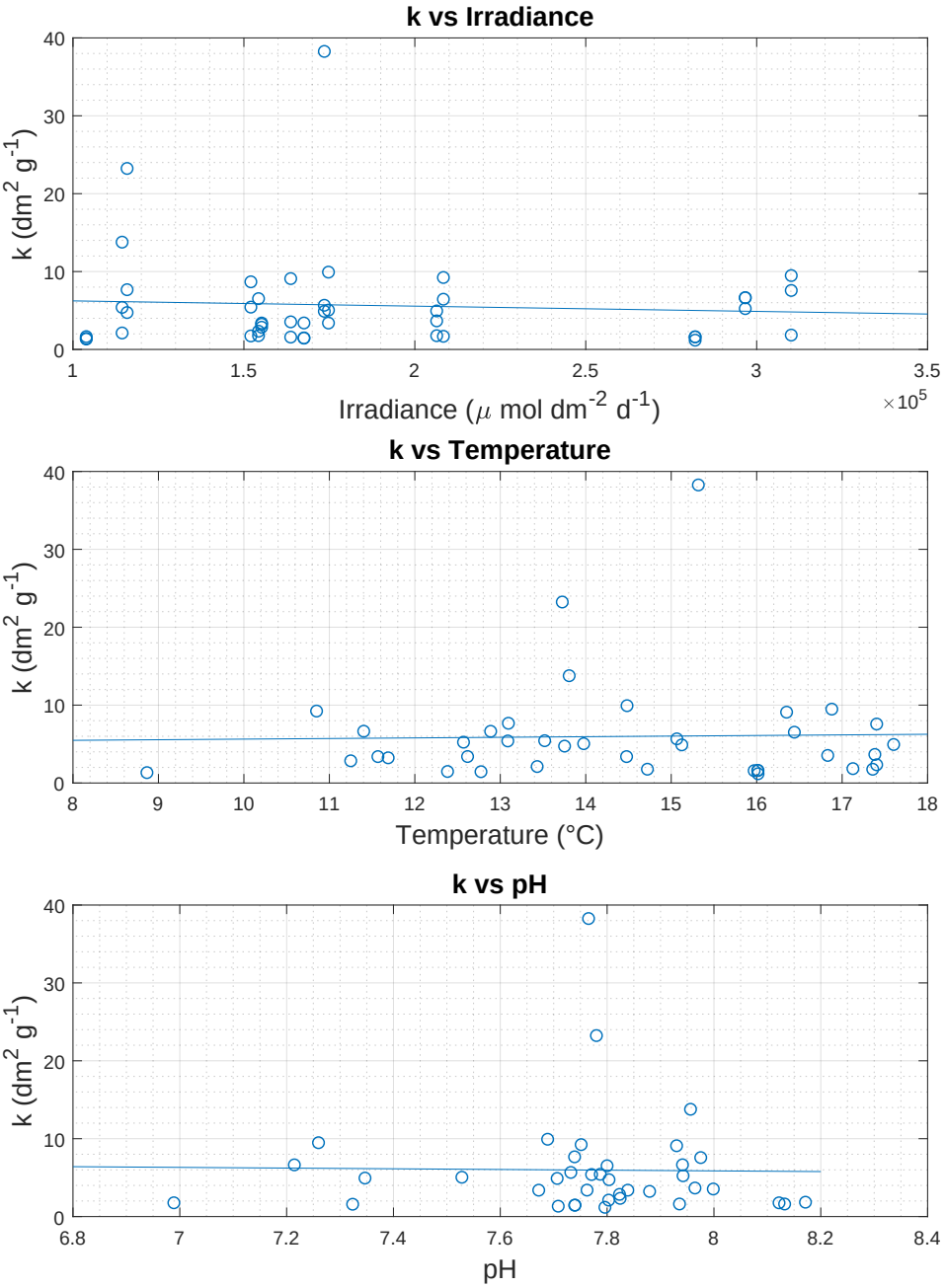

Figure 36: Scatterplot of k versus average irradiance, average temperature and average pH.

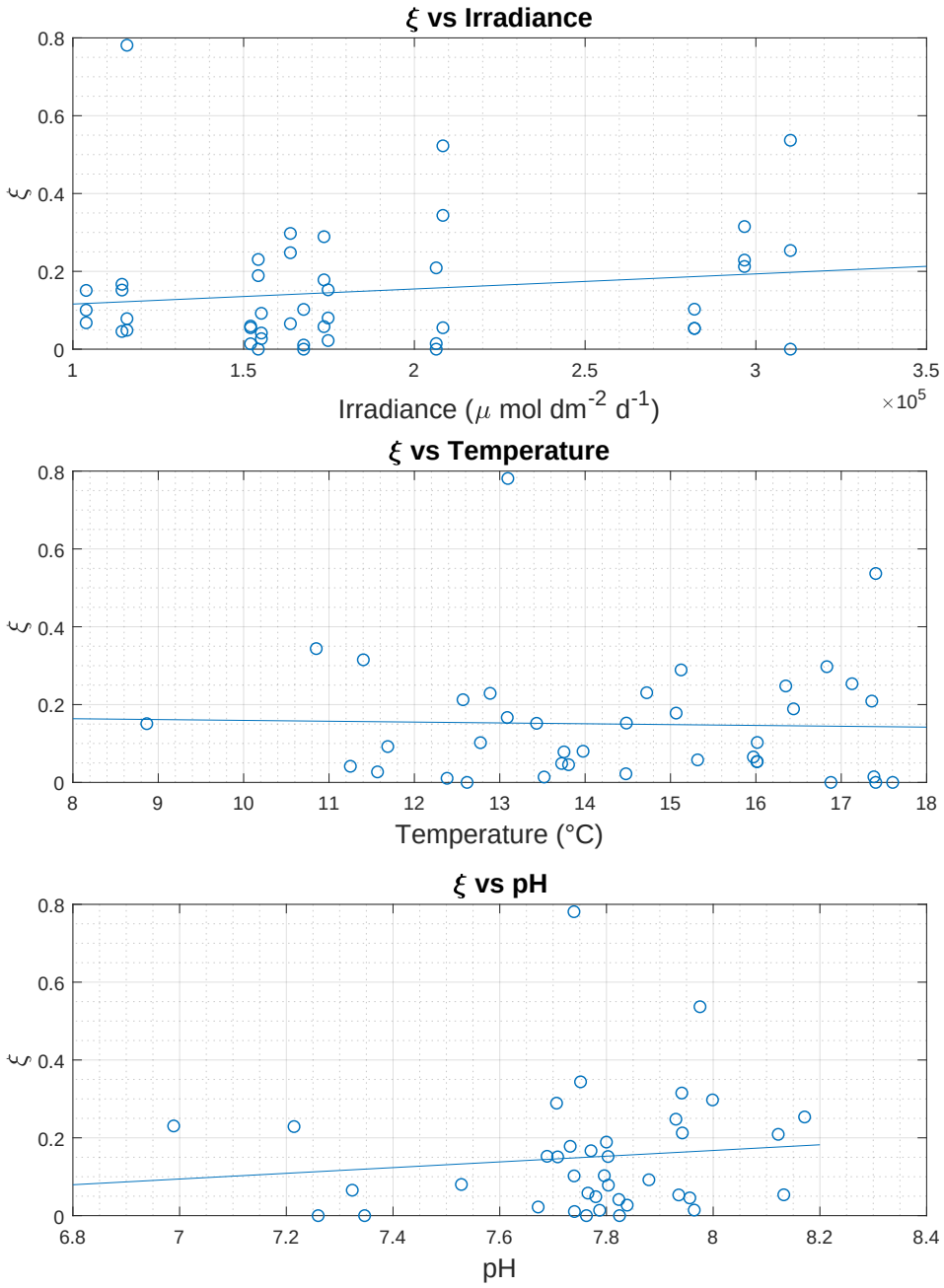

Figure 37: Scatterplot of ξ versus average irradiance, average temperature and average pH.

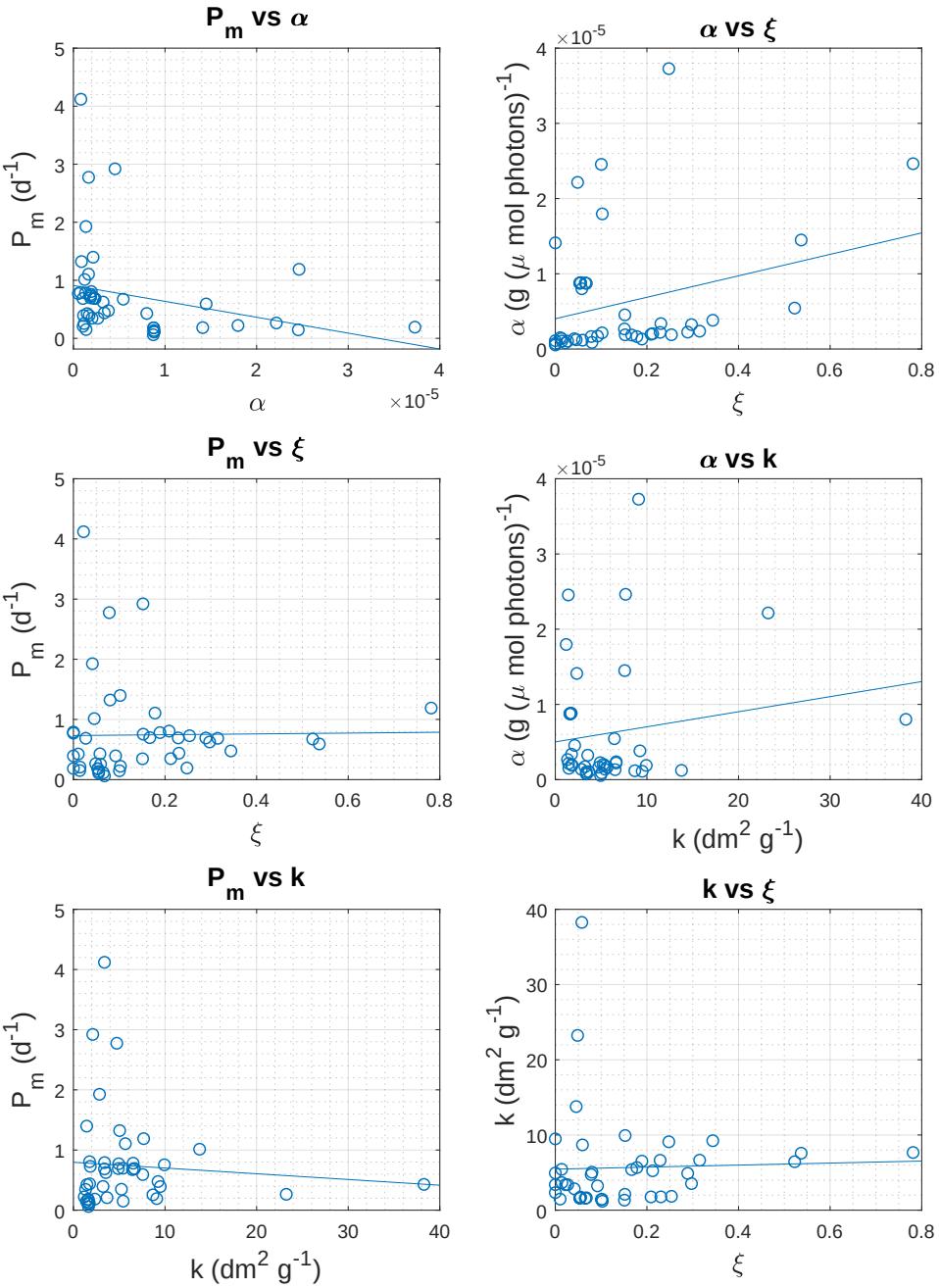

Figure 38: Scatterplot of P_m versus α, k and ξ, α versus k and ξ, and k versus ξ.

Figures 34, 35, 36 and 37 show, respectively, how P_m depends on average irradiance, average temperature and average pH, how α (with units $g(\mu mol$ photons$)^{-1}$) depends on average irradiance, average temperature and average pH, how k depends on average irradiance, average temperature and average pH, and how ξ depends on average irradiance, average temperature and average pH. Figure 38 shows how P_m depends on α, k and ξ, how α depends on k and ξ, and how k depends on ξ. Note, however, that in this results section (section 5.2), the average irradiance, average temperature and average pH does not mean the average values of these quantities between biomass points, but for entire measurement series.

In Figure 34, we can see how P_m depends on irradiance, temperature and pH. The spread in data points tells us that there is a low correlation, but it seems that there is a slight negative correlation between P_m and irradiance and temperature.

In Figure 35, we can see how α depends on irradiance, temperature and pH. The data points for α versus irradiance seem to be distributed mostly in a horizontal band, and so there is barely a connection. The correlation between α and temperature and pH is a little larger, but still the distribution seems to be mostly in the form of a horizontal band.

In Figure 36, we can see how k depends on irradiance, temperature and pH. The least square line in each case is almost entirely flat, and the data points are almost completely distributed along a horizontal band. Hence, the correlations are very small.

In Figure 37, we can see how ξ depends on irradiance, temperature and pH. Again, there barely seems to be any correlation between this variable (ξ) and irradiance, temperature and pH.

In Figure 38, we can see how the parameters P_m, α, k and ξ depend on each other. In all cases the variables seem to be almost completely uncorrelated.

Table 13: Correlations between parameters P_m, α, k, ξ, and average irradiance, average temperature and average pH.

Parameter	Irradiance [μmol photons $dm^{-2}d^{-1}$]	Temperature (Celsius)	pH
P_m [d^{-1}]	-0.20	-0.17	-0.024
α [$g(\mu mol$ photons$)^{-1}$]	-0.11	0.23	0.14
k [dm^2g^{-1}]	-0.067	0.025	-0.017
ξ	0.15	-0.030	0.12

From Table 13 we can see that most of the correlations are very weak. The strongest negative correlation is the one between P_m and average irradiance, which is approximately -0.20, while the strongest positive correlation is the one between α and average temperature, which is approximately 0.23. These correlations are, however, quite weak, as can also be seen from the plots in figures 34, 35, 36 and 37.

By looking at the highest negative correlation (-0.20), we find the following: even though the correlation is quite low, there is somewhat of a dependency between the variables. If, for example, it is really the case that P_m decreases with increasing irradiance, then an increase in irradiance, based only on this correlation and depending on not only whether or not there is an optimal P_m value but also what P_m value we already have will yield either an increase or a decrease in the maximum growth. If, for example, there is an optimal value for $P_m = 0.8\text{d}^{-1}$ and our current value for $P_m = 1.0\text{d}^{-1}$, then an increase in irradiance will yield an increase in the maximum growth. However, if the optimal value for $P_m = 0.8\text{d}^{-1}$ and our current value for $P_m = 0.6\text{d}^{-1}$, then a decrease in irradiance will yield an increase in the maximum growth.

By looking at the highest positive correlation (0.23), we find the following: even though the correlation is quite low, there is somewhat of a dependency between the variables. If, for example, it is really the case that α increases with increasing temperature, then an increase in temperature, based only on this correlation and depending on not only whether or not there is an optimal α value but also what α value we already have will yield either an increase or a decrease in the maximum growth. If, for example, there is an optimal value for $\alpha = 1{\cdot}10^{-6}$ and our current value for $\alpha = 1.1{\cdot}10^{-6}$, then a decrease in temperature will yield an increase in the maximum growth. However, if the optimal value for $\alpha = 1{\cdot}10^{-6}$ and our current value for $\alpha = 0.9{\cdot}10^{-6}$, then an increase in temperature will yield an increase in the maximum growth.

Table 14: Correlations between parameters P_m, α, k and ξ.

Parameter	P_m $[d^{-1}]$	α $[g(\mu mol$ photons$)^{-1}]$	k $[dm^2g^{-1}]$	ξ
P_m $[d^{-1}]$	1	-0.27	-0.076	0.014
α $[g(\mu mol$ photons$)^{-1}]$	-0.27	1	0.16	0.29
k $[dm^2g^{-1}]$	-0.076	0.16	1	0.034
ξ	0.014	0.29	0.034	1

In Table 14 we can see that most of the correlations are very weak. The strongest negative correlation is the one between P_m and α, which is approximately -0.27, while the strongest positive correlation is the one between α and ξ, which is approximately 0.29.

By looking at the highest negative correlation (-0.27), we find the following: given that there is a negative dependency between P_m and irradiance and a positive dependency between α and temperature, in addition to a negative correlation between P_m and α, an increase in irradiance will yield a decrease in P_m which will yield an increase in α. An increase in α is also yielded by an increase in temperature, and hence an increase in irradiance will yield an increase in temperature, which is in accord with what we have previously discussed.

By looking at the highest positive correlation (0.29), we find the following: given that there is a positive dependency between α and ξ and a positive dependency between α and temperature, an increase in temperature will yield an increase in ξ. That is, an increase in temperature will yield a decrease in the maximum growth rate. It is important to keep in mind, however, that we have only dealt with a few of the correlations; an increase in temperature need not actually yield a decrease in the maximum growth rate. In addition, the correlations are quite weak.

5.2.3 Maximal growth parameters

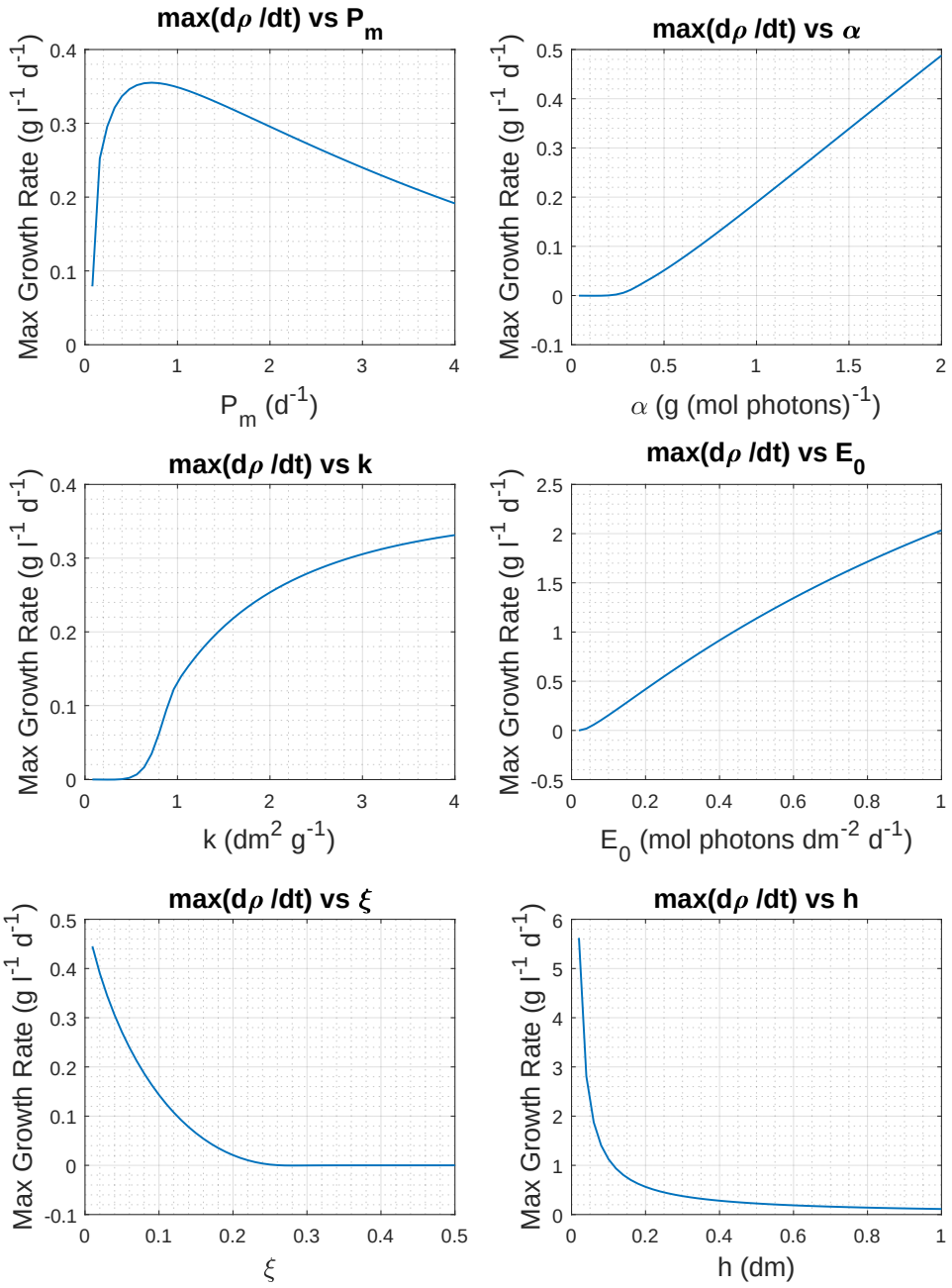

Figure 39: Maximum model based growth rate versus model parameters P_m (upper left), α (upper right), k (middle left), E_0 (middle right), ξ (lower left) and h (lower right). Figure is based on measurement series one for FITO.

Figure 39 shows the relationships between the maximum model based growth rate and P_m, α, k, E_0, ξ and h. These graphs are obtained by setting all parameter values constant while varying the 6th parameter, and seeing how the maximum model based growth rate changes with it.

The relationship between the maximum model based growth rate and P_m has a steep curve for low P_m values, reaches a plateau, and then decreases until it becomes zero and stays zero. This means that it is important to keep P_m from becoming too small, yet there is a somewhat wide range of values for P_m where the maximum growth is more or less constant. When P_m, is too small or too large, it becomes difficult for the culture to grow efficiently in the point of maximum growth, that is, when the maximum production P_m is too small or too large, the maximum (net) growth rate of the culture is sub-optimal.

When α is very small, the maximum model based growth rate is zero. Once α reaches a certain value, the maximum growth rate increases. The increase, however, seems mostly linear in the given range of α values, and so any increase in α within this range of α values will yield the same increase in the maximum growth rate.

The relationship between the maximum model based growth rate and k is somewhat similar to the relationship between the maximum growth and P_m. For small values of k the maximum growth rate is zero, as expected. When k reaches a certain value, the maximum growth seems to increase quite quickly, and further increases in the absorption cross section lead to smaller and smaller increases in the maximum growth rate. Hence, it is important that the absorption cross section is high enough for decent maximum growth.

The relationship between the maximum model based growth rate and the irradiance E_0 is somewhat similar to the relationship between the maximum growth and α. In this range of irradiance values the increase in maximum growth rate does seem to decrease with increasing irradiance, and so the higher the irradiance, the more of an increase in irradiance you would need to increase the maximum growth rate. However, photoinhibition is not taken into account.

When the loss factor ξ is small, the maximum model based growth rate is large. As ξ increases, the maximum growth decreases quite a bit until the maximum growth is zero, staying at zero. Hence, there exists a threshold value for the loss factor, where smaller values for the loss factor yield growth and larger values do not. This means that the loss factor must be smaller than the threshold value.

When the depth h goes to zero, the maximum model based growth rate seems to go to infinity, while when the depth h becomes large, the maximum model based growth rate seems to go towards zero or some small value. It is important to keep in mind here that the growth rate is, as it usually is in this thesis, in terms of a change in the volumetric mass density. Since a change in depth also change the volume, this graph does not give us a full picture of how the depth affects growth.

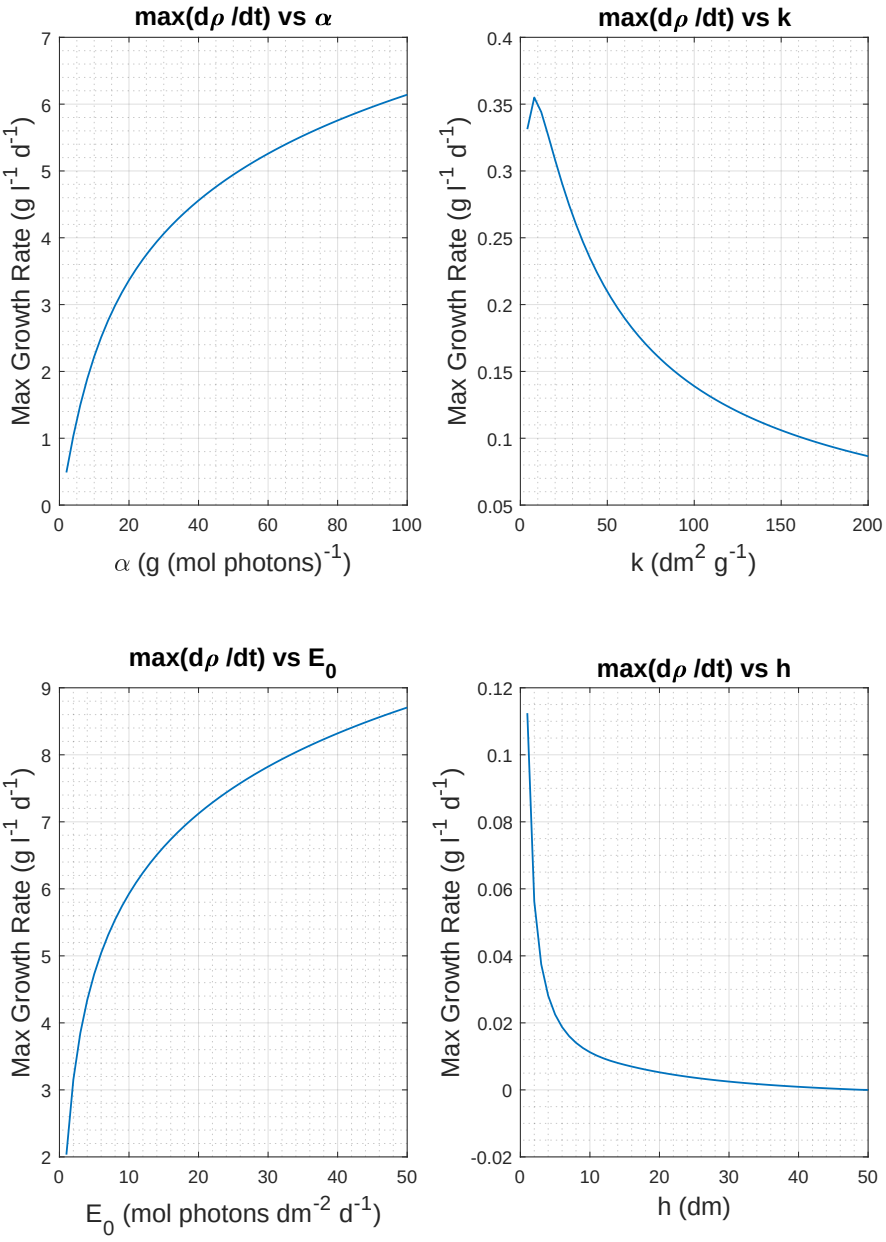

Figure 40: Maximum model based growth rate versus high values for the model parameters α (upper left), k (upper right), E_0 (lower left) and h (lower right). Figure is based on measurement series one for FITO.

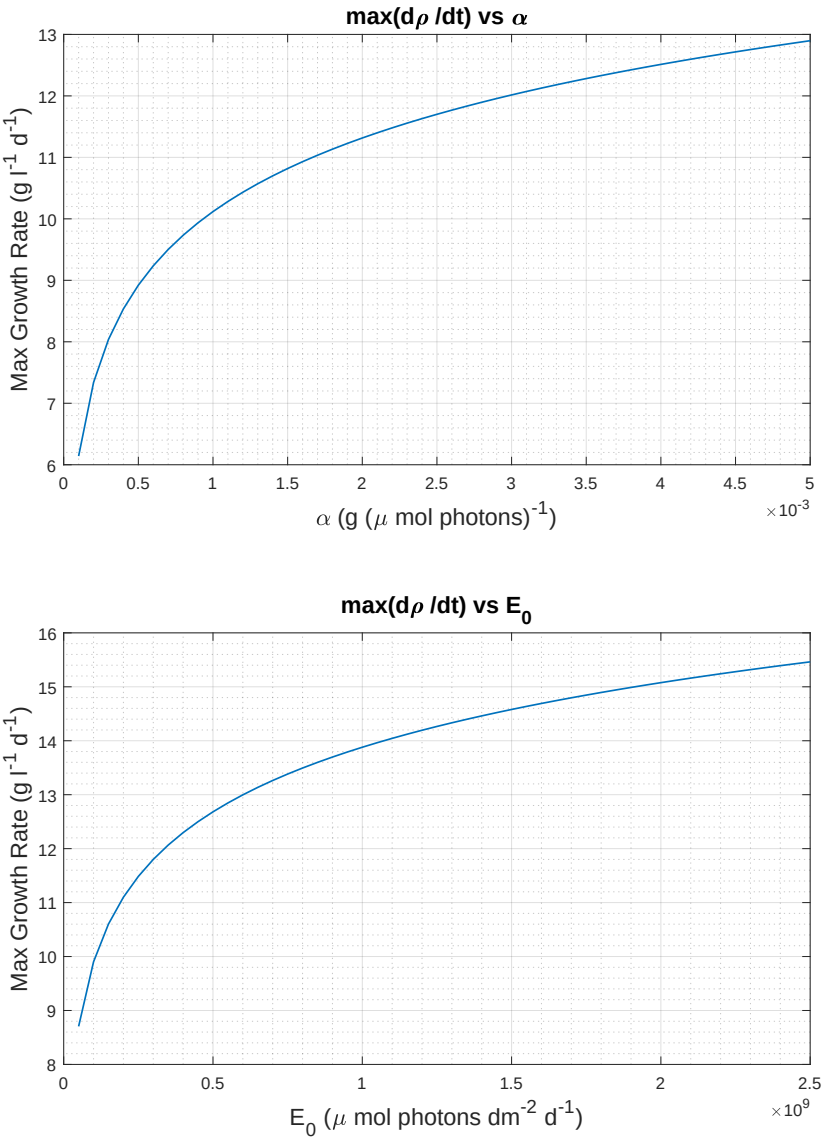

Figure 41: Maximum model based growth rate versus extreme values for the model parameters α (upper) and E_0 (lower). Figure is based on measurement series one for FITO.

As we can see from figures 40 and 41, as α and E_0 become very large, the maximum model based growth rate does not seem to reach a peak, but rather a saturation level since the graphs seem to flatten. When h becomes very large, the maximum model based growth rate seems to go towards zero (again, this does not give us a full picture). There is a peak value for k, but when k becomes large, the maximum model based growth rate decreases.

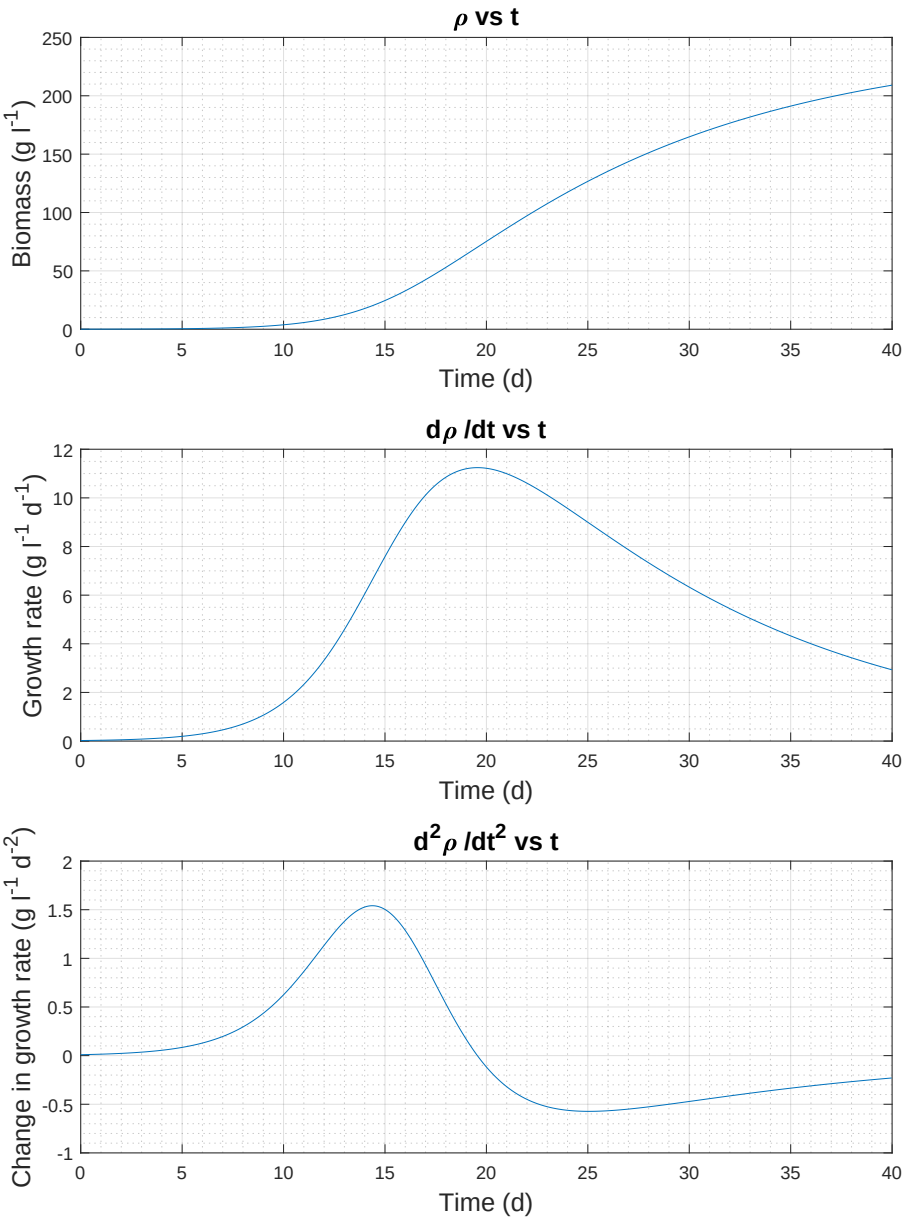

Figure 42: Model curve for small depth (h = 0.01 dm). Figure is based on measurement series one for FITO.

When the depth h becomes small, the maximum growth rate (change in volumetric mass density) becomes large. The relative growth however is not particularly large because of the large biomass (volumetric mass density) at the point of maximum growth, as can be seen in Figure 42.

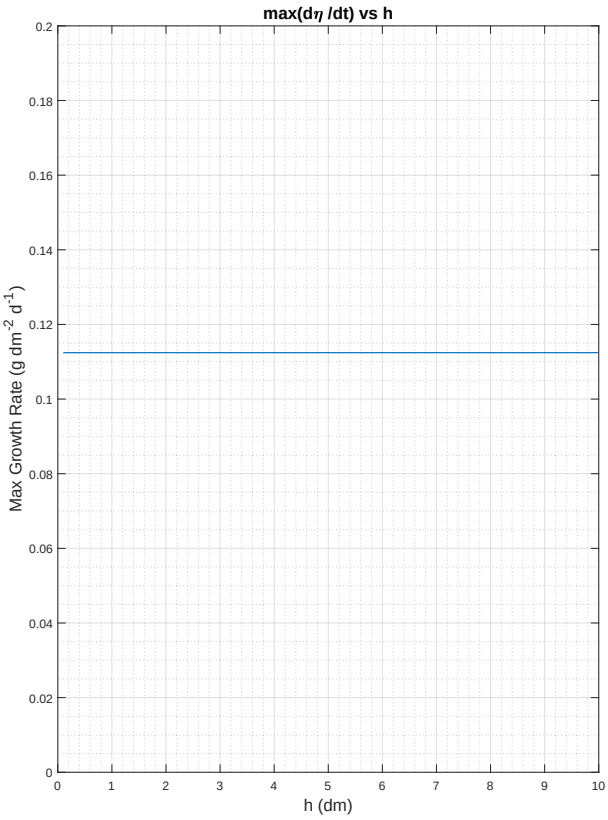

Figure 43: Maximum model based growth rate (change in mass per area) versus very small depths h. Figure is based on measurement series one for FITO.

Figure 43 tells us something interesting. Although the maximum change in volumetric mass density gets quite large with decreasing depth h, the maximum change in mass per area seems to be constant with depth, or in other words, the maximum change in mass per area in the water column is independent of depth. This means that whether the water column is deep or shallow, the maximum net change in mass per area for the depth layers in the water column is constant. That is, to maximize growth, we should increase the area of the water column, not just because of what has been discussed here, but also because the irradiance is a physical quantity with units per area; the total radiation received by the water column will then increase with the area even though the incoming irradiance remains the same. Since the maximum growth per area is constant with depth (at least between 1 cm and 1 m), the depth does not affect the maximum growth rate in terms of the total mass.

We will now look at how the maximal model based growth rate depends on the parameters P_m and k for all measurement series, however we will only look at figures for 9 measurement series so as to not have too many figures. Even though there are 6 model parameters we could investigate, only two of them (P_m and k) seem to yield peak values for the maximal growth.

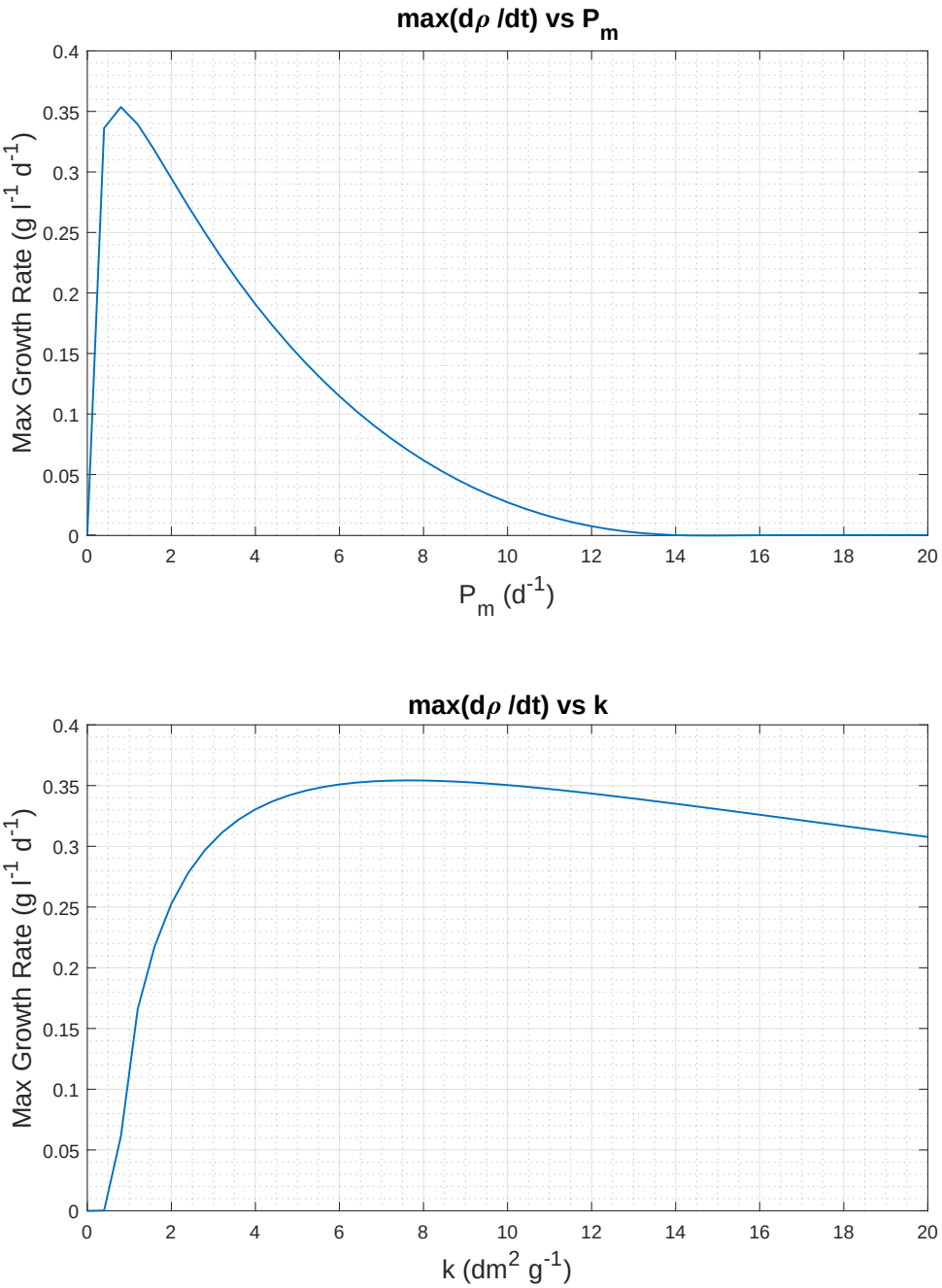

Figure 44: Maximal model based growth versus different values of the parameters P_m and k for the 1st measurement series of FITO. Only one parameter changes value at a time.

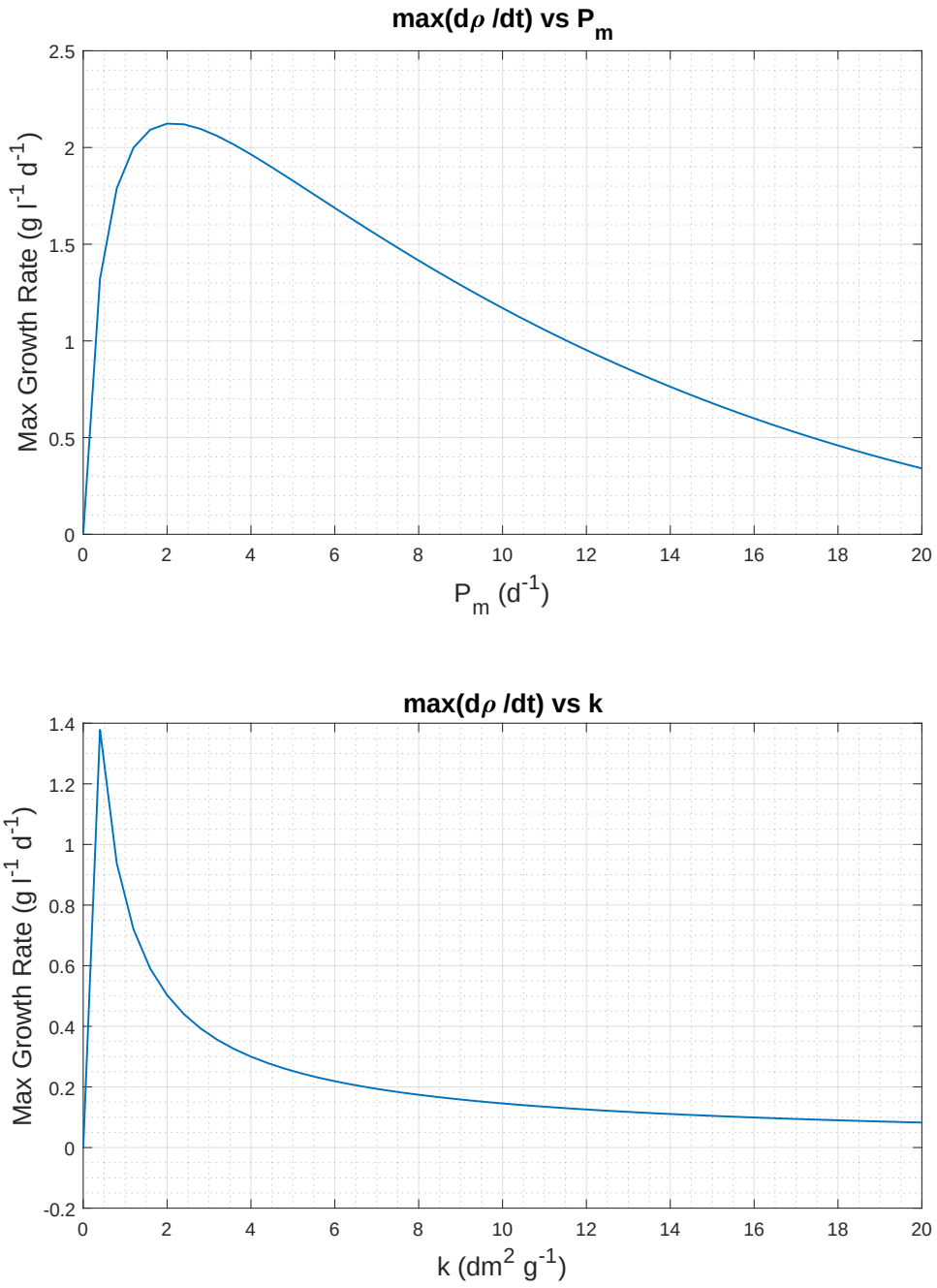

Figure 45: Maximal model based growth versus different values of the parameters P_m and k for the 6th measurement series of FITO. Only one parameter changes value at a time.

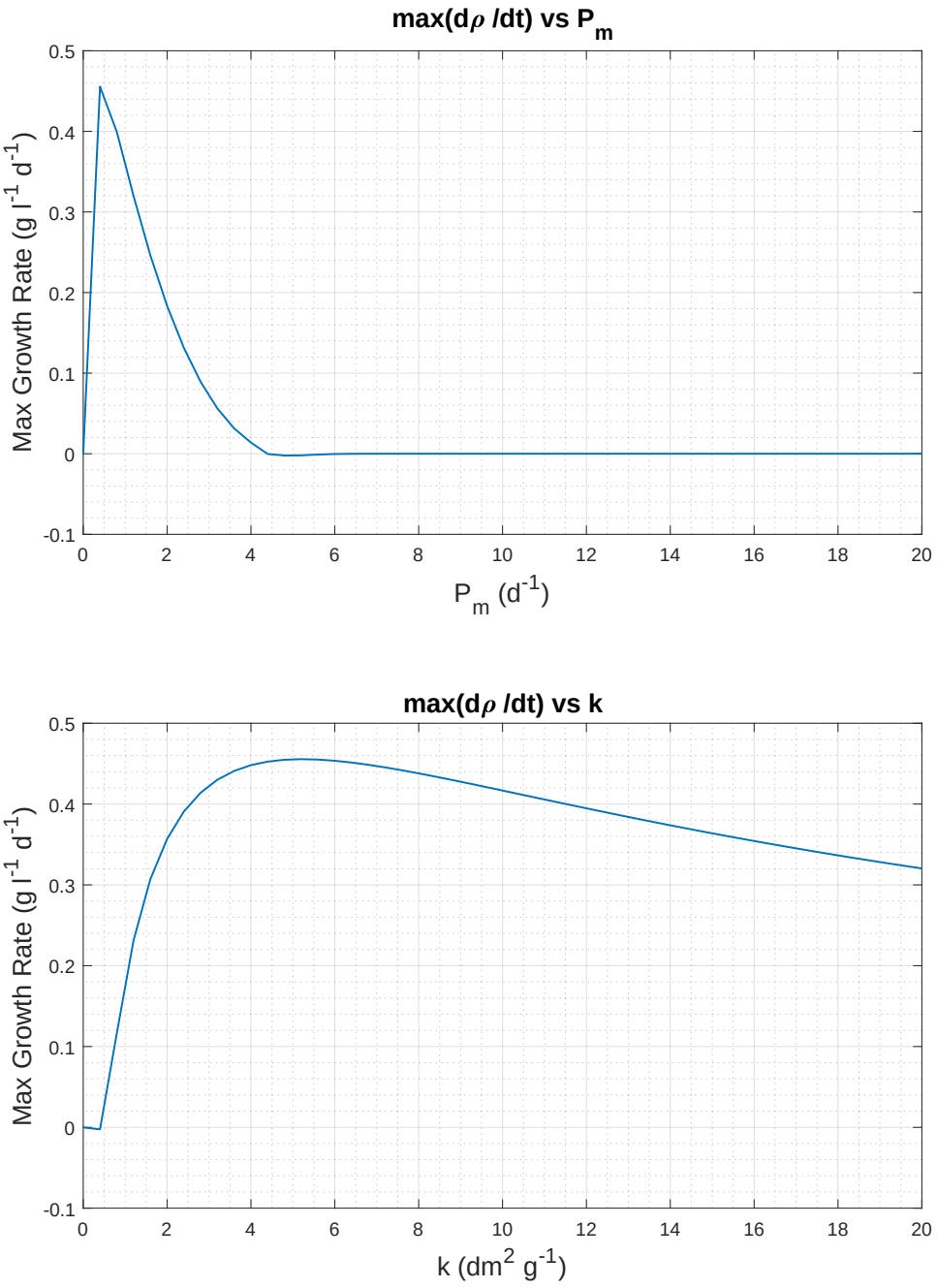

Figure 46: Maximal model based growth versus different values of the parameters P_m and k for the 11th measurement series of FITO. Only one parameter changes value at a time.

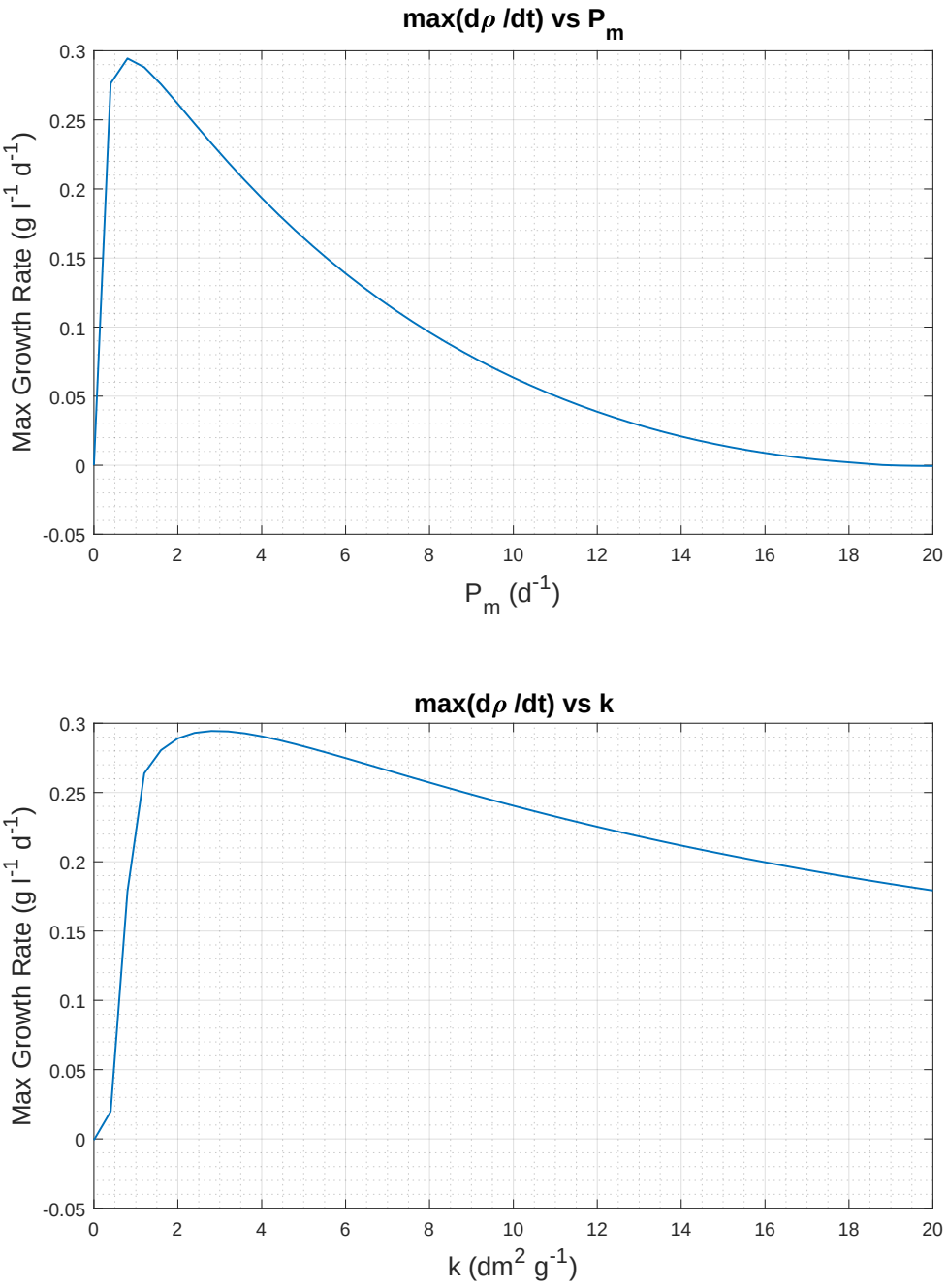

Figure 47: Maximal model based growth versus different values of the parameters P_m and k for the 1st measurement series of M28. Only one parameter changes value at a time.

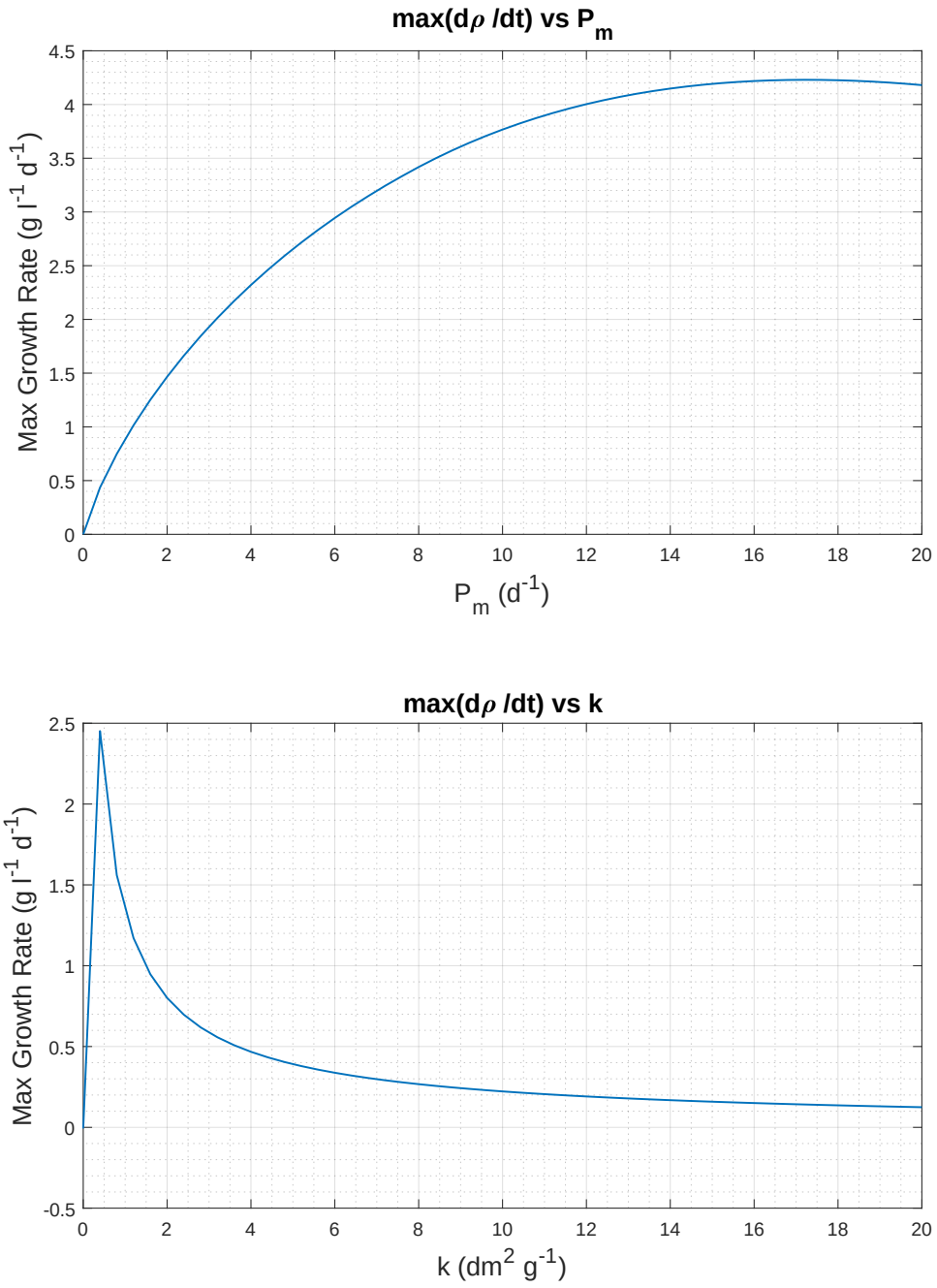

Figure 48: Maximal model based growth versus different values of the parameters P_m and k for the 6th measurement series of M28. Only one parameter changes value at a time.

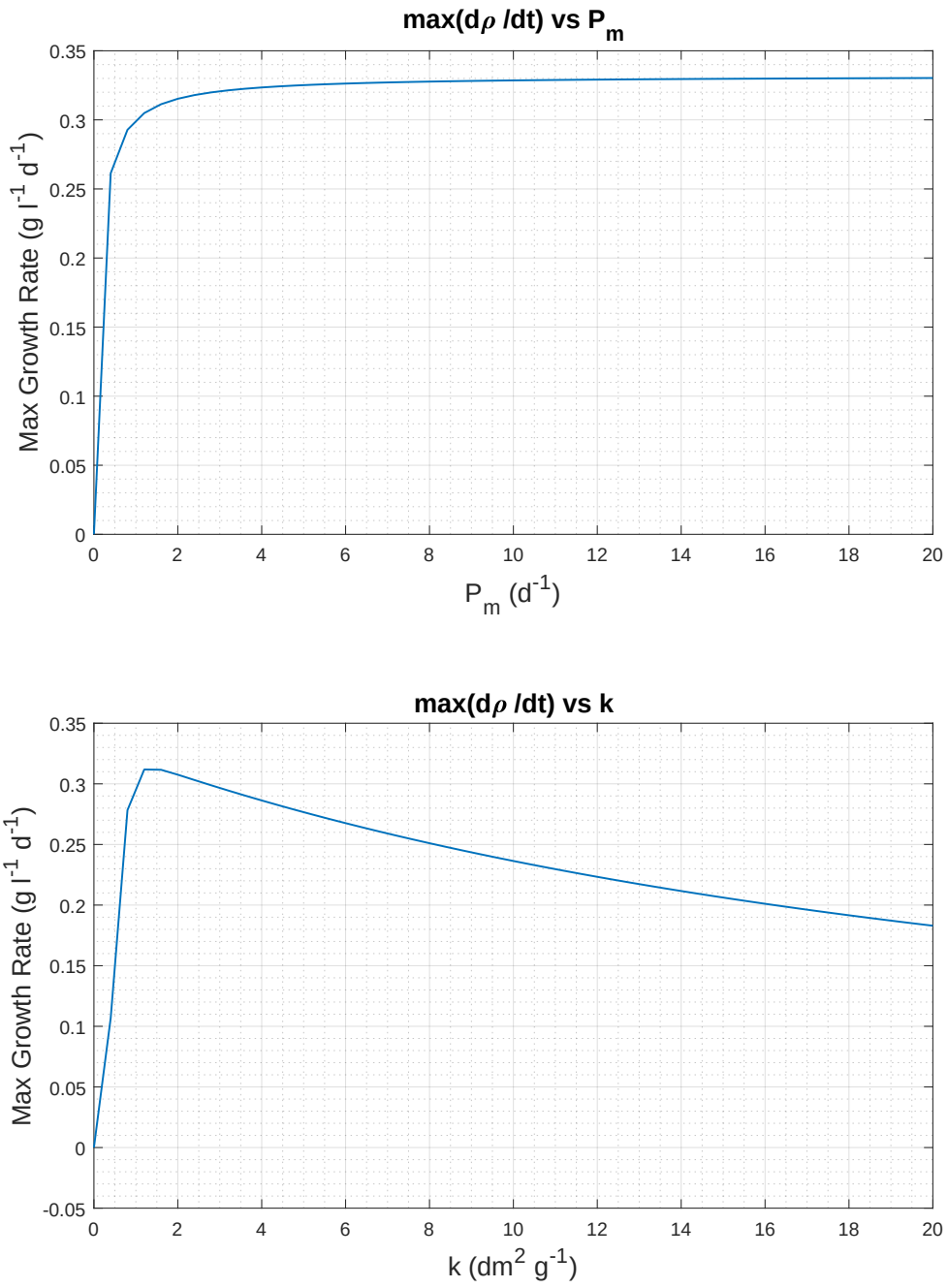

Figure 49: Maximal model based growth versus different values of the parameters P_m and k for the 11th measurement series of M28. Only one parameter changes value at a time.

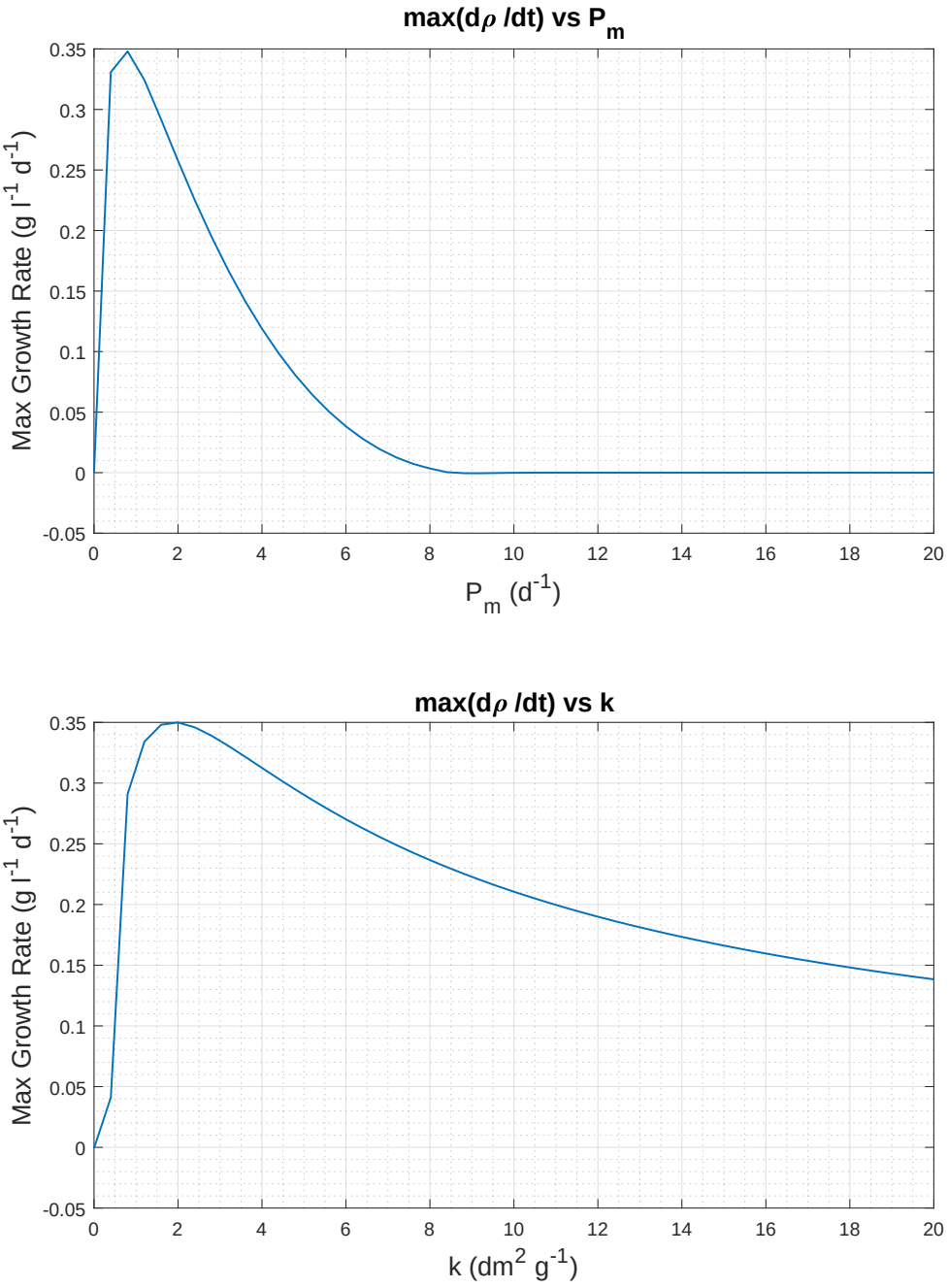

Figure 50: Maximal model based growth versus different values of the parameters P_m and k for the 1st measurement series of B58. Only one parameter changes value at a time.

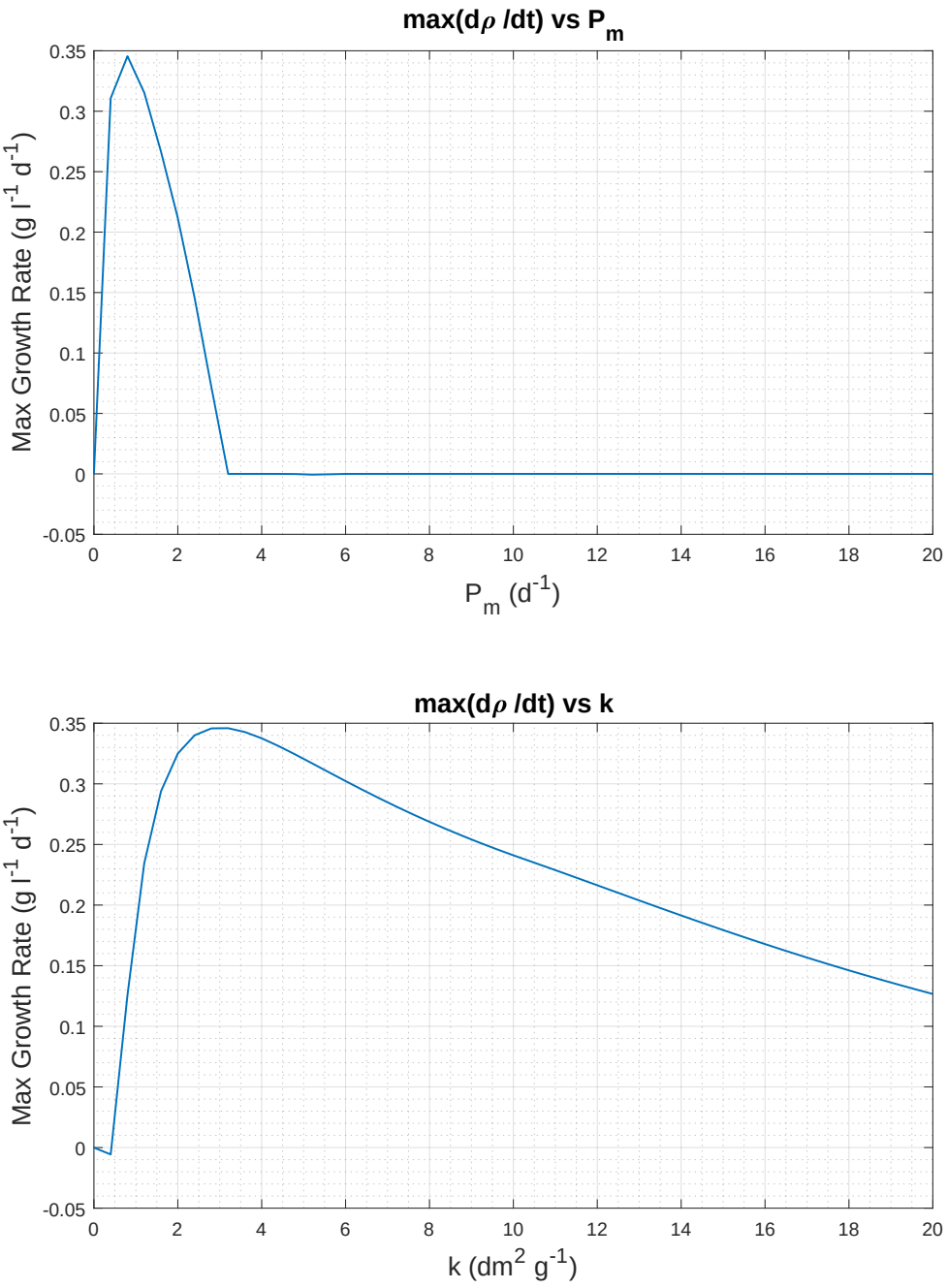

Figure 51: Maximal model based growth versus different values of the parameters P_m and k for the 6th measurement series of B58. Only one parameter changes value at a time.

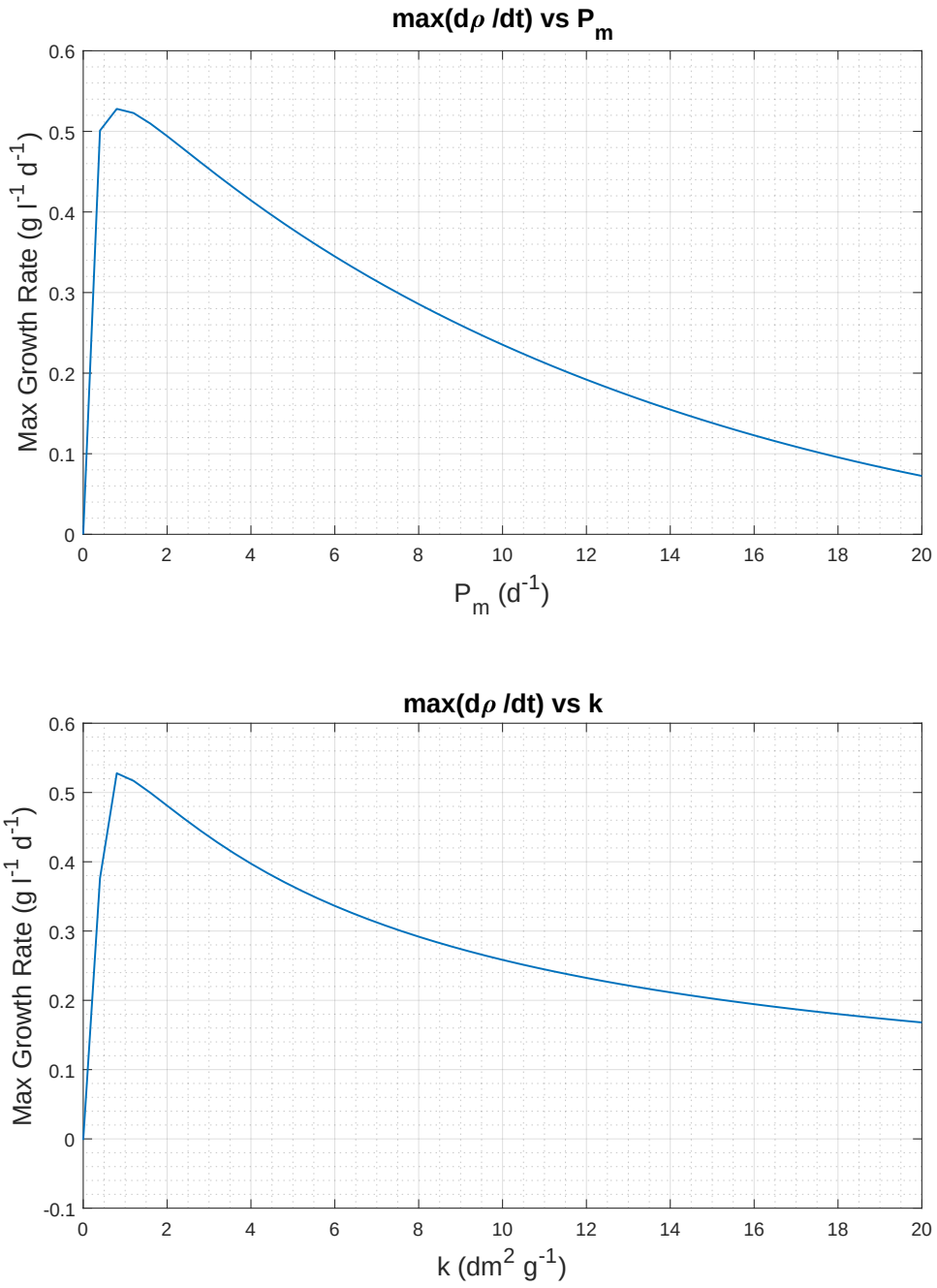

Figure 52: Maximal model based growth versus different values of the parameters P_m and k for the 11th measurement series of B58. Only one parameter changes value at a time.

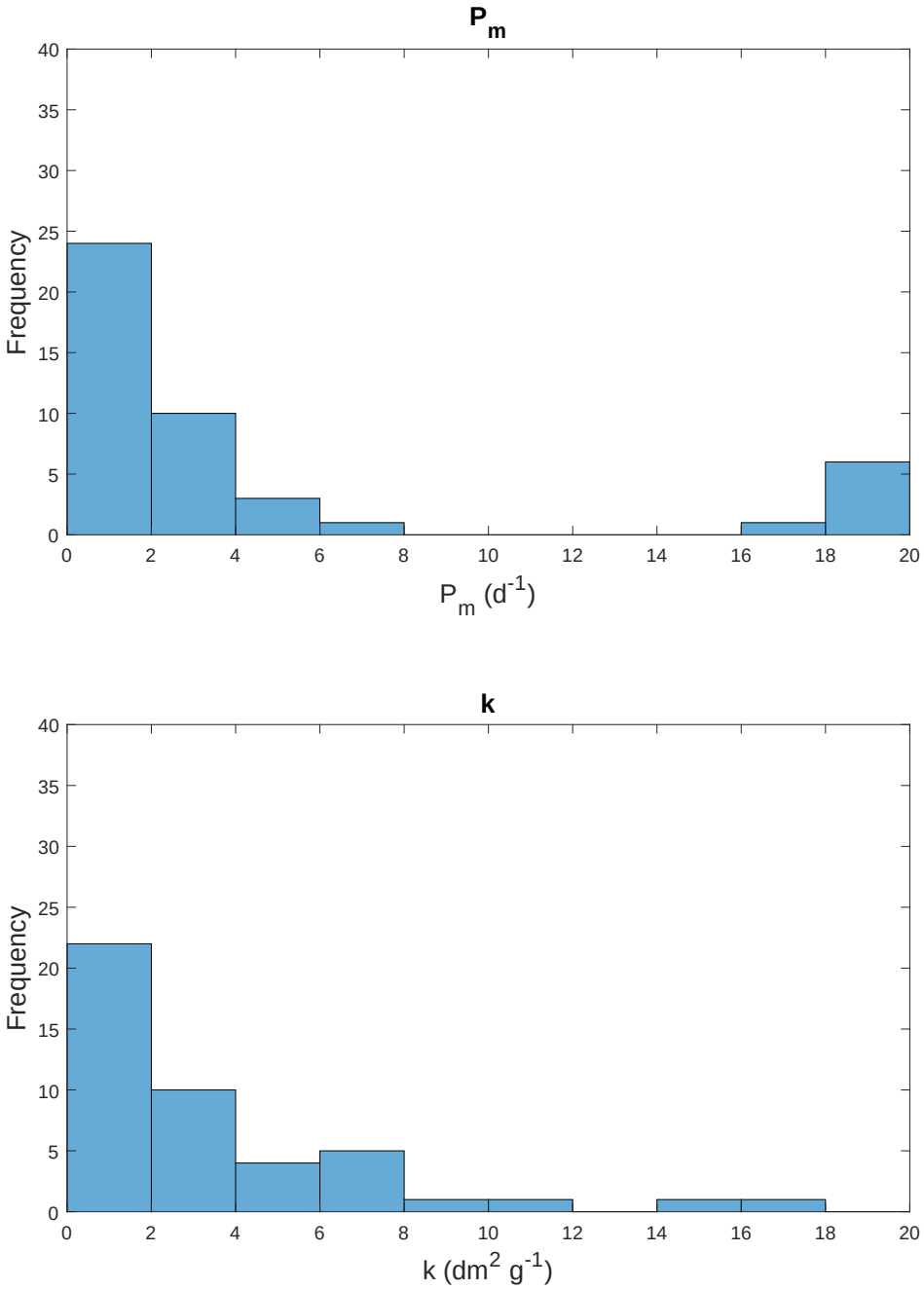

Figure 53: Histogram of the distributions of optimal parameter values P_m and k gained by finding the optimal parameter value for every parameter for every measurement series.

Figure 44-52 show the distributions of maximal model based growth rates versus different values of the parameters P_m and k for the 1st, 6th and 11th measurement series for each strain of algae. In some cases of maximum growth rate versus P_m the peaks are very wide, but in some cases they are quite thin. If the peak is thin the range of values for P_m that yield high growth is quite narrow and so to optimize growth in these situations we need to pay close attention to the value of P_m. When the peak is wide there is a large range of P_m values that yield optimized growth, and so by changing the P_m value in this case does not necessarily yield a very large change in the maximum growth. However, in most cases the value of P_m should be above a certain value since the increase in the maximum growth versus P_m in these cases is quite large for small values of P_m.

In the case of the absorption cross section k, the peaks are usually quite wide, yet the change in the maximum growth is quite large for small values of k. This means that the absorption cross section must not be too low. When the absorption cross section is such that the peak value for maximum growth has been reached, a further increase in the absorption cross section decreases the maximum growth, but not by a lot. Hence, in most cases, the absorption cross section must be above a certain value, and it can even be at a higher value than the value needed for maximum growth and still yield decent growth, but it must not become too large.

Figure 53 shows the distributions of optimal parameter values P_m and k for the maximum model based growth rate. The distributions are gained by finding the optimal parameter values P_m and k for every measurement series. Some of the measurement series are shown in the nine figures preceding the histogram. Note that not all the plots for maximum growth versus P_m seemed to have a peak, at least not in the interval given. Effectively, this means that on the right side of the histogram, some of the values for P_m are probably greater than 20, that is, if there are any peaks for P_m greater than 20 at all.

Table 15: Average and standard deviations of the distributions in Figure 53.

Parameter	Average	Std. Dev.
P_m $[d^{-1}]$	4.5	6.7
k $[dm^2 g^{-1}]$	3.2	3.7

Table 15 shows the averages and the standard deviations for the distributions of P_m and k that gave us the optimal growth for every measurement series. As we can see, the standard deviation is larger than the mean for both P_m and k, which means the uncertainty in both of these parameters is large. This can also be seen from the histograms.

To summarize, the average optimal value for P_m is 4.5 d^{-1}, while the average optimal value for k is 3.2 $dm^2\ g^{-1}$. In comparison, the average values for P_m and k based on the fitting procedure (least square sum and fminsearch) are 0.74 d^{-1} and 5.7 $dm^2\ g^{-1}$, respectively. The standard deviation in each case is larger than the average value, which means that there is great uncertainty in the values of P_m and k.

By comparing these values, we see that the optimal average value of P_m is more than 6 times larger than the fitted average value of P_m. This means that, on average, the fitted values of P_m probably do not yield optimal growth. By increasing P_m we will probably, in at least some measurement series, increase the maximum growth rate.

We also see that the average optimal value for the absorption cross section k is smaller than the average fitted value of k. This means that, on average, the fitted values of k probably do not yield optimal growth.

As explained, there is however great uncertainty in the values of P_m and k. The average fitted value of P_m, for example, does lie within one standard deviation of the optimal P_m values, and so it is possible that some of the measurement series do have optimal values for P_m. In addition, the average fitted value of k does lie within one standard deviation of the optimal k values, given that we ignore the standard deviation of the fitted k values, and so it is possible that some of the measurement series do have optimal values for k.

By studying other strains and species of algae, we might find a type of algae that has more or less the same properties as FITO, M28 and B58 (P. tricornutum), but also have other, more optimal values for P_m and k.

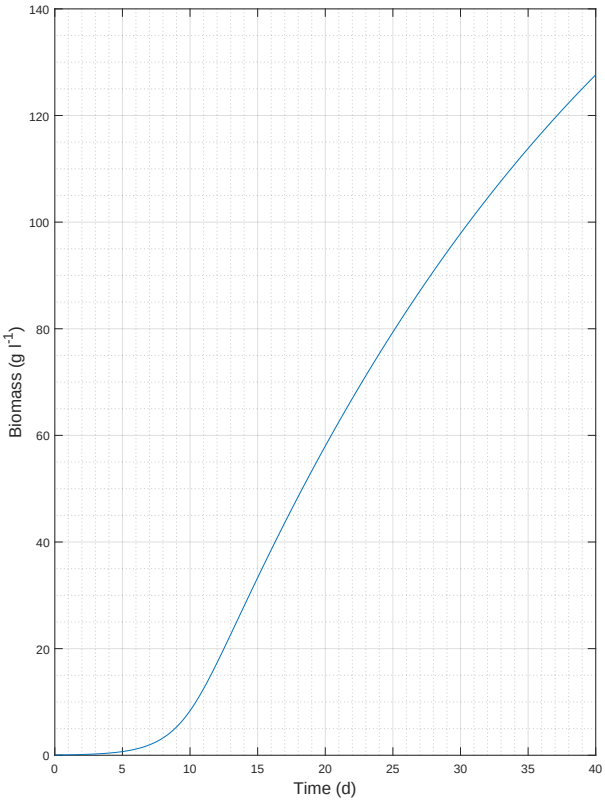

Figure 54: Model biomass versus time based on optimal growth conditions. Figure is based on measurement series one for FITO.

In Figure 54 we have inserted the following values into the model: $E_0 = 0.16$ mol photons dm^{-2} d^{-1}, $h = 0.15$ dm, $P_m = 0.58$ d^{-1}, $\alpha = 11$ g $(\text{mol photons})^{-1}$, $k = 1.1$ dm^2 g^{-1} and $\xi = 0.051$. The graph in Figure 54 is an example of a model graph with ultimate growth conditions.

By comparing these parameter values with the fitted parameter averages, we see that the optimal P_m is a bit smaller than the average value of the fitted P_m values, which was 0.74 d^{-1} with a standard deviation of 0.8 d^{-1}. The difference between these P_m values is not very large, and the standard deviation of the fitted P_m values certainly includes $P_m = 0.58$ d^{-1}.

We also see that the optimal α is a bit larger than the average value of the fitted α values, which was 6.1 g $(\text{mol photons})^{-1}$. The difference between these α values is quite large; the average fitted value of α is almost half as large as the optimal α, however, the standard deviation of the fitted α values does include the optimal α value.

In addition, the optimal value of k is much smaller, almost 5 times smaller, than the average value of the fitted k values, which was 5.7 dm^2 g^{-1}. However, again, the standard deviation of the fitted k values includes the optimal k value.

The optimal value of ξ is 0.051, which is one third of the average fitted value for ξ , which was 0.15. Once again, the standard deviation of the fitted ξ values includes the optimal value of ξ.

The optimal irradiance E_0 was approximately equal to the irradiance in the first measurement series, and the optimal depth h was 0.15 dm, while the depth in the water columns we used was 0.375 dm.

Hence, to optimize growth, we should, on average, use a smaller depth than what was used in addition to a smaller P_m, a larger α, a smaller absorption cross section k and a smaller loss factor ξ. It is always beneficial to use a large α and a small ξ, however.

By comparing the graph in Figure 54 with some of our measurement series, we find that the graph in Figure 54 has a much higher biomass (a factor of approximately 20) in the different parts of its growth cycle. Its maximum growth occurs after 13 days and 12 hours and has a magnitude of 5.4 g l^{-1} d^{-1}, while in a lot of the measurement series the maximum growth occurs, from the same starting biomass, after approximately 8 days with a magnitude of approximately 0.3 g l^{-1} d^{-1}. Hence even if we can find optimal growth conditions, an algae culture with a small starting biomass might need some time to reach the point of maximum growth.

6 Conclusion

In order to grow algae most efficiently the average irradiance should be high as long as it is not too high, and this is true for all the three strains examined. Too high irradiance will cause photoinhibitory damage, yet it is not clear whether or not any of the average irradiances we had caused significant photoinhibitory damage. Photoinhibitory damage may still occur at low average irradiances given that there is both a high level of irradiance at some time during the day and that this high level of irradiance has a long exposure time.

With regards to average temperature all three strains seem to have high growth for high average temperatures within the range of average temperatures given, yet the correlation between average temperature and growth varies quite a bit between the different strains. Within the average pH range given the link between average pH and growth varies a lot between the strains. The growth rate for FITO barely reacts to differences in average pH, while the growth rate for B58 reacts the most.

Nevertheless, a trend is clear: in the given ranges for the average values of irradiance, temperature and pH, all strains have positive correlations between growth and average irradiance, average temperature and average pH, although to a varying extent. That is, within these ranges, higher average irradiance, average temperature and average pH yields higher growth. Although, it should be noted that there is a pretty strong correlation between average irradiance and average temperature, which means that even if an average irradiance does not inflict photoinhibitory damage it still helps raise the temperature, and if the temperature caused by this level of average irradiance is a detriment to growth, it means that there is an optimal value or an optimal range of values somewhere for average irradiance and average temperature, even when ignoring photoinhibition. It should also be noted that to predict growth rates, it is irrelevant whether PAR or PUR is used to measure irradiance; that is, it is not necessary, for the purpose of predicting growth rates, to have knowledge about the absorption cross sections of the strains.

In addition to investigating the data as explained above, we also create a model for growth as shown in Equation 15. According to our model, the maximum growth rate occurs in the turning point between exponential growth and the flattening of the model curve. In addition, this turning point is in the linear part of the curve, where the growth rate does not change very quickly with time. This is important because in order to gain information on the biomass of the algae culture, even if we take a sample around the point of maximum growth, given that the sample is not too large, the growth rate is almost unaffected. But it is even more important for another reason: in order to maximize production of algae, we want to grow algae as quickly as possible. If the growth rate barely changes around the point of maximum growth, we can harvest quite a bit of algae near the biomass point of maximum growth without significantly affecting the growth rate.

The model parameters P_m, α, k and ξ barely seem to depend on average irradiance, average temperature or average pH. In addition the model parameters barely seem to depend on each other. Therefore, it seems unlikely that it is possible to create any mathematical relationship between these variables and hence get a model in terms of average irradiance, average temperature and/or average pH instead of these model parameters. However, with more data points for biomass, especially in the flattening part of the growth, perhaps this would change somewhat, but even still the model curves are quite sensitive to changes in parameter values, and so if there are still somewhat low correlations between the model parameters and average irradiance, average temperature and average pH, the new model without the model parameters P_m, α, k and ξ would not necessarily be accurate in predicting growth rates.

It seems that in most if not all cases there is a peak value for the maximum growth as a function of both P_m and k. In addition, most of these peak values seem to exist for small values of both P_m and k, yet there are some peak values for somewhat larger parameter values. In the case of k, all the maximum growth rates occur below 18 $\mathrm{dm}^2\ \mathrm{g}^{-1}$, while in the case of P_m there seems to be some missing peaks or peaks for P_m greater than 20 d^{-1}. It is, after all, reasonable to expect there to be an optimal value for the absorption coefficient k; as explained in the theory section, a small absorption cross section barely absorbs any radiation, which reduces growth, while a large absorption cross section absorbs too much in the top layer, which also reduces the growth in the culture. Interestingly, when the maximum production P_m is too small or too large, the maximum (net) growth rate of the culture is sub-optimal.

We find the average fitted P_m and k values to be equal to 0.74 d^{-1} and 5.7 $\mathrm{dm}^2\ \mathrm{g}^{-1}$, respectively, and we also find the average optimal P_m and k values to be equal to 4.5 d^{-1} and 3.2 $\mathrm{dm}^2\ \mathrm{g}^{-1}$, respectively. By comparing the average fitted P_m and k values to the average optimal P_m and k values, we find that for P_m the average optimal value is much higher than the average fitted value, while for k the average optimal value is lower than the average fitted value. Perhaps by studying other strains or species of algae we can find a type of algae with almost the same properties as FITO, M28 and B58, but with other average values for P_m and especially k.

The maximum growth rate seems to increase indefinitely with increasing α and increasing E_0. However, as previously mentioned, if the irradiance is too high, the algae cells may suffer from photoinhibition, which the model does not take into account. Not surprisingly, if the loss factor ξ is small enough, the growth is large, and if the loss factor ξ is large enough, the growth stagnates. Although the maximum growth rate is large for small depths, there are some limitations as to how small the depth can be in reality. For one the algae cells have certain sizes, so if the depth becomes too small, it becomes physically impossible for the algae cells to exist in the water column. In addition to algae cells, water, nutrition, CO_2 and other substances are in the bag, which require space. For small depths the maximum growth rate seems quite large, however, as explained in the thesis, the relative growth rate is not very large because of the large biomass in the point of maximum growth for small depths. In addition, even though the maximum change in volumetric mass density (maximum growth rate) is large for small depths, the maximum change in mass per area seems to be constant with depth, and if this indeed is the case, the maximum growth rate in terms of total mass is constant with depth. Hence we can choose our bags to have any depth (at least between 1 cm and 1 m) given that the other model parameters are constant with depth.

7 Further work

Because of the limitation on the number of biomass points for each measurement series, especially in the exponential part and even more so in the flattening part of each measurement series, the model curve fits to the data points we had might not have been good curve fits for possible extra biomass points. Since there are only so many data points for each measurement series, and often a severe lack of data points in the flattening parts, the model fits we got via the method of the least square sum combined with fminsearch only got us so far because there were often no flattening part data points that we could incorporate into our least square sum. For future work, you should use more data points especially in the exponential and flattening parts to put more of a limitation on what parameter values you will get.

Although we did use three strains of algae, maybe it would be a good idea to use more strains or even species of algae. That way you get not only more data, but you also get a broader picture of how the growth depends on the different parameters and physical quantities (irradiance, temperature and pH). The drawback, of course, is that by including more strains or species of algae you might get a much larger variation in your data and/or parameter values. Then again, the aim of this thesis has been to find a model for growth more or less independent on the particular algae strain or specie.

In addition, even though the individual parameters have low correlations with average irradiance, temperature and pH, perhaps it is possible to find relationships between these parameters and these physical quantities that make it so that when you have equations for all the parameters and then plug these equations into the model, you might be able to predict the growth anyway. Although this perhaps is not possible, by having more data points like I recently mentioned, the correlations between the parameters and the physical quantities (irradiance, temperature and pH) might increase.

The model could be modified so that the growth rate, or maximum growth rate, would be reduced with increasing ρ. This could possibly be done by making the loss factor ξ proportional to ρ.

The mathematical criterion we used to fit the model curves to the data points was, as mentioned earlier, with the method of sum of least squares. Perhaps, with or without increasing the amount of data points for biomass, there is another mathematical criterion that would give us better model fits and/or higher correlations between parameters and physical quantities (irradiance, temperature and pH). Additionally, some method other than fminsearch could be used to fit the model curves to the data points.

References

Agar. (2017). Retrieved 20.11.2017, from https://www.britannica.com/topic/agar-seaweed-product

Alters, S. (2000). *Biology: understanding life*. Jones & Bartlett Learning.

Amthor, J. S. (1994). Respiration and carbon assimilate use. *Physiology and Determination of Crop Yield. American Society of Agronomy, Madison, WI*.

Blankenship, R. E. (2013). *Molecular mechanisms of photosynthesis*. John Wiley & Sons.

Bohren, C. F., & Clothiaux, E. E. (2006). Fundamentals of atmospheric radiation.

Brennan, J. (2017). *Earth's first atmosphere contained what gases?* Retrieved 09.10.2017, from https://sciencing.com/earths-first-atmosphere-contained-gases-2034.html

Cain, F. (2009). *Earth's early atmosphere.* Retrieved 09.10.2017, from https://www.universetoday.com/26659/earths-early-atmosphere/

Chatterjee, A., Singh, S., Agrawal, C., Yadav, S., Rai, R., & Rai, L. (2017). Role of algae as a biofertilizer.

Chisti, Y. (2007). Biodiesel from microalgae. *Biotechnology advances*, *25*(3).

Falkowski, P. G., & Raven, J. A. (2007). Aquatic photosynthesis. , *Second Edition*.

Govindjee. (2012). *Energetics of photosynthesis*. Elsevier.

Hannon, M., Gimpel, J., Tran, M., Rasala, B., & Mayfield, S. (2010). Biofuels from algae: challenges and potential. *Biofuels*, *1*(5).

Henriques, M., Silva, A., & Rocha, J. (2007). Extraction and quantification of pigments from a marine microalga: a simple and reproducible method. *Communicating Current Research and Educational Topics and Trends in Applied Microbiology Formatex*, *2*.

Hill, G. E. (2014). Cellular respiration: the nexus of stress, condition, and ornamentation. *Integrative and comparative biology*, *54*(4).

Kirk, J. T. (1994). *Light and photosynthesis in aquatic ecosystems*. Cambridge university press.

Lee, K. Y., & Mooney, D. J. (2012). Alginate: properties and biomedical applications. *Progress in polymer science*, *37*(1).

Liu, Z. (2013). Review on the role of terrestrial aquatic photosynthesis in the global carbon cycle. *Procedia Earth and Planetary Science*, *7*.

Nedrebø, S. (2017). Use of market ready light dosimeters for patients with erythropoietic protoporphyria disorder.

Ntc thermistors. (-). Retrieved 09.11.2017, from http://www.microchiptechno.com/ntc_thermistors.php

Operating instructions mettler toledo mt/umt balances. (-). Retrieved 09.11.2017, from https://www.mt.com/dam/mt_ext_files/Editorial/Generic/5/UMT-MT_BA_Editorial-Generic_1101387228265_files/mt-umt-ba-e-11780223a.pdf

Ph meter. (-). Retrieved 09.11.2017, from https://www.britannica.com/technology/pH-meter

Prokaryotic cells. (-). Retrieved 20.11.2017, from https://nb.khanacademy.org/science/biology/structure-of-a-cell/prokaryotic-and-eukaryotic-cells/a/prokaryotic-cells

Ptc thermistor. (-). Retrieved 09.11.2017, from http://www.resistorguide.com/ptc-thermistor/

Sakshaug, E., Bricaud, A., Dandonneau, Y., Falkowski, P. G., Kiefer, D. A., Legendre, L., ... Takahashi, M. (1997). Parameters of photosynthesis: definitions, theory and interpretation of results. *Journal of Plankton Research*, *19*(11), 1637–1670.

Steinrücken, P., Erga, S. R., Mjøs, S. A., Kleivdal, H., & Prestegard, S. K. (2017). Bioprospecting north atlantic microalgae with fast growth and high polyunsaturated fatty acid (pufa) content for microalgae-based technologies. *Algal Research*, *26*.

Tveiterås, J. (2013). Characterization of hyper spectral irradiance and radiance sensors.

Vidyasagar, A. (2016). *What are algae?* Retrieved 09.10.2017, from https://www.livescience.com/54979-what-are-algae.html

Wang, H.-M. D., Chen, C.-c., Huynh, P., & Chang, J.-S. (2015). Exploring the potential of using algae in cosmetics. *Bioresource technology*, *184*.

Zahnle, K., Schaefer, L., & Fegley, B. (2010). Earths earliest atmospheres. *Cold Spring Harbor perspectives in biology*, *2*(10), a004895.